United States
Department of
Agriculture

**Agricultural
Research
Service**

ARS-29

November 1985

BRDRFLW: A Mathematical Model of Border Irrigation

Abstract

Strelkoff, Theodor. 1985. BRDRFLW: A Mathematical Model of Border Irrigation, U.S. Department of Agriculture, Agricultural Research Service, ARS 29, 104 p., illus.

BRDRFLW is the documentation for a computer program of the same name, written in FORTRAN and designed to predict the behavior of the surface stream flowing down an irrigation border. The infiltration is assumed a given function of infiltration time. Other physical characteristics required as input to the model are the border length, slope, roughness, and downstream boundary condition; that is, whether the stream is blocked by an end check or allowed to drain freely into a drainage ditch. The management parameters—required depth of application, inflow rate, and cutoff time—complete the physical input to the model. Upon entry of certain numerical-solution and display parameters, the computer program solves the equations governing the flow in the surface stream. The key solution variables are the advance, recession, and runoff as functions of time, and the ultimate distribution of applied water. These results can be displayed in both tables and graphs. Also displayed are various figures of merit of the irrigation; for example, distribution and application-efficiency parameters. Input can be made in either English or metric units or in dimensionless form; output appears in all three.

The governing (nonlinear) equations are comprised of a mass-conservation relation and either a statement of equilibrium among pressure, gravity, and drag forces on elements of the surface stream (zero-inertia formulation) or one of equilibrium between gravity and drag forces (kinematic-wave model, suitable for steep slopes). The user can also choose a hybrid model, utilizing zero-inertia concepts for advance and kinematic-wave analysis for recession.

KEYWORDS: irrigation engineering, surface-irrigation hydraulics, border irrigation, mathematical models, computers, water distribution, irrigation efficiency

Copies of this publication may be purchased from the National Technical Information Service, 5285 Port Royal Road, Springfield, Va. 22161.

ARS has no additional copies for free distribution.

United States
Department of
Agriculture

**Agricultural
Research
Service**

ARS-29

BRDRFLW: A Mathematical Model of Border Irrigation

By Theodor Strelkoff
Hydraulic Engineer
1376 Seventh Avenue
San Francisco, Calif. 94118

Prepared for
U.S. Department of Agriculture
Agricultural Research Service
U.S. Water Conservation Laboratory
4331 East Broadway
Phoenix, Ariz. 85040

Under Contract No. 53-9AHZ-1685

Foreword

This manuscript represents the results of several decades of work on the development of models to describe the flow of water within irrigation borders. Of the two basic types of surface irrigation, borders and furrows, borders are the simplest mathematically and so have been given the most attention initially. The purpose of surface-irrigation models is to improve the overall state-of-the-art of surface irrigation. This improvement could eventually lead to the more efficient use of water and water conservation. The U.S. Water Conservation Laboratory became interested in surface irrigation modeling in the mid-1970's after the Western Regional Research Project on surface irrigation modeling W-65 was terminated. This group, along with others, had made significant advances in the theoretical development of border-irrigation flow. A major breakthrough was the development of the zero-inertia model by Theodor Strelkoff and Nikolaos D. Katopodes (under cooperative agreement between the U.S. Water Conservation Laboratory and the Department of Land, Air, and Water Resources, University of California, Davis). This information was published in 1977. The model had significant advantages over previous models since it was far less complicated than the more complete hydrodynamic models and far more widely applicable than the kinematic-wave models.

Versions of this original model are being used by a number of researchers. These versions have been modified to handle a variety of situations; however, a number of computational problems have arisen and the model as such has never been fully reliable. Accordingly, it was never fully documented since an unfamiliar user may not be able to differentiate a good run from a poor one.

Continual development has taken place since the original model was produced through cooperative efforts with the University of California, Davis, and currently through a contract with Strelkoff (formerly of U.C., Davis). This ongoing cooperative effort with Strelkoff over the last 6 or 7 years has resulted in the mathematical model and computer program described herein. This publication consists of two theoretical models (the kinematic wave and a new fully nonlinear zero-inertia or equilibrium model) and a hybrid of the two. The user may select the appropriate model for his or her particular situation. New techniques have been used to perform the computations and a considerable

amount of flexibility has been added. This new program is sufficiently more reliable than its predecessor that sawtooth profiles and aborted runs can be avoided and consistent solutions can be obtained. This new program, along with its documentation, will provide a useful tool for analyzing border irrigation flow. It can be used to develop design criteria, to develop or modify specific designs, to evaluate current systems, to develop optimum management practices, and to improve our understanding of border-irrigation flow. As such, it can be a valuable tool for teaching, for research, and for application to improvements in border-irrigation practices. Those interested in the computer program can obtain a copy by sending a 9-track magnetic tape to me at the following address:

Albert J. Clemmens
U.S. Water Conservation Laboratory
4331 East Broadway
Phoenix, Ariz. 85040
ATTN: BRDRFLW

Contents

1. Introduction

1.1 BRDRFLW: An Overview

BRDRFLW is a computer program designed to model the flow of water over the surface of an irrigation border. It was implemented at the computer center of the Lawrence Berkeley Laboratory, University of California, Berkeley. The inflow is assumed to be distributed evenly across the width of the border at its upper end, and the transverse slope of the border is assumed to be zero. Roughness and infiltration characteristics are assumed not to vary transversely either, so that the resulting flow is plane, that is, two dimensional. The subject of analysis is a strip of field of unit width to which water is introduced at a known volumetric rate per unit width at the upper end and which possesses known roughness and infiltration characteristics as well as known bottom configuration, length, and downstream-boundary condition, either a free outflow into a drainage ditch or ponding behind a dike.

On the basis of the physical principles of conservation of mass and one or another approximation to the impulse-momentum relationship, the longitudinal variation of depth and discharge along the length of the surface stream is computed at a sequence of times after the start of an irrigation. As byproducts of these calculations, the movement of the wave front during stream advance and of the trailing edge of the stream profile in recession are obtained. With infiltration a known function of opportunity time, the ultimate post-irrigation longitudinal distribution of infiltrated water depth (volume infiltrated per unit plan area of field) is readily obtained. With the irrigation requirement known, the volume lost to deep percolation is then determined. An additional byproduct of the profile computations, the runoff rate from the end of the field, is integrated over time to provide the volume of runoff. Final computations by the program provide the water-application efficiency and various distribution parameters stemming from the inputted conditions of the irrigation.

1.2 Significant Features

The zero-inertia border mathematical model was last documented in 1977 (10). At that time a locally linearized set of algebraic equations was used to approximate a mix of integrated and differential forms of the equations of continuity and motion. The present equilibrium model is based wholly on integrated forms. Statements of mass conservation and equilibrium of forces are applied to thick slices of the surface stream; furthermore, the continuity equation is integrated over small increments of time. Simple quadrature formulas, notably the trapezoidal rule, are used to approximate the integrals by algebraic expressions. The model described by Strelkoff and Katopodes (10) was not programmed to treat irrigation streams ponded behind dikes raised at the downstream end of the field. Recession from the front of the irrigation stream, either before advance was completed or after, also could not be modeled. The present model is capable of treating both of these circumstances.

Additional bases for mathematical modeling are provided in the current model by normal-depth kinematic-wave theory. If the depth gradient in the surface flow is sufficiently small compared with the bottom slope, the depth and discharge at every point in the stream are uniquely related through a normal-depth stage-discharge relationship. This allows simpler, quicker, more robust[1] computations than those provided by equilibrium (zero-inertia) theory. The range of applicability of the kinematic-wave model can be greatly extended if application of kinematic-wave theory is deferred until water starts to recede from the upper end of the field. Such a hybrid model constitutes a subset of BRDRFLW, as does pure kinematic-wave theory. These can be called for as desired by the user.

The present equilibrium model differs also from its more recent, undocumented predecessors in several substantial ways. The length δx of cells making up the surface stream has been divorced from the time step δt. For quick, rough computations the number N of cells can be set to a small constant, say, $N = 5$. Previously, the number of cells equaled the number of time steps of advance, which results in unnecessarily large numbers of computations. The present system also allows the computational field length to be precisely equal to the given field length, rather than somewhat larger in accordance with the advance achieved in an integral number of time steps, as in the earlier models.

Further, irregular bottom profiles can be input to the model, in contrast to the strictly plane borders allowed in the earlier versions. If an irregular bottom breaks through the stream surface, however, an error may be incurred, as the program will compute the motion of only one continuous length of surface stream. If the stream breaks up into several pieces with islands in between, only the largest piece will be followed in detail. The other pieces are assumed to infiltrate as stagnant ponds.

The surface-stream profile is found at each time step either iteratively, through the Newton-Raphson method of solving the nonlinear governing equations, or in a single set of implicit computations utilizing locally linearized forms of the equations. The latter calculation is merely the first step of the former. When used, the Newton-Raphson method typically converges in about three or four iterations.

[1]Less subject to computed saw-tooth profiles and spontaneous aborts of computer runs.

The skeleton of BRDRFLW is built in such a way that variations in the functional form of inputted conditions are relatively easily accommodated. For example, when in the course of computation the program requires a value of inflow discharge at time t, a call is made to the function subprogram QF(t). Any desired inflow-hydrograph function of time can be programmed into the subprogram. Similarly, the program's need for a value of time step, say at time t, results in a call to DTF(t,. . .); any desired variation in time-step size can be specified in that one subprogram. Variable bottom slope is handled as follows: In the statement of equilibrium among all forces acting on the water in a cell, the pertinent geometrical feature of the bottom is the difference in elevation at the upstream and downstream ends of the cell. The subprogram BF(x,. . .) provides the bottom elevation of point x. Any desired variation can be programmed into that routine. Current programming allows either a constant bottom slope or a table of bottom elevations.

The roughness of the bottom is characterized by the Chezy C, which in general is a function of depth y. The subprogram CHEZYC, which has among its arguments y, RUF, a_n, and RUFMOD, computes the Chezy C on the basis of the computer-supplied y and the roughness parameter RUF, read in at the start of the computation. The index RUFMOD, also supplied by the user, determines the nature of the roughness formula to be used. With RUFMOD set to 1, RUF is interpreted as a constant Chezy C value. With RUFMOD = 2, RUF represents the Manning n. Some researchers allow the Manning n to vary as a power law of depth (reflecting the fundamental unsuitability of the Manning formula for shallow flow). To allow comparison with the results of these researchers, the CHEZYC routine utilizes the following formula when RUFMOD = 2: $n = RUF \cdot y^{a_n}$; in the usual case, $a_n = 0$. With RUFMOD = 3, RUF is interpreted as the Sayre-Albertson χ (chi) in their logarithmic formula (6), considered theoretically more sound than the Manning formula.

Cumulative infiltration z (and infiltration rate) is also relegated to a subroutine whose principal argument is τ, the infiltration time. The formula currently programmed is rather general: $z = k\tau^a + b\tau + c$, with a, b, and c supplied by the user. With b = 0 and c = 0, the formula is the Kostiakov function; with b = 0, the results represent the Soil Conservation Service formula (11) typifying their infiltration families; with a = ½, c = 0, the result is the Philip formula. Other infiltration functions of time can be programmed into this routine, if desired.

To save computation time in the ponded case and with some irregular bottom configurations, the computer can recognize a nearly stagnant state of the surface stream and compute recession times directly, based on a succession of level water surfaces. Alternately, the program works in the usual mode, computing at successive times the positions of the nearly horizontal water surface as it slowly lowers, as the result of infiltration, into the soil.

Input data can be entered in either metric or English units or in dimensionless form. Setting an index (DMLMOD) determines the system of nondimensionalization used by the program. With data entered in dimensional form, the desired set of characteristic values is used to put them in dimensionless form. The computations, in any case, are carried out in dimensionless form, with intermediate results, say, at each time step, printed in dimensionless form. Final results—the advance and recession functions, ultimate distribution of infiltered water, runoff volumes, efficiencies—are presented in all sets of units.

To enhance the significance of dimensionless input, the program computes the corresponding dimensioned values for a hypothetical border. Hypothetical values of border roughness, slope, and inflow, needed to interpret physically the given dimensionless input (see sec. 3.8), are entered by the user, or default values can be supplied by the program.

In general, most input data defining solution methods and parameters rather than physical-problem parameters have program-supplied default values, which are enabled by entering 0 (zero) for each such variable value called for.

2. Influence of Computer-Facility System Software

In moving a computer program from one facility to another, certain portions require modification because of system software peculiar to the facility that is utilized by the program. BRDRFLW was constructed in FORTRAN4 language (MNF4 at BKY) using the computing facilities at the Lawrence Berkeley Laboratory, University of California at Berkeley (BKY).

The program was designed for interactive use, with a terminal capable of printing 132 characters per line, such as the DIGITAL DECWRITER III. Requests for data are made in the form of prompts to the operator who then enters the necessary information from the keyboard. The program may be used in batch mode by deleting the subroutine calls, CALL CONNECT(5) and CALL CONNECT(6) (these subroutines are part of the library at BKY and allow interactive communication). The prompts for data should then be anticipated by the operator who submits a small data deck (typically, a dozen cards), one card for each group of data requests expected (see ch. 3).

It is also possible to allow entry of input data from a terminal, while shunting output to a line printer. In the program, unit number U1 is designated for reading input, U2 for printing program output, and U3 for providing input-entry prompts to a terminal operator. Numerical values are assigned to these variables in the data statement following the type-variable declaration and dimension statements in the main program. The values 5 and 6 correspond, respectively, to input and output units at many computer centers.

In addition, the program was designed for graphic output, in conjunction with a computer-center-library graphics package (GRAFPAC at BKY) and a plotter, for example, the TEKTRONIX 4662. It is possible to display depth or water-surface profiles, as well as advance and recession trajectories, runoff as a function of time, and the post-irrigation infiltration profile. With the kinematic-wave option in force, the wave trajectories in the x-t plane can also be plotted.

For use at computer centers where no graphics capabilities exist, reference to the GRAFPAC routines TVINIT, TVWIND, TVVIEW, TVPLOT, TVSEND, and TVEND must be deleted from BRDRFLW or dummy routines must be added, unless the software at the given center allows reference in a program to a nonexistent routine as long as it is not actually called. Calls to these graphics routines are avoided by setting all graphics input parameters (see Section 3.12, LINE 12) to zero. Computer centers with graphics packages different from GRAFPAC, will require calls in BRDRFLW different from those to TV. . . cited above. The call to CONNECT(4LFILM) also refers to BKY software and allows interactive graphing.

Other calls in BRDRFLW peculiar to BKY software that will likely require modification for use at other computing facilities are the control cards (records 1 to 9) up to and including the PROGRAM card and DATE, CLOCK, and STATUS, all of which are called from the BRDRFLW subroutine RNINF. These subroutines provide information on real date and time at the moment they are called, the amount of central processor time used up to that point, and other information pertinent to the computer run.

To reduce the difficulties of program adaptation to various computer centers, free format has been used but sparingly, specifically only for input. The star (*) in input statements READ (U1, *). . . signifies at BKY that the list of input data specified is in free format, that is, in either integer or decimal form, and in fields of arbitrary length, set off by commas. This provides maximum user flexibility in input format. All output format is achieved through FORMAT statements, and textual material therein is introduced as a specified number of Hollerith characters.

BRDRFLW is a large program. At BKY the memory requirement for compilation and loading is about 176,000 words (octal), that for execution about 153,000 (octal).

3. Input

As indicated in chapter 2, the input to the model is in the form of keyboard entries during an interactive session, or as a series of punched cards for batch processing. The individual records, call LINES in the sequel, are therefore either a set of data preceding a carriage-return (send) strike on a keyboard, or a card of data input fed into a card reader. Input data received by the program are immediately echoed back to unit U2 (see ch. 2 for description of input/output units).

Much of the data called for define solution options, rather than describing particulars of a border irrigation. Often, the former have program-supplied default values, which the inexperienced user can enable by entering a 0 (zero) for the particular value. The variables so endowed, and the default values for each, are identified in the sequel, which describes each variable entry in turn. See appendix for sample input.

3.1 LINE 1 (Class of Computer Run)

The first line (or card) of input is aimed at interactive users. It allows the user to position the paper at the terminal to whatever vertical placement he or she desires before beginning the run. For example, a fresh page can be brought up for recording prompts and data input, uncluttered by information pertaining to log-in, computer-center messages, and so on. Then, entry of a single digit, between 1 and 5 inclusive, signifies that the operator is ready; a 0 brings about a normal termination. The significance of this parameter, TSTMOD, follows

TSTMOD — *indicates the relationship, if any, of the current simulation to the last one executed during the current program connection.*

= 1 : the current simulation is independent of any preceding one; a complete new set of data will be entered.

= 2 : geometrical data are assumed the same as in the preceding simulation. Following entry of LINE 2 (see below), the program in effect jumps to entry of LINE 7. This option is convenient for management-optimization studies. The management variables z_{req}, q_{in}, t_{co} can be changed relative to their value stored in the preceding run. Entry of a zero for any of these causes retention of the previous value.

Prompts will be made for entry of solution modes and parameters (LINES 9, 10). Zero entries will cause retention of the value from the previous run. Diagnostic and plotting parameters (LINES 11, 12) must be entered anew.

= 3 : all physical data are assumed the same as in the preceding run. Following entry of the run identification (LINE 2), the program, in effect, jumps to entry of LINE 9. The solution modes (LINE 9) and parameters (LINE 10) can be changed by entry of non-zero values. Zeroes cause retention of previous values. Diagnostic and plotting parameters are entered anew.

= 4 : physical parameters and solution technique are identical to those of the preceding run, but numerical-solution parameters (LINE 10) can be changed. Diagnostic and plotting parameters (LINES 11, 12) are entered anew.

= 5 : all parameters are retained except diagnostic and plotting flags (LINES 11 and 12). These are entered anew.

= 0 : stop

The program, after completing an irrigation simulation, or upon encountering certain error states, returns to this point to allow entry of a new set of conditions without the need for program reloading. When the operator has completed all the runs contemplated, or notes his execution-time limit approaching (this information is supplied by RNINF, prior to the prompt for TSTMOD), entry of a 0 ends program control.

3.2 LINE 2 (Run Identification)

The next line (or card) of input requested is data identifying the run. This can be any 78 characters, including blanks, the user wishes to have printed near the top of the printed output from the run.

3.3 LINE 3 (Dimension Control)

The next line (or card) requested contains the values of two integer variables, in free format, that is, separated by commas, defining the simulation conditions. In order, these are:

INPMOD — *alerts the program to the dimensions of the irrigation parameters to be entered.*

= 1 : causes the program to expect irrigation parameters in the metric system: required depth of infiltration in cm; field length and elevations in meters, coefficient of power term in infiltration formula in cm/hr^a in which a is the exponent, coefficient of time term in infiltration formula in cm/hr, constant in cm, cut-off time, time step, and maximum irrigation time computed, in minutes, inflow rate in liters per second per meter width, flow depths in meters.

= 2 : causes the program to expect irrigation parameters in the English system: required depth of infiltration in inches, field length and elevations in feet, coefficient of power term in infiltration formula in in/hr^a, coefficient of time term in infiltration formula (final intake rate) in in/hr, constant in inches, cut-off time, time step, and maximum irrigation time computed, in minutes, inflow rate in cfs/foot width, flow depths in feet.

= 3 : causes the program to expect irrigation parameters in dimensionless form.

DMLMOD — *The program works with dimensionless variables. DMLMOD defines the reference (characteristic) depth, length, time, Y_0, X_0, T_0, respectively, computed by the program and used, subsequently, to put dimensioned input data into dimensionless form.*

= 0 : enables one of the following two default values. If the average bottom slope of the border $S_{0_{avg}}$ is greater than 0, DMLMOD is set to 1. If $S_{0_{avg}} = 0$, DMLMOD is set to 2.

= 1 : $Y_0 = y_n$ (normal depth for the given inflowing discharge q_{in}, average bottom slope, $\widetilde{S}_0$, and field roughness). Thus, DMLMOD = 1 cannot be used with horizontal borders.

$X_0 = y_n / \widetilde{S}_0$

$T_0 = X_0/(q_{in}/y_n)$.

As a consequence, the dimensionless average bottom slope S_0^* is always unity, as is the dimensionless drag coefficient D^*. Dimensionless cutoff time t_{co}^* is variable, and so is the dimensionless infiltration power-law coefficient K^*. DMLMOD = 1 is the routine choice for sloping borders, although DMLMOD = 2 is permissible.

= 2 : Y_0 satisfies the equation $Y_0^5 C_h^2 = q_{in}^3 t_{co}$, in which C_h is the Chezy C.

$X_0 = q_{in} t_{co}/Y_0$

$T_0 = t_{co}$

DMLMOD = 2 is the proper value for horizontal borders. Then $t_{co}^* = 1$ always, and D^* also. S_0^* is variable and equals zero in horizontal borders.

3.4 LINE 4 (Soil and Crop Properties)

The data on line (card) 4 describe the hydraulic properties of the soil and crop. The entries differ, depending upon whether input is dimensioned or dimensionless. In the dimensioned case (INPMOD = 1 or 2), the required variables, eight in number, are

RUFMOD — *determines how program interprets roughness parameters entered.*
- = 1 : parameter RUF (below) is interpreted as fixed Chezy C.
- = 2 : parameter RUF is interpreted as the coefficient in a power law of depth for Manning n; namely, $n = RUF \cdot y^{a_n}$; usually, $a_n = 0$ and RUF is the Manning n.
- = 3 : parameter RUF is interpreted as the Sayre-Albertson chi.

RUF, AN : roughness characteristics of field (see explanation of RUFMOD, above).

INFMOD — *determines how the program interprets infiltration parameters entered.*
- = 1 : interprets K, A, B, C (below) as parameters in the following modified power law for cumulative infiltration z as a function of infiltration time τ:

$$z = K \tau^A + B \tau + C$$

A user who had programmed some other time variations of infiltration would signal which function he or she wished enabled by entering an appropriate value of INFMOD.

K,A,B,C — *infiltration characteristics of field (see preceding explanation of INFMOD).*

If dimensionless variables are being entered (INPMOD = 3), the four infiltration parameters are required, plus the kind of roughness formula used; in the Sayre-Albertson formula, a dimensionless χ must be given.

RUFMOD, INFMOD — *same as above.*

K^*, A, B^*, C^* : the dimensionless forms of K, A, B, C above.

LINE 4a

With use of the Sayre-Albertson formula, request is made to enter

CHI^* : the dimensionless form, $\chi^* = \chi/Y_0$, of the Sayre-Albertson roughness parameter.

3.5 LINE 5 (Border Geometry)

The fifth record describes, in part, the border geometry. The three entries are

L : field length.

DBC — *defines the downstream boundary condition.*
= 1 : open-end border; stream reaching downstream end of field runs off into a drainage ditch.
= 2 : blocked-end border; stream reaching field end is ponded behind a dike.

S0MOD — *defines the way bottom configuration is described.*
= 1 : field is assumed plane; the bottom slope will be requested.
= 2 : field bottom can be irregular; pairs of values—distance *vs.* elevation—will be requested.

3.6 LINE(S) 6 (Bottom Configuration)

Description of field geometry continues with specification of bottom configuration, in accordance with S0MOD, above. With S0MOD = 1, enter—

S0AVG : the average slope of the border.

With S0MOD = 2, enter instead—

NZ0 : the number of value pairs, distance *vs.* elevation, that will be entered (minimum of 2, maximum of 21).

XZ0(1), Z0(1), XZ0(2), Z0(2)..., XZ0(NZ0), Z0(NZ0) : the NZ0 value pairs, distance *vs.* elevation, describing bottom configuration. As many records as necessary are used to enter the information. Any location upstream from XZ0(1) is assumed to lie on the same slope as between points 1 and 2; any location downstream from XZ0(NZ0) is assumed on the same slope as the last two points.

3.7 LINE 7 (Management Parameters)

The management variables are called for next. The choice of variables depends upon whether the input is dimensioned or dimensionless. With dimensional input (INPMOD = 1 or 2), the three entries are—

ZREQ : the required depth of infiltration; this figure does not affect the advance, recession, runoff, or infiltration, but only the assessment of the merit of the irrigation, deep percolation losses, etc. If this variable is of no interest[2], or it is desired to set the requirement, *ex post facto*, to the minimum or average-low-quarter depths of infiltration, z_{req} can be set here simply to zero. The merit of the irrigation is presented in the post-irrigation synopsis on the basis of all three possible values of z_{req}—a given value, inputted here, the minimum depth of infiltration, and the average-low-quarter depth of infiltration.

Q : volumetric inflow rate per unit width of border.[3]

TCO : time that inflow is cut off.

With dimensionless input (INPMOD = 3), and DMLMOD = 1, one enters instead, the two values—

ZREQ*, TCO* : the dimensionless counterparts of ZREQ, TCO.

If DMLMOD = 2, only ZREQ* is called for.

3.8 LINE 8 (Hypothetical Dimensioned Border)

These records are requested only in the event that all input is dimensionless (INPMOD = 3). To increase the significance to the user of entered dimensionless variables, the variables are translated by the program into corresponding dimensioned variables for a hypothetical border. This hypothetical border is specified by inflow, by roughness if RUFMOD = 1 or 2, by slope if DMLMOD = 1, and by cutoff time, if DMLMOD = 2. These parameters, plus the dimensionless variables entered as indicated above are sufficient to define all pertinent dimensioned variables for the hypothetical irrigation. These are computed and displayed in the header material at the top of the output. Default values are supplied for the required hypothetical values below, if zeroes are entered for the requested data.

---

[2]. . . say, in a nonjudgemental study , in which it is simply the factual result—distribution of infiltered water and volume of runoff—from a given combination of soil and crop properties, and design and management parameters, that is needed.

[3]The program as written assumes a constant value for inflow until cutoff. Other inflow hydrographs can be programmed into the subprogram QF.

INPMDH — *determines the dimensional system in which hypothetical values will be given.*

= 0 : enables default values for all variables in this group.

= 1 : metric system (see INPMOD = 1, sec. 3.3); this is the default value of INPMDH.

= 2 : English system (see INPMOD = 2, sec. 3.3).

S0AVG : average bottom slope; requested only if DMLMOD = 1; default value is 0.001.

QIN : unit inflow rate; default value is 6 L/sm.

TCO : cutoff time, requested only if DMLMOD = 2; default value is 120 min.

LINE 8a

If INPMDH is not zero, and RUFMOD is not 3, request is made to enter

RUF : hypothetical constant Chezy C, if RUFMOD = 1

or

RUF, AN : hypothetical Manning n coefficient and exponent if RUFMOD = 2.

3.9 LINE 9 (Solution-Mode Parameters)

Five integer solution parameters are entered next.

SOLMOD — *determines the type of solution, see section 3.16 for a discussion on the relative merits of each type.*

= 0 : enables the default value, SOLMOD = 2.

= 2 : enables the zero-inertia (equilibrium) model.

= 3 : enables the normal-depth kinematic-wave model.

= 5 : enables the hybrid: equilibrium model for advance, then when advance is completed and recession is underway, the kinematic-wave model is used.

LINMOD — *controls the linearity of solution at each time step.*

= 0 : enables the default value, 2.

= 1 : solution is locally linearized at each time step. This is the cheaper and less accurate option.

= 2 : fully nonlinear solution; nonlinear algebraic equations are solved iteratively at each time step. Larger time steps can be used. Nonlinear solution is recommended at least until the user becomes familiar with model behavior. The strongest argument for nonlinear solution pertains to the zero-inertia solution mode. With LINMOD = 2, the user is *assured* that the equations of mass and force balance are indeed satisfied in every cell at every time step. With the locally linearized solution (LINMOD = 1), one only knows that a single try has been made to correct the first guesses for values of depth, discharge, runoff, and advance.

In the kinematic-wave mode, use of LINMOD = 2 ensures treatment of the wave-trajectory segments as parabolas, rather than as straight lines.

DTMOD — *controls the variation of the time increment δt in the zero-inertia solution. In principle, δt can vary. In the kinematic-wave solution DTMOD has no pertinence, and its value is ignored. In the zero-inertia solution, whatever the value of DTMOD, certain variations in time-step size occur automatically in the calculations. For example, if convergence of a nonlinear, iterative solution is not achieved within a specified number of iterations, the time step is automatically cut in half. (Also, see ch. 6, pt. II.)*

= 0 : enables the default value, 2.

= 1 : δt = constant = DT(STD), entered in line 10.

= 2 : DT(STD) is divided into N(STD)[4] equal parts to form a smaller δt. The small increment is used for the first N(STD) time steps. During this period, the number of cells comprising the stream increases at each step, from one to N(STD). Subsequently, the number of cells remains constant, while the time step gradually increases until the full value DT(STD) is achieved. Thenceforth, except as noted above, this serves as the time step. This procedure is designed to minimize the influence of the assumed shape of the stream profile in the first time step.

[4]. . . entered in line 10.

ISUPZA — *Limitations in the numerical solution can lead to the exclusion of portions of the surface stream from computation.*[5] *In the event islands are formed, BRDRFLW chooses the longest length of stream on which to continue the calculations. The remainder of the stream is excluded. The excluded portions can be assumed*[6] *to infiltrate approximately as stagnant ponds, to preserve an overall mass balance.*

= 0 : the default value, causes such an adjustment of the recession curve as to effect at each excluded node the addition of the surface depth there to the local infiltrated depth. The user is cautioned that this procedure may lead to irregular aberrations in the recession curve, say if the excluded portions of the stream profile exhibit large-amplitude saw teeth.

= 1 : suppresses these additions to the infiltration profile. The consequent neglect of some of the stream volume leads to volume error, as will be noted in the program output.

ZADMOD — *controls the nature of the solution after stream flow has become essentially stagnant. With very low infiltration rates, and little or no runoff, very great irrigation times can result. Array dimensions in the program limit the number of time steps to 800.*

= 0 : enables the default value, 2.

= 1 : normal procedure is followed regardless of the values of flow velocities encountered.

= 2 : the program monitors the water surface in the stream. When this becomes essentially level, recession is assumed to occur as for a still pond (or a series of ponds, if the bottom is sufficiently irregular). The water surface in each pond is assumed to fall at a time-varying rate equal to the current distance-averaged infiltration rate in that pond.

---

[5]Islands can form in shallow flow over a border with an irregular (nonplane) bottom. Further, even in a plane border, an imperfect calculation can lead to saw-tooth stream profiles. Computation of a negative depth anywhere implies formation of an island. BRDRFLW is designed to compute only a single length of flowing stream; surges in tandem, separated by islands, are not allowed.

[6]. . .with varying degree of error.

3.10 LINE 10 (Numerical Solution Parameters)

Numerical parameters governing the behavior of the solution are entered next, four with the locally linearized solution, five with the fully nonlinear solution.

N(STD) : the number of increments (slices) into which the stream length is divided. Array dimensions limit this value to 80. Typical values are 10 to 20. A value of 5 gives relatively crude, inexpensive results. 0 (zero) enables the default value of 20.

RDX : the ratio of adjacent-cell lengths. A value less than unity leads to a gradual decrease in cell length, from the middle of the stream outwards towards the stream boundaries. Small cell lengths in regions of sharp profile curvature make the choice of ϕ weighting factors (see sec. 6.2) less critical than it would be otherwise. Thus, small cells can be concentrated in regions where they are most needed.

The value, unity, leads to uniform cell size. A zero value entered for RDX leads to the default value 0.8, if N(STD) is less than 20, and 0.9 if N(STD) is greater than 20.

Too small a value of RDX can lead to a cell length so small at the stream front, that during advance it is exceeded by the correction to the first-guess advance increment. When this happens, the nodes are automatically repositioned within the corrected stream length and the calculation of the time step is begun anew.

Furthermore, a small value of NSTD coupled with small RDX leads to large cell lengths in the interior of the flow. This can lead to inaccuracies if the profile is not smooth and gradually changing in the interior. For example, in the event of ponding behind a dike blocking the end of a relatively steep border, the juncture between the fast moving stream in the upstream portions and the nearly stagnant pool in the downstream portion can make a relatively sharp angle, rather than a smooth and gradual transition.

DT(STD) : standard time step upon which δt is based in accordance with DTMOD, entered in line 9.

TMAX : The computation will stop when computed irrigation time exceeds TMAX. Such an upper limit is introduced to allow a limited study. TMAX also prevents excessive computation in case a peculiar combination of input parameters is entered (for example, ponded border with nearly zero infiltration rate). To avoid exceeding array dimensions, which allow a maximum of 800 time steps, set TMAX ≤ 800 • DT(STD) (when time step is constant). A 0 (zero) enables the default value, approximately 800 • DT(STD).

If the fully nonlinear, iterative solution (LINMOD = 2) is used, the number of iterations must be limited. The user supplies this maximum number, namely—

JMAX : (requested only if LINMOD = 2); limits the number of iterations in selected nonlinear procedures; rarely are more than 10 required. 20 is a recommended value to allow the program more leeway in convergence problems. 0 (zero) enables the default value, JMAX = 20.

3.11 LINE 11 (Diagnostics)

Four integer entries and one real entry are required in this record, which controls the output of diagnostic information.

IDIAG — *determines the level of diagnostic information printed, to facilitate troubleshooting. A given level enables all lower levels as well.*

= 0 : almost no diagnostic information is printed—merely the input in dimensional and dimensionless form, advance and recession data, and ultimate distribution of infiltered water, efficiencies, and so forth. Evidences of irregularities in the solution, however, are also printed, to alert the user.

= 1 : a brief survey of the stream at each time step (or for each kinematic-wave trajectory) is printed. When the computation of the irrigation has concluded, also printed is a listing of the advance and recession trajectories as computed at each time step.

= 2 : Zero-inertia mode

. . . informs the user that the time step has been automatically cut in half, following computational difficulties.

Kinematic-wave mode

. . . enables print of runoff calculations for each kinematic-wave.

. . . in the hybrid mode, enables print of profile used as starting point for kinematic-wave analysis; also prints advance curve as computed by zero-inertia model.

= 3 : Zero-inertia mode

...enables printing of a stream profile at each time step.

Kinematic-wave mode

...enables printing of variation of stream variables along the kinematic-wave trajectory, for each trajectory calculated.

= 4 : Zero-inertia mode

...in the ponded case, shows computations leading to first guess for downstream pool elevation in the first step after stream has reached field end.

Kinematic-wave mode

...in the ponded case, shows computations leading to pool dimensions at start of standing-pool recession.

Higher levels of diagnostics allow the user to explore the internal workings of the program in ever greater detail. Level 5 refers both to the zero-inertia and kinematic-wave modes of solution, while values of IDIAG equal to 6, 7, or 8 refer only to the zero-inertia mode.

Kinematic-wave mode

= 5 : prints the results of each iteration.

Zero-inertia mode

= 5 : prints the results of each iteration in selected computations. In particular, at each iteration, it prints residuals from both continuity and force-equilibrium equations, as well as values of stream variables and predicted and resulting values of pressure, weight, and drag in the force equation. Because of its high degree of nonlinearity, the force equation usually exhibits the greatest lack of correspondence between predicted and actual variable values. This level of diagnostic produces one line of data for each cell.

Level 5 also enables printing of the new cell dimensions, after the computational stream length has been shortened.

= 6 : prints the six components of the continuity and force equations, the sensitivity of each to each of the stream variables, and the incremental changes to these variables, for each cell, in each iteration (six lines of data for each cell).

= 7 : prints the raw output from the double-sweep routine.

= 8 : displays the coefficients, solution vector, and right-hand sides of the set of linear equations solved at each iteration.

IDCH : the number I of the time step at which it is desired to change IDIAG; for example, a program may work well up to the 132nd time step, then some irregularities are noted. IDIAG may be held to, say, zero or one for the first 132 time steps, and IDCH set to 132 to cause a change in the value of IDIAG at the 132nd step; if no changes in IDIAG are desired, set IDCH = 0.

ID2 : the new value of IDIAG, from I = IDCH onward. If no changes in IDIAG are desired, set ID2 = 0.

IPRZA — *for certain evaluations of the ultimate profile of infiltrated depths, it is desirable to construct an equivalent profile with monotonic increasing depths. The program performs this reordering.*

= 1 : enables printing of equivalent profile.

= 0 : suppresses such printing.

FLGPVE — *value of overall relative volume error, which if exceeded will cause a special print message.*

= 0 : the default signal, which sets FLGPVE = 0.015.

.12 LINE 12 (Plotting Parameters)

This line (card) of data contains 5 integers, all related to plotting. If no plots are desired, or in the absence of facilities for automatic plotting, all 5 items should be set to zero. Descriptions of these variables follow:

IPLOTW : = 1 : advance, recession, and runoff data are plotted as functions of time; ultimate, post-irrigation infiltration depths are plotted *vs.* distance; = 0: no plotting of these variables.

IPLOTY : = N : with positive integer N, depth or water-surface-elevation profiles are plotted at intervals N; =0: no plots of depth or water surface.

IPLOTH : = 1 : water-surface elevation rather than depth is plotted; = 0: water surface not plotted.

IPLOTC : = 1 : trajectories of computed kinematic waves are plotted; = 0: no plots of these waves.

IPWAIT — *sometimes, in interactive use, a pause is needed before automatic plotting of each profile begins; this allows some adjustment in the plotter, for example, a change in pen color.*

= 1 : prompts the user to enter a zero, before plotting commences. Following any necessary adjustments, the user enters 0, and the profile is plotted. Prior to plotting the next profile, the prompt appears again.

= 0 : profiles are plotted one after the other, at intervals dictated only by the rate of data transmission.

3.13 LINE 13a (Plot Scales)

(Called for only if profile plotting is enabled)

FSX : full-scale value of abscissa; a zero enables a default value.

FSY : full-scale value of ordinate; a zero enables a default value.

LINE 13b

(called for only if trajectory plotting is enabled)

PLTXMX : full-scale value of the x-coordinate. A zero here enables the default value, border length. A negative entry allows retention of value from preceding run.

PLTTMX : full-scale value of the time coordinate. A zero enables the default value. A negative entry allows retention of value from preceding run.

3.14 LINE(S) 14 (Dummy Pause Variable)

MP : enter 0 repeatedly, before *every* profile plot if IPWAIT = 1

.15 Summary of Input

Record	Parameter	Function	Permissible values	Defaults
Line 1:		Class of computer run		
	TSTMOD	terminate, or continue with certain data stored, some new data entered	0,1,2,3,4,5	
Line 2:		Run identification	any 78 characters	blanks
Line 3:		Dimension control		
	INPMOD	indicates units of input data	1,2,3	—
	DMLMOD	controls form of dimensionless variables	0,1,2	0 → 1 or 2
Line 4:		Soil and crop properties		
With dimensioned input (INPMOD = 1,2):				
	RUFMOD	determines roughness formula	1,2,3	
	RUF	roughness coefficient	user entry	
	AN	exponent for variable Manning n	user entry	0
	INFMOD	determines infiltration formula	1	
	K A B C	terms in $z = K\tau^A + B\tau + C$	user entry	
or: With dimensionless input (INPMOD = 3):				
	RUFMOD	determines roughness formula	1,2,3	
	INFMOD	determines infiltration formula	1	
	K^* A B^* C^*	terms in $z^* = K^*\tau^{*A} + B^*\tau^* + C^*$		
Line 4a:		(called for only if INPMOD = 3, RUFMOD = 3)		
	CHI^*	dimensionless Sayre-Albertson χ	user entry	
Line 5:		Border geometry		
	L	field length	user entry	
	DBC	downstream boundary condition	1,2	
	S0MOD	plane, or irregular bottom	1,2	

Record	Parameter	Function	Permissible values	Defaults
Line 6:		Bottom configuration		
	For plane bottom (S0MOD = 1):			
	With dimensioned input (INPMOD = 1,2):			
	S0AVG	bottom slope	user entry	
or:	With dimensionless input (INPMOD = 3, DMLMOD = 2):			
	$S0^*$	dimensionless bottom slope	user entry	
or:	For irregular bottom (S0MOD = 2):			
	NZ0	number of value pairs (x_{z_0}, z_0) to be entered	2-21 (inclusive)	
XZ0(1), Z0(1), XZ0(2), Z0(2), . . ., XZ0(NZ0), Z0(NZ0)			user entry	
Line 7:		Management parameters		
	With dimensioned input (INPMOD = 1,2):			
	ZREQ	required depth of infiltration	user entry	
	Q	unit inflow rate	user entry	
	TCO	cutoff time	user entry	
or:	with dimensionless input (INPMOD = 3)			
	. . . and DMLMOD = 1:			
	$ZREQ^*$	dimensionless required depth	user entry	
	TCO^*	dimensionless cutoff time	user entry	
or:	. . . and DMLMOD = 2			
	$ZREQ^*$	dimensionless required depth	user entry	
Line 8:	Hypothetical dimensioned border (called for only if INPMOD = 3)			
	With DMLMOD = 1			
	INPMDH	controls units of hypothetical example	0,1,2	0 → 1
	S0AVG	hypothetical average bottom slope	≥ 0	0 → 0.001
	QIN	hypothetical unit inflow rate		0 → 6 L/sm
or:	With DMLMOD = 2			
	INPMDH	controls units of hypothetical values	0,1,2	0 → 1

Record	Parameter	Function	Permissible values	Defaults
	QIN	hypothetical unit inflow rate	user entry	0 → 6 L/sm
	TCO	hypothetical cutoff time	user entry	0 → 120 min
Line 8a:	(called for only if INPMDH ≠ 0, RUFMOD ≠ 3)			
	With RUFMOD = 1			
	RUF	hypothetical constant Chezy C	user entry	0 → 12.55
or:	With RUFMOD = 2			
	RUF	hypothetical Manning-n coefficient	user entry	0 → 0.05
	AN	hypothetical Manning-n exponent	user entry	0 → 0
Line 9:	Solution-mode parameters			
	SOLMOD	solution technique	0,2,3,5	0 → 2
	LINMOD	solution linearity	0,1,2	0 → 2
	DTMOD	controls time-step variation	0,1,2	0 → 2
	ISUPZA	controls option for treatment of excluded portions of stream	0,1	0
	ZADMOD	controls option for stagnant ponding	0,1,2	0 → 2
Line 10:	Numerical solution parameters			
	N(STD)	number of stream increments	0-80	0 → 20
	RDX	spatial rate of cell-size decrease	0-1	0 → 0.8 or 0.9
	DT(STD)	basic time step	user entry	
	TMAX	maximum irrigation time allowed	user entry	0 → 800 • DT(STD)
	JMAX	(requested only if LINMOD = 2) maximum number of iterations	user entry	0 → 20
Line 11:	Diagnostics			
	IDIAG	controls amount of diagnostic information	0-8	0 → summary only
	IDCH	time step at which IDIAG is changed	user entry	0 → no change

Record	Parameter	Function	Permissible values	Defaults
	IDIAG2	new level of diagnostics after change	0-8	0
	IPRZA	if $\neq 0$, prints equivalent monotonic increasing ultimate-infiltrated-depth distribution	0,1	0 → no print
	FLGPVE	flags overall relative volume error in excess of FLGPVE	≥ 0	0 → 0.015
Line 12:	Plotting parameters (total of 5)			
	IPLOTW	controls plot of advance, recession trajectories, runoff function, ultimate infiltrated-depth profile	0,1	0:no plot 1:plot
	IPLOTY	controls frequency of plotting depth or water-surface elevation	integer	0:no plot of depth profile
	IPLOTH	controls plot of water-surface elevation profile	0,1	0:no plot 1:plot
	IPLOTC	controls plotting of kinematic-wave trajectories	0,1	"
	IPWAIT	allows a pause before profile plot	0,1	0:no pause 1:pause to read a dummy variable
Line 13a:	Profile-plot scales			
	FSX	full-scale value of abscissa	user entry	0
	FSY	full-scale ordinate value	user entry	0
Line 13b:	Trajectory plot scales			
	PLTXMX	full-scale x-coordinate value	– 1, or user entry	0
	PLTTMX	full-scale t-coordinate value	– 1, or user entry	0
		(– 1 leads to retention of values stored in a previous run)		
Line 14:	Dummy pause variable (called for only if IPWAIT = 1)			
	MP	entered repeatedly, before *every* profile plot		0

For the interactive user, the program contains a bail-out feature that can be used if incorrect data have been inadvertently transmitted, and the mistake is noted before completion of data input. Entry of -1 for the first variable value (and appropriate numbers for the remaining entries in the line) in any of lines 3, 4, 4a, 5, 7, 8, 8a, 9, 10, 11, 12 returns the user to the beginning of data input, without loss of program control.

3.16 Relative Merits of the Submodels (With Reference to SOLMOD, Section 3.9)

The zero-inertia technique is the usual for computations of border-irrigation streamflow. Under conditions of very steep bottom slope (typically greater than about one-half pct.), poor numerical approximations in the solution algorithms (for example, determination of average value of drag on a cell of shallow water from drag-per-unit-length values at the upstream and downstream boundaries of the cell, or determining the weight of the most downstream cell from the depth at its upstream end, its length, and an assumed shape factor ϕ_y) lead to computed profiles exhibiting a saw-tooth character. If the amplitude of the oscillations is not too great a fraction of the depth, this does not constitute a serious problem, because the computation is fundamentally stable, and the irregularities do not tend to grow at each time step. However, if a computed depth drops anomalously below zero, somewhere in the interior of the stream, the computed recession will occur too quickly, and the relative volume error of the computation will become high (say, substantially greater than $+0.01$). While such problems can often be alleviated by the use of smaller time steps and cell lengths, the cost of computations then increases. An alternate approach to the problem, since it arises with high values of bottom slope, utilizes the concepts of kinematic-wave theory.

Kinematic-wave theory based on a normal-depth stage-discharge relationship is an inexpensive, robust technique and yields results very close to those of zero-inertia theory, provided the depth gradient is everywhere small compared with the bottom slope. This eliminates kinematic-wave theory completely in horizontal borders. But in sloping borders, during advance, the upstream depth is of the order of normal depth, so that by the time the stream has advanced to a distance, say, 20 times y_n/S_0, the depth gradient is less than 5 percent of the bottom slope. In practice, once $L^* = L\,S_0/y_n$ is greater than about 10, advance is accurately computed by kinematic wave theory.

Right after inflow cutoff, however, the upstream depth drops sharply while depths in the interior of the stream reduce more gradually. Thus, there is a substantial depth gradient in the stream for a while after cutoff. This leads to inaccurate computation of recession by kinematic-wave theory, even at substantial values of L^*.

If, however, application of kinematic-wave theory is delayed until recession as computed by zero-inertia theory begins, the depth gradient has generally had the opportunity to decrease in magnitude to the point where kinematic-wave theory becomes applicable. This is the basis of the hybrid model. In operation of this model, application of kinematic-wave theory is delayed until both recession starts and the advancing stream has reached field end. This simplifies the computation of the kinematic-wave trajectories, which otherwise would have to be computed simultaneously with the trajectory of the advancing front. The hybrid model exhibits good accuracy for L^* as low as unity.

As a comparison of typical execution costs, if the zero-inertia model costs $1.00 to run, the kinematic-wave model could be run for $0.16 and the hybrid for $0.36.

4. Printed Output

The first output to appear following standard printouts originating with the computer system will be the line. . ***BORDER-IRRIGATION-FLOW PROGRAM***. . This is followed (provided the subprogram RNINF or its counterpart in the given computer system—see ch. 2—is in operation) by certain real, on-line computing information: calendar date and time, elapsed central processor time, and computation units used and remaining available for use. This is followed by prompts for the input data and the data themselves, if these have been routed to the output printing unit (ch. 2).[7] See appendix for sample printout.

Formal output begins with the line:

********************* BORDER IRRIGATION FLOW *********************

Then, if the subprogram RNINF or its counterpart is in operation, the calendar date and time are printed.

This is followed by the run identification entered as data in LINE 2.

The header information that follows is divided into five groups. The first three describe the problem; the fourth lists the computed characteristic reference parameters which enter into the dimensionless problem parameters, and the last group describes the parameters of the numerical solution.

The problem parameters consist of (1) the hydraulic properties of crop and soil, that is, roughness and infiltration, (2) the border geometry, that is, bottom configuration, and (3) the management parameters, that is, required depth of application, inflow rate, and cutoff time.

The characteristic, reference-parameter information consists, first, of a statement (governed by DMLMOD—see sec. 3.3) defining the reference variables. Next, normal depth for the inflow, average slope, and roughness and Froude number at normal depth are printed (if the slope is greater than zero). These are followed by the characteristic depth, length, discharge, and time.

The parameters XOP, TOP, P refer to the system of nondimensionalization used in (5), and are not used in the program; they are included only for comparison with the earlier work.

The solution parameters define the solution technique, and also the numerical elements thereof; namely, the number of cells, size of time step, and maximum number of iterations allowed in a nonlinear solution.

---

[7]In the event DMLMOD = 2 and IDIAG $\geq$ 5, the progress of the iterations for the characteristic depth Y_0 will be printed next; this will not usually be the case.

In general, the first column of data appears in English units, the second is in metric units; dimensionless forms appear in the third column. In the event that data are entered in dimensionless form, corresponding dimensioned values computed for a hypothetical border irrigation are also printed for added significance.

The next series of output records to appear depends upon the values entered for IDIAG, IDCH, and ID2 (see sec. 3.11).

In the output for IDIAG = 1, the index J refers to the number of iterations, I is the number of time steps (t = 0 when I = 1), LB refers to the left (upstream) boundary of the stream, and RB refers to the right (downstream) boundary of the stream. FIYLN and FIYRN refer to the shape factors ϕ_y applied at the left and right boundaries, respectively, of the last computational cell. The variable TOOTH is a measure of the irregularity, or lack of smoothness, of the computed surface-water profile. It represents the largest value, in the absolute sense, of the variable

$$s = (y_{k+2} + y_k - 2\,y_{k+1}) - (y_{k+1} + y_{k-1} - 2\,y_k) \tag{4.1}$$

within the profile. KTOOTH is the value of k for which s is maximum. The variable PCVERR is the relative volume error incurred over the extant period of irrigation; it is the volume error divided by the volume of inflow. The volume error is the inflow volume, minus the sum of surface, infiltrated, and runoff volumes. All diagnostic data are given in dimensionless form. If needed, dimensional values can be obtained through multiplication by the appropriate characteristic parameter (Q0, Y0, X0, or T0) listed in the header section of the output.

At the conclusion of the irrigation-modeling computations, the results of post-irrigation analysis (see sec. 5.5) are printed—the ultimate infiltrated-depth profile, measures of the merit of the computation, and a synopsis of the irrigation results.

As a general note—appearance of the code number -7777 in place of a variable value signifies that the output variable in question has not been properly defined, for example, if the definition formula contains a divide by zero.

The final bit of output from the run is a statement of the number of computing units used for the run (provided subprogram RNINF or a substitute is attached). The program then returns to the beginning with a prompt for TSTMOD (see sec. 3.1).

5. Overview of Instruction Sequence in BRDRFLW: Major Branches

5.1 Input

Input data is requested and read. Data entered in the English system is converted to metric (SI). Characteristic variables are defined, and input data are converted, if necessary, to dimensionless form. Dimensioned input variables, computed characteristic variables, and dimensionless input variables are printed.

The program then branches on the choice of solution mode, SOLMOD.

5.2 SOLMOD = 2 Zero-Inertia (Equilibrium) Model

For each of a succession of time steps, the profile of depth and discharge in the surface stream is computed. Each profile except the first is based on the results of the preceding time step. The computations are based on satisfaction of mass conservation and equilibrium of forces in each of the N slices (cells) comprising, together, the total length of the surface stream. The profiles gradually lengthen until the stream front reaches the end of the field (under certain input conditions, advance will halt spontaneously, short of the field end). Stream length, more specifically the location of the stream front at each instant of time, is stored for subsequent construction of the advance curve. Once the end of the field is reached, either runoff or ponding takes place there; runoff rate is monitored and integrated over time to yield the volume of runoff. Some time after cut off of the inflowing stream, the computed profiles begin to shorten, with recession occurring from either the upstream or downstream end of the stream, or both. Locations of the stream boundaries are stored for construction, ultimately, of the recession curve. With IDIAG = 1, a line of output descriptive of the stream is printed at every computational time step. With IDIAG = 3, the computed profiles of dimensionless bottom elevation b, depth y, water surface elevation h, discharge q, and depth of infiltration z are also printed. When the stream length has been reduced to zero, the irrigation is over, and the program skips to Post-Irrigation Analysis (sec. 5.5). The zero-inertia computations are described in detail in chapter 6.

5.3 SOLMOD = 3 Kinematic-Wave Analysis

As described in chapter 7 (also Bassett and others (1) and the pioneering paper (7)), kinematic-wave theory applied to the partial differential equation of mass conservation (equation of continuity) and a given stage-discharge relation (say, normal-depth assumption everywhere in the stream) yields a simultaneous pair of ordinary differential equations. One describes a curve in the x-t plane—the so-called kinematic-wave trajectory—in terms of the depth at points on the curve, while the other describes the variation in depth along the curve. During advance, the kinematic-wave trajectories end abruptly when they reach the trajectory of the wave front, with an abrupt, step rise in depth and discharge from zero values on the field ahead of the wave to non-zero values at the wave front, in the wave. At the wave front, water velocity in the wave and speed of propagation of the wave front down the border are equal.

Kinematic-wave trajectories are constructed in the x-t plane separated by constant time intervals at the left boundary $x = 0$, from whence they emanate; depths (and discharge) are known there. Their intersections with the advance trajectory, simultaneously under construction, are recorded by the program, for they constitute the coordinates of the advance curve. When advance is complete, subsequent kinematic-wave trajectories either intersect the downstream field boundary $x = L$, or trail off to end spontaneously at points in the x-t plane at which the depth on the trajectories has fallen, gradually, to zero. On those trajectories reaching $x = L$, the discharge there is recorded, for it constitutes the runoff, when the stream is flowing off freely, and the rate of ponded-volume buildup when runoff is blocked by a dike. The end points of those trajectories that trail off with zero depths are also recorded, for they constitute the coordinates of the recession curve. At the instant of cutoff of the inflowing stream, however, the upstream depth drops instantaneously to zero, in accord with the normal-depth, stage-discharge relation presumed in force everywhere and for the entire duration of the irrigation. If trajectories were constructed only for the instant just before cutoff and the instant just after, all the detail of the recession curve and some of the runoff function would be lost. Consequently, the "instant" over which cutoff occurs is subdivided into N portions, and wave trajectories are computed for each value that the upstream depth takes on (at the end of each portion of the "instant") as it drops to zero. Since the instant is indeed infinitesimal in size, all these trajectories emanate from the single point in the x-t plane $(0, t_{co})$.

When all trajectories have been computed, either to their intersections with the advance curve or to the field end or to their trailing ends where $y = 0$, as described above, the streamflow calculation is over. If the stream is, in fact, ponded behind an end check, the infiltration of the still pool is computed next. Finally, the program skips to Post-Irrigation Analysis (sec. 5.5).

5.4 SOLMOD = 5 Hybrid: Zero-Inertia plus Kinematic Wave

The great disparity in recessions computed by kinematic-wave and zero-inertia theories, especially near the upper end of the field, as discussed in section 3.16, led to the development of a hybrid model. Zero-inertia theory is used until both advance is complete and recession has started.

Then, N kinematic-wave trajectories are constructed emanating from the node points on this time line and utilizing the existing values of depth there as starting values (in case the last depth profile computed by zero-inertia theory is highly irregular, it is smoothed somewhat prior to passage to kinematic-wave theory). Node points are utilized in order from left to right. As in the description of the pure kinematic-wave model (SOLMOD = 3), intersections of the kinematic-wave trajectories with field end yield runoff or ponded-volume buildup rates. The trailing ends of those trajectories that fail to reach field end comprise points on the recession curve. When all kinematic-wave trajectories have been computed, and any still-pool infiltration calculated, the program skips to Post-Irrigation Analysis (sec. 5.5).

5.5 Post-Irrigation Analysis

The advance and recession curves computed at each time step or for each kinematic-wave trajectory are printed, if IDIAG $\geq$ 1, and are used to determine the infiltration-opportunity time at n + 1 equally spaced locations in the border (n is defined in the sequel). This together with the given infiltration function yields the post-irrigation infiltration profile and the total volume infiltrated. Smooth profiles need only a small value of n for proper definition, while highly irregular profiles require a large value. Starting with n = 10, the volume is computed and compared with that stemming from a doubled value of n. If the two computed values of volume substantially agree, the larger value of n is accepted. Otherwise n is doubled again. In any case, n is not allowed to exceed 80; if it appears that a greater value is necessary, a warning statement is printed, but the results with n = 80 are accepted.

The ultimate infiltration profile and advance and recession trajectories are printed in dimensionless, metric, and English units. If IDIAG = 0, only 11 equally spaced values are printed; with higher levels of diagnostics, all n + 1 computed values are printed.

This is followed by some indicators of the goodness of the computation. The principal measures of such merit are the degree of satisfaction of overall mass balance and the smoothness of the computed surface-water profiles. Dimensionless values of inflow volume V_Q, infiltrated volume V_z, and runoff volume V_{ro} are printed as well as the relative volume error = $(V_Q - V_z - V_{ro})/V_Q$.

The surface-water profiles were scanned during the period of their construction and the largest value of TOOTH (eq. 4.1) encountered is stored as TOOTHM. At the same time, the largest relative value of saw tooth RTOOTH, defined as

$$\mathrm{RTOOTH} = \mathrm{TOOTH}/y_{avg} \tag{5.1}$$

with

$$y_{avg} = (y_{k+1} + 2\,y_k + y_{k-1})/4 \tag{5.2}$$

is stored as RTOOTM. The smoothness of the computation is described by the following printed variables

ITM : the time index at which the maximum value of TOOTH is encountered

KTM : the cell index pertaining to this maximum

TOOTH : the maximum

IRTM : the time index at which the maximum relative value RTOOTH is encountered

KRTM : the cell index pertaining to this maximum

RTOOTM : this relative maximum

The figures of computational merit are followed by a synopsis of the results of the irrigation. If IPRZA = 1 (line 11), this commences with the monotonic-increasing infiltration-depth distribution derived from the computed ultimate infiltration profile, together with the corresponding total infiltrated volume, all in dimensionless units.

The remaining factors presented in the synopsis are given, where applicable, in English, metric, and dimensionless units, as well as in percentage of the applied depth. The variables presented are:

t_{co} : time of cutoff

t_L : duration of advance

t_R : time recession starts at upstream end

t_{FR} : time recession starts at downstream end

t_E : time all surface water disappears

V_Q : applied (inflow) volume

V_z : ultimate computed infiltrated volume

V_{ro} : total computed runoff volume

y_{max_U} : maximum depth of surface stream encountered at upstream end of field

y_{max_D} : maximum depth of surface stream encountered at downstream end of field

y_{max} : maximum depth of surface stream encountered anywhere

$x_{y_{max}}$: location of y_{max}

z_{min} : minimum post-irrigation infiltration depth

z_{max} : maximum post-irrigation infiltration depth

z_{LQ} : average-low-quarter depth of infiltration

z_{req} : inputted required depth of infiltration

z_Q : average applied depth = V_Q/L

z_{avg} : average infiltrated depth = V_z/L

z_{ro} : average depth of runoff = V_{ro}/L

The next three parameters comprise average depth z_{dp} of deep-percolation volume V_{dp},

$$z_{dp} = \frac{V_{dp}}{L} \tag{5.3}$$

with deep percolation based on different definitions of required depth, as follows:

$z_{dp_{zreq}}$: deep percolation defined as infiltration in excess of given input value, z_{req}

$z_{dp_{zmin}}$: deep percolation defined as infiltration in excess of minimum infiltration depth

$z_{dp_{zLQ}}$: deep percolation defined as infiltration in excess of average-low-quarter infiltration depth

This is followed by three conceptions of average useful depth of infiltration z_u

$$z_u = \frac{V_u}{L} = \frac{V_z - V_{dp}}{L} \tag{5.4}$$

in which V_u is the useful infiltrated volume (comprised of infiltration depths less than or equal to the required depth), namely,

$z_{u_{zreq}}$: z_u with deep percolation based on inputted z_{req}

$z_{u_{zmin}}$: z_u with deep percolation based on minimum infiltration depth

$z_{u_{zLQ}}$: z_u with deep percolation based on average-low-quarter depth of infiltration

These are followed by the Christiansen uniformity coefficient,

$$UC_C = 1 - \frac{1}{n} \sum_{k=1}^{n} \left| \frac{\bar{z}_k}{z_{avg}} - 1 \right| \tag{5.5}$$

with

$$\bar{z}_k = \frac{z_k + z_{k+1}}{2} \tag{5.6}$$

the HSPA uniformity coefficient,

$$UC_H = 1 - 0.798 \sqrt{\frac{\left(\frac{\bar{z}_k}{z_{avg}}\right) - 1}{n - 1}} \tag{5.7}$$

the distribution uniformity,

$$DU = \frac{z_{min}}{z_{avg}} \tag{5.8}$$

the low-quarter distribution uniformity,

$$DU_{LQ} = \frac{z_{LQ}}{z_{avg}} \tag{5.9}$$

and the runoff fraction in percent,

$$RP = 100 \frac{V_{ro}}{V_Q} \tag{5.10}$$

The remaining parameters are also presented in terms of the three interpretations of required depth—the inputted value z_{req}, the minimum in the distribution z_{min}, and the average-low-quarter depth in the distribution z_{LQ}. These comprise the irrigation efficiency,

$$IE = 100 \frac{z_u}{z_Q} \tag{5.11}$$

the useful fraction of the infiltrated volume,

$$UZ = \frac{z_u}{z_{avg}} \tag{5.12}$$

the storage efficiency,

$$SE = \frac{z_u}{z_{req}} \tag{5.13}$$

in which z_{req} stands for each of the three interpretations in turn; the percent of total area adequately irrigated,

$$AAP = 100 \frac{L - x_{ui}}{L} \tag{5.14}$$

in which x_{ui} is the total length of border receiving less than the required depth of infiltration. This figure is obtained from the monotonic increasing equivalent distribution of infiltrated depths by noting the x-value therein at which the infiltrated depth equals the requirement (interpolating as necessary between tabulated values).

The last parameter of the group is the deficiency ratio, DR, the average deficit in the underirrigated portion of the field, expressed as a percentage of the required depth,

$$DR = 100 \left(1 - \frac{\forall_{ui}}{X_{ui} \cdot Z_{req}} \right) \tag{5.15}$$

Here, $\forall_{ui}$ is the volume infiltrated in the underirrigated portions of the border.

6. Equilibrium (Zero-Inertia) Model

The program operations outlined in section 5.2 are detailed in this chapter. The first nine sections provide the underlying theory; the rest sets forth the program logic constituting the mathematical model embodying that theory.

Part I: Theory

6.1 The Equilibrium Concept: Subdivision of the Stream Into Cells

In a useful approximation to reality, the forces on a slice of the surface stream due to the component of weight acting down slope, the drag of vegetation and soil surface acting upstream, and the pressure gradient resulting from nonuniform depth can be assumed in equilibrium. In reality, any imbalance among these forces would result in momentum changes in the surface stream. In most cases, however, water velocities are so low that the momentum of all portions of the stream is nearly zero, and changes therein truly negligible.

The flow in the surface stream is analyzed by subdividing its length into a number, N, of cells and applying the principles of conservation of mass and equilibrium of forces to each of the cells. If the shape of the depth and discharge profiles were known, subdivision would be unnecessary, and these physical principles could be used directly to find the flow depths and advance rate or any other property of the stream. The subdivisions (cells) are taken short enough, so that variation of depth and discharge over the length of a cell can be assumed known, usually linear. The physical principles are applied to these cells over time steps short enough for the shape of the time variation also to be known (usually, again, linear). The result is a set of mathematical relationships among the values of the pertinent variables at the juncture sections. Solution of the equations yields the size and shape of the stream at all times and, by the way, the trajectories of the stream boundaries in the x-t plane.

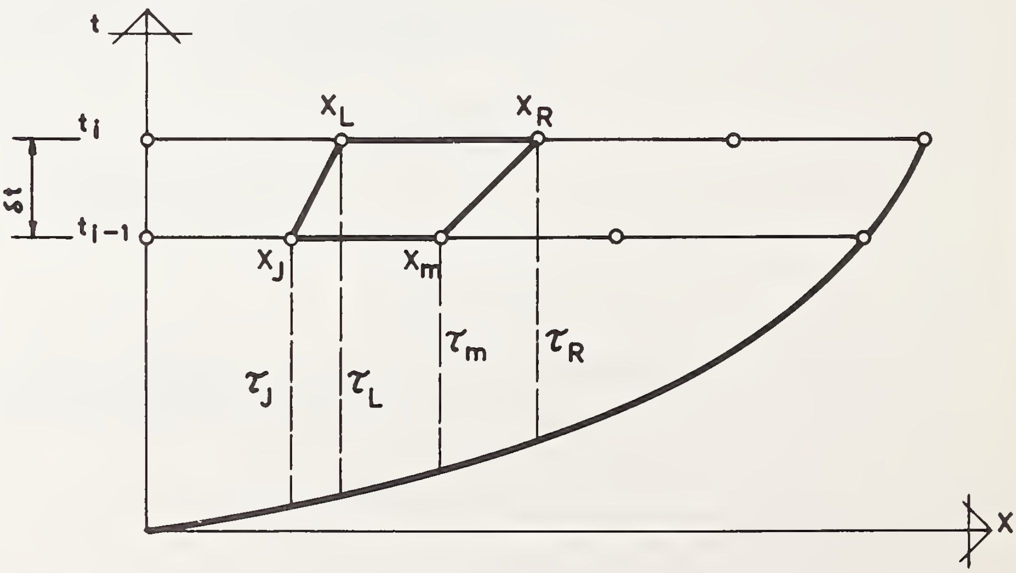

Figure 6.1.—Computational network in x-t plane.

Because the surface profiles are steep and relatively strongly curved when the stream is short, and vary more gradually as it lengthens, it is desirable to have small cells at small times and larger cells at large times. It is convenient to keep the number of cells in a profile constant, from time step to time step as pictured in figure 6.1. Consequently, the locations of the juncture sections are moved over the duration of a time step, as shown. In principle, a cell of the surface stream is bounded by the juncture cross sections U and D on its upstream and downstream sides, respectively, by the soil surface, and by the moving free surface, so that the cell is always filled with water.

In figures 6.1 and 6.2, the location of U at the beginning of the time step is x_J, at the end of the time step, x_L; the downstream face is moved from x_M to x_R.

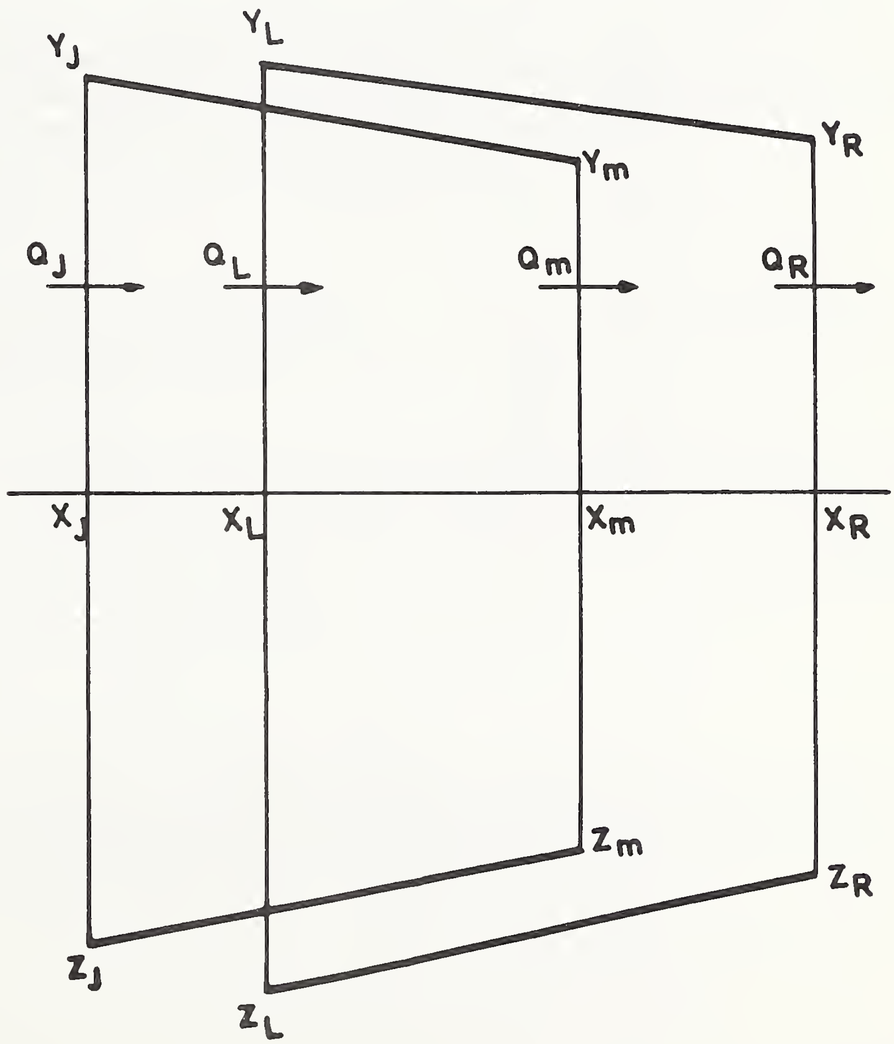

Figure 6.2.—Water cell with moving faces.

6.2 Mass Conservation Within Cells

It is convenient, when expressing mass conservation, to view the cell volume as consisting of both the water above ground and that which has infiltrated into the soil. The cross sections "U" and "D" are simply extended below the ground surface. Thus, the lower boundary of the cell lies below the soil surface by an amount equal to the depth of infiltration there; that is, by the volume infiltrated per unit area of infiltrating surface.

Water enters or leaves the cell through the juncture sections by virtue of the relative velocity between water and juncture section. The rate Q_{r_U} at which water actually enters the cell across the moving upstream face U (as opposed to the absolute value Q, say Q_J at the beginning of the time interval) is given by

$$Q_{r_U} = (V_U - w_U)\, A_U - w_U\, A_{z_U} \tag{6.1}$$

Here, V_U is the water velocity at the location occupied by U, as seen by a stationary observer, w_U is the velocity of movement of U, A_U is the cross sectional area of the surface stream at the location of U, and A_{z_U} is the volume infiltrated per unit length of channel at U. Inherent in equation 6.1 is the assumption that infiltrated water moves solely in the vertical direction.

Similarly, Q_{r_D} is the rate at which water flows out from the cell:

$$Q_{r_D} = (V_D - w_D)\, A_D - w_D\, A_{z_D} \tag{6.2}$$

with the symbols defined as before, but for the location of the downstream juncture section D.

Mathematical expression of mass conservation of an incompressible liquid in the given cell over a time increment is given by

$$\int_{t_{i-1}}^{t_i} Q_{r_U} dt - \int_{t_{i-1}}^{t_i} Q_{r_D} dt = \int_{x_L}^{x_R} A(x,t_i)dx + \int_{x_L}^{x_R} A_z(x,t_i)dx \tag{6.3}$$

$$\int_{x_J}^{x_M} A(x,t_{i-1})dx - \int_{x_J}^{x_M} A_z(x,t_{i-1})dx$$

The first and second integrals on the left represent the volumes of inflow and outflow, respectively; the first two integrals on the right are the volumes of surface and infiltrated water, respectively, in the cell at the end of the time increment; the last two represent these same volumes at the beginning of the time increment.

There remains to approximate these integrals by algebraic expressions involving depth and discharge at the node points J, M, L, R of figure 6.1. The x – integrals are expressed as follows

$$\int_{x_L}^{x_R} A(x,t_i)dx = \delta\forall_{y_{LR}} = (\phi_{y_L} A_L + \phi_{y_R} A_R)(x_R - x_L) \tag{6.4}$$

$$\int_{x_L}^{x_R} A_z(x,t_i)dx = \delta\forall_{z_{LR}} = (\phi_{z_L} A_{z_L} + \phi_{z_R} A_{z_R})(x_R - x_L) \tag{6.5}$$

$$\int_{x_J}^{x_M} A(x,t_{i-1})dx = \delta\forall_{JM} = (\phi_{y_J} A_J + \phi_{y_M} A_M)(x_M - x_J) \tag{6.6}$$

$$\int_{x_J}^{x_M} A_z(x,t_{i-1})dx = \delta\forall_{z_{JM}} = (\phi_{z_J} A_{z_J} + \phi_{z_M} A_{z_M})(x_M - x_J) \tag{6.7}$$

in which the ϕ are shape factors, which depend upon the assumed variation of the areas with distance. Usually, in most cells, a straight-line variation of the variables can be assumed, so that,

$$\phi_{y_L} = \phi_{z_L} = \phi_{y_J} = \phi_{z_J} = \phi_{y_R} = \phi_{z_R} = \phi_{y_M} = \phi_{z_M} = \frac{1}{2} \tag{6.8}$$

When a straight-line variation is considered inappropriate, such as in the leading cell of the stream during advance, these factors are changed accordingly (see sec. 6.5).

The time integrals in the left side of eq. 6.3 are similarly approximated through a weighting factor, θ, but first, an average face velocity w is expressed in terms of face location at the beginning and end of the time interval. With δt chosen small enough so that the velocity of stream advance (or recession) can be assumed essentially constant over the time interval, the upstream-face velocity can be approximated by

$$w_U = \frac{x_L - x_J}{\delta t} \tag{6.9}$$

with a similar expression for w_D. (One recalls that the stream length is divided into N cells, so that the cell faces move in conjunction with the advancing [and receding] front and rear stream boundaries.) Then one can write

$$\int_{t_{i-1}}^{t_i} Q_{r_U}dt = I = \theta[Q_L\,\delta t - (A_L + A_{z_L})(x_L - x_J)] + (1 - \theta) \tag{6.10}$$

$$[Q_J\,\delta t - (A_J + A_{z_J})(x_L - x_J)]$$

and

$$\int_{t_{i-1}}^{t_i} Q_{r_D} dt = O = \theta[Q_R\,\delta t - (A_R + A_{z_R})(x_R - x_M)] + (1 - \theta) \quad (6.11)$$

$$[Q_M\,\delta t - (A_M + A_{z_M})(x_R - x_M)].$$

The factor θ is taken slightly greater than the value one-half, corresponding to straight-line variation of the integrands over time. This is for reasons of computational stability as the equations are applied successively over a long sequence of time steps, rather than for more accurate representation of the average value of the integrands.

Equation 6.3 can thus be approximated by the algebraic equation

$$R_c = I - O - \delta\forall_{y_{LR}} - \delta\forall_{z_{LR}} + \delta\forall_{y_{JM}} + \delta\forall_{z_{JM}} = 0 \quad (6.12)$$

In which R_c is a *residual*, discussed subsequently.

In a border, with Q, A, and A_z given per unit width by q, y, and z, respectively, the face values of depth and discharge at the node points J, M, L, R are thus related by equation 6.12, with

$$I = [\theta q_L + (1 - \theta)q_J]\,\delta t - \delta x_{JL}\,[\theta(y_L - z_L) + (1 - \theta)(y_J + z_J)] \quad (6.13)$$

$$O = [\theta q_R + (1 - \theta)q_M]\,\delta t - \delta x_{MR}\,[\theta(y_R + z_R) + (1 - \theta)(y_M + z_M)] \quad (6.14)$$

$$\delta\forall_{y_{LR}} = (\phi_{y_L}\,y_L + \phi_{y_R}\,y_R)\,\delta x_{LR} \quad (6.15)$$

$$\delta\forall_{z_{LR}} = (\phi_{z_L}\,z_L + \phi_{z_R}\,z_R)\,\delta x_{LR} \quad (6.16)$$

$$\delta\forall_{y_{JM}} = (\phi_{y_J}\,y_J + \phi_{y_M}\,y_M)\,\delta x_{JM} \quad (6.17)$$

$$\delta\forall_{z_{JM}} = (\phi_{z_J}\,z_J + \phi_{z_M}\,z_M)\,\delta x_{JM} \quad (6.18)$$

in which

$$\delta x_{JL} = x_L - x_J \quad (6.19)$$

$$\delta x_{LR} = x_R - x_L \quad (6.20)$$

$$\delta x_{MR} = x_R - x_M \quad (6.21)$$

$$\delta x_{JM} = x_M - x_J \quad (6.22)$$

With nodal locations J, M, L, R, in the $x - t$ plane given and advance up to time t_{i-1} known, the infiltration times τ_J, τ_M, τ_L, τ_R are known. In a uniform border, z depends virtually on τ alone, (is virtually independent of flow depth), so that z_J, z_M, z_L, z_R are also known. Assuming that the flow has been solved up to time t_{i-1}, depth and discharge at J and M are also known. The equation 6.12 contains the four unknowns y_L, q_L, y_R, q_R. R_c represents a residual that results from incorrect values of these variables; correct values reduce R_c to zero. An additional equation relating the same four variables is provided by the statement of equilibrium amongst all forces acting on the cell at time t_i.

6.3 Equilibrium of Forces Acting on a Cell

Figure 6.3 shows, schematically, the longitudinal components of forces acting on the surface water contained in the cell at time t_i. The forces of hydrostatic pressure exerted by the water in the neighboring cells upstream and downstream from the given cell, divided by the unit weight of water, are given by P_L and P_R, respectively. W is the component of the weight acting in the downstream direction, and D is the drag of soil surface and vegetation acting upstream, each also divided by the unit weight of water. With P the resultant $P_L - P_R$ of the pressure forces, the statement of equilibrium is simply

$$P + W - D = 0 \tag{6.23}$$

In a unit width of border, the resultant of the pressure forces is given by

$$P = \frac{y_L^2 - y_R^2}{2} \tag{6.24}$$

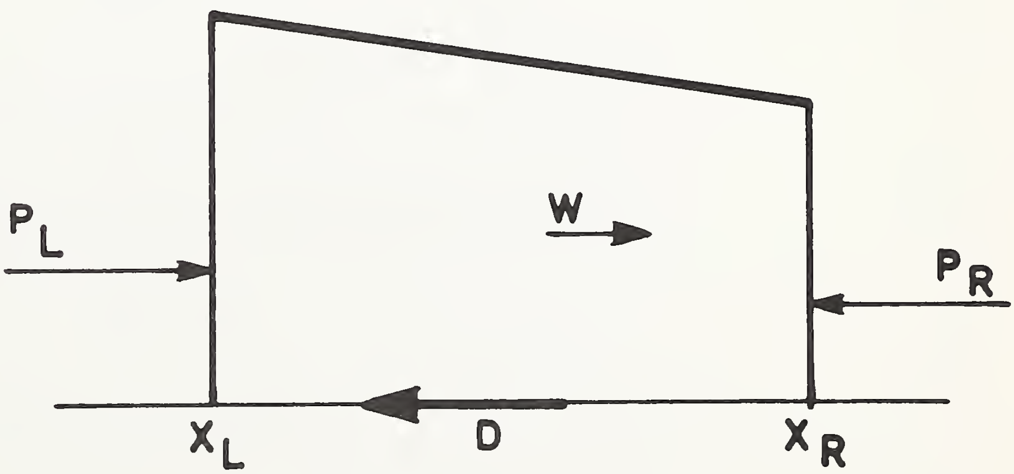

Figure 6.3.—Equilibrium of forces on suface-water cell.

The weight component W in a unit width of border is

$$W = (\phi_{y_L} y_L + \phi_{y_R} y_R)(b_L - b_R) \tag{6.25}$$

in which b_L and b_R are the bed elevations at x_L and x_R, respectively.

The drag d per unit length of stream (divided by the unit weight γ of water), called here the drag intensity, depends upon the velocity and depth of flow. The relationship is put in concrete terms through the use of a dimensionless drag coefficient C_D defined, in effect, by the following equation

$$\gamma d = w\, C_D\, \varrho \frac{V|V|}{2} \tag{6.26}$$

in which w is the wetted perimeter of the flow, unity in a unit width of border, and ϱ is the mass density of water. The absolute-value signs are put on the velocity V to insure that the drag is always in a direction opposite that of the flow velocity. The drag coefficient can be expressed in terms of the well known Chezy C_h as follows. First a definition is given to the so-called friction slope S_f through which C_h is usually defined. S_f is the drag per unit length divided by the weight of the stream per unit length, the latter being the product of unit weight and cross-sectional area. In symbols,

$$S_f = \frac{d}{A} \tag{6.27}$$

The Chezy C_h is usually defined in terms of the friction slope, by the expression

$$S_f = \frac{V|V|}{C_h^2\, R} \tag{6.28}$$

in which R is the hydraulic radius

$$R = \frac{A}{w} \tag{6.29}$$

It follows that C_D and the Chezy C_h are related as follows:

$$C_D = \frac{2g}{C_h^2} \tag{6.30}$$

in which g is the ratio of unit weight to mass density.

A variety of empirical expressions have been used to predict the value of C_h, which, in fact, depends upon the geometry of the roughness elements or vegetation, the cross-sectional dimensions of the stream, and the Reynolds number of the flow. The program choices are discussed in section 3.4. The most common formula in use in the United States expresses the Chezy C_h in terms of the Manning n

$$C_h = \frac{C_u}{n} R^{1/6} \tag{6.31}$$

in which C_u is a units coefficient (C_u = 1.0 $m^{1/2}/s$ in the metric system; $C_u \cong 1.486\ ft^{1/2}/sec$ in the English system).

In any event, the total drag on the water in the cell (divided by the unit weight) is

$$D = \int_{x_L}^{x_R} d\, dx = \tilde{d}\, \delta x_{LR} \tag{6.32}$$

in which $\tilde{d}$ is defined as the average drag intensity. It is not a trivial matter to express the average drag intensity in terms of its values at L and R. With

$$d = \frac{Q|Q|}{A\, C_h^2\, R} = \frac{V|V|w}{C_h^2} \tag{6.33}$$

small values of flow depth make the denominator very small, with the result, of possibly very large values of d and very nonuniform variation of d over the cell length. Two variants are proposed for estimating $\tilde{d}$ in a border, now computed per unit width. The first, for a cell in which velocity varies gradually, as in the lead cell during advance

$$d = \frac{\tilde{V}|\tilde{V}|}{C_h^2\ (\tilde{y})} \tag{6.34}$$

Here $\tilde{V}$ is the average velocity in the cell, approximated by

$$\tilde{V} = \phi_{V_L} V_L + \phi_{V_R} V_R \tag{6.35}$$

with most commonly

$$\phi_{V_L} = \phi_{V_R} = \frac{1}{2} \tag{6.36}$$

The function C_h is evaluated at an average value of depth

$$\tilde{y} = \phi_{D_{y_L}} y_L + \phi_{D_{y_R}} y_R \tag{6.37}$$

in which the ϕ_D are shape factors pertinent to the calculation of drag. In interior cells, with nearly straight-line variation of y over a cell length

$$\phi_{D_{y_L}} = \phi_{D_{y_R}} = \frac{1}{2} \tag{6.38}$$

The second variant, especially suited to cells in which discharge varies gradually over a cell length, such as in the downstream-most cell during run off, or, for that matter, in the interior of the flow, is

$$\tilde{d} = \frac{\tilde{q}|\tilde{q}|}{K_D(\tilde{y})} \tag{6.39}$$

with

$$\tilde{q} = \phi_{q_L} q_L + \phi_{q_R} q_R \tag{6.40}$$

Here, commonly,

$$\phi_{q_L} = \phi_{q_R} = \frac{1}{2} \tag{6.41}$$

The term $K_D(\tilde{y})$ represents the function of y, $\tilde{y}^2\tilde{C}_h^2$, evaluated at an average value of depth, as given by equation 6.37.

The companion equation to (12) expressing equilibrium of forces is then

$$R_m = P + W - D = 0 \tag{6.42}$$

Like R_c, R_m is a function of the unknown variable values q_L, y_L, q_R, y_R. It is evident that between them, the two equations, 12 and 42, contain four variables and are in themselves insufficient for solution. Application of these equations to N cells yields 2N equations and 2N + 2 unknowns. Additional information for the boundary cells at front and rear closes the system by supplying two more values of unknowns.

6.4 Boundary Conditions

At the upstream boundary of the stream, the discharge is presumed known for all time of interest. The inflow discharge hydrograph constitutes the upstream boundary condition. Most commonly, the inflow rate is constant until cut off and is zero thenceforth.

The downstream boundary condition depends upon the progress of the irrigation and upon the assumed nature of the downstream end of the border or furrow; that is, whether it is free flowing or diked by a check.

During advance, the depth and discharge at the wave front are both zero. However the x-position of the wave front is not known. Yet the preceding set of algebraic equations is simpler to solve if the locations x_L, x_R are known *a priori* for all cells. So, only x_R of the most downstream cell is carried in the equations as an unknown. The interior values are set by estimating the increment of advance occurring in the given time step (by extrapolating the advance in the previous time step) and dividing the estimated stream length into cells. If the cell division is not too fine at the front, and the time steps are not so great as to cause significant error between estimated and ultimately determined stream advance, the potential problem of negative cell lengths does not arise. If, indeed, a negative cell length is generated, the stream is redivided into new cells.

The boundaries of the stream in recession are set as follows: At a stream boundary at which recession is imminent, the discharge is zero. Recession from the boundary location during a given time step is signalled by the computation of a negative depth there. When this happens, the computational stream boundary is moved into the interior of the stream until a location is found at which the depth exceeds some minimum small value y_{rec} (perhaps 1 pct. of the normal depth for the initial inflowing discharge). This constitutes the new location x_{LB} (or x_{RB}, if the recession occurs from the downstream end) of the computational stream boundary. The discharge there is set to zero, with the implication that all water outward from that point is stagnant and simply seeps vertically into the soil.

Prior to any recession from the downstream, or front, end of the surface stream, one of three conditions prevails there. Either the stream is advancing, as discussed previously, or it is running off the field into a drainage ditch or it is ponded behind a dike. Other conditions are possible, for example, flow over a dike of insufficient height to contain the stream, but these have not been programmed. With a dike in place at field end, the discharge there is simply zero.

In the event of free overfall into a drainage ditch, the depth of flow is, perhaps startlingly, zero. This conclusion, supported in Strelkoff and Katopodes (9), stems directly from the assumption of zero inertia in the flow. In the usual hydraulic treatment of subcritical flow approaching a free over-

fall, it is noted that the water accelerates in the vicinity of the brink, until the depth drops to critical, at which section the specific energy of the flow is a minimum, and the velocity head is a given fraction of the flow depth, the fraction depending on the cross section (one-half, with a rectangular section). In section 6.8, the assumption of zero inertia without zero weight is tantamount to assuming a ratio of mass density to unit weight of zero, or an infinite value of g. Thus, all velocity heads are zero, relative to flow depths; all flows are necessarily infinitely subcritical. The ratio of critical depth, to normal depth, or any other depth in the flow is thus zero.

The result that velocity at the brink is infinite is dealt with from several points of view by Strelkoff and Katopodes (9). From the theoretical standpoint, this result, obviously in gross error, stems from strict adherence to the equilibrium assumption, even in the vicinity of the brink, where, in fact, the forces are not in equilibrium. To a lesser degree, the same problem arises with the use of the Saint-Venant equations or the equation of gradually varied steady flow near a brink. The latter formula,

$$\frac{dy}{dx} = \frac{S_0 - S_f}{1 - F^2} \tag{6.43}$$

in which F is the local Froude number of the flow

$$F = \frac{V}{\sqrt{g\, A/B}} \tag{6.44}$$

with B the top width, yields the result $\frac{dy}{dx} = \infty$ at the critical section, where $F = 1$. Now observations of the phenomena in real life show that $\frac{dy}{dx}$ is not infinite at all, but rather small, well less than unity. The grossly incorrect results of equation 6.43 stem from the strict adherence to the assumption of hydrostatic pressure distribution, even when it does not apply, such as close to the brink where the streamlines are distinctly curved.

If it were necessary to model the flow in the vicinity of the brink accurately, a more accurate theory would have to be invoked. In general practice, it has become customary to ignore the errors incurred by use of equation 6.43 or its counterpart in unsteady flow, the Saint-Venant equation, because in comparison to the long reaches of open channel usually considered, the length of channel over which significant errors arise is actually very small. Similarly, as shown by numerical comparisons in the foregoing reference, provided the Froude number everywhere in the flow is in fact small, say, less than about 0.3, the longitudinal extent of the region with abnormally high velocity values—computed in the assumption of force equilibrium—is also very small, relative to the overall stream length. Thus, from a practical standpoint, one can simply ignore the very high velocity values that are computed for this very small

fraction of the stream length. From the standpoint of the present computational technique, it is not even velocity, but discharge, which constitutes the primary variable, and the variation of discharge with distance is well behaved, even near the brink. Only the computation of average drag intensity (eq. 6.32) in the cell at the brink requires special care. Clearly, right at the brink, drag intensity is infinitely great (eq. 6.33) and is not at all representative of conditions within the cell; consequently, equation 6.39 is used.

A similar situation arises in the leading cell during advance. While the velocity variation is well behaved near the front, the zero depth there again results in an infinite drag intensity again not representative of average conditions in the cell, and equation 6.34 is appropriate.

The matter of expressing cell averages in terms of end-point values is, in general, not trivial. The question is dealt with in some detail in the next section.

6.5 Cell-Profile Shape Factors: The ϕ Weighting Factors

The weighting factors are the key to a precise solution of the governing equations for the water in the cells, and hence of the entire stream profile. The algebraic cell equations are precise equivalents of the integral formulas (which are exactly correct) if the weighting factors are chosen just right. Usually, the smaller the cell length, the less troublesome is selection of appropriate values of the weighting factors. Economical calculation, however, suggests use of large cells, and consequently less obvious values of the ϕ. Poorly chosen ϕ can result in the development of saw-tooth profiles; this can be troublesome, because of the potential for calculating negative depths in the interior of the stream. This would not represent a true instability of calculations, because small errors are not amplified without bound as the computations proceed over the succession of time steps. The end result, however, can be the same: an aborted computation.

As suggested in sections 6.2 and 6.3, the variation of depth and discharge in the interior of the stream is sufficiently gradual and close to linear that the trapezoidal rule of numerical integration can be readily applied even when the number of cells is small and the length of each, consequently, large. Then, the ϕ weighting factors all have the value one-half as in equations 6.8, 6.36, 6.38, and 6.41. Near the boundaries of the surface stream, however, variables can change rapidly and curvilinearly. This is clearly true near the front of an advancing stream or near a free overfall. It is true, also, at an end check for a short period after the stream arrives. Finally, conditions near the trailing edge of a stream in recession on a steep slope may also require special treatment.

The tip cell is investigated first. In the advancing tip, velocity variation is smooth and gradual, while discharge is not. In the free overfall, discharge variation is smooth and gradual, while velocity is not. In both, the variation in depth is highly curvilinear. The depth variation in the tip cell can be approxi-

mated by assuming it identical to that of a corresponding steady flow. In the advancing stream, the corresponding steady flow is obtained by postulating that the stream advances without changing shape, that is, that all cross sections move at the same average velocity (that is, averaged over the cross-sectional area) V_A, equal to the velocity of advance. Indeed, the average fluid velocity in the surface stream changes but slowly with both time and distance. The details of flow at the very front of the wave are obscure, but it is a reasonable postulate that the streamlines intersect the wave front, as shown in figure 6.4. There is a velocity gradient in the surface stream, with velocity increasing with distance from the bed, because of bed resistance and infiltration. This concept agrees with the rolling advance of the front evident in the field, as opposed to bulk sliding, which might at first seem to be the consequence of the flow pattern postulated in figure 6.4. In any event, equation 6.33, with the Chezy C_h defined as in the bulk of the wave[8], is assumed to apply all the way to the stream front. The depth profile near the front is then obtained as follows.

Equation 6.23 written for a very thin, unit-width slice of stream moving downstream at the velocity V_A is given by

$$\frac{y_L^2 - y_R^2}{2} + \frac{y_L + y_R}{2} S_0 \,\delta x = \frac{V_A^2}{C_h^2} \delta x \tag{6.45}$$

in which C_h is the Chezy C_h for an average depth in the slice. As the slice thickness is decreased, the average value of depth therein approaches the depth y at midsection. Division of equation 6.45 by the volume of the slice and passage to the limit as $\delta x \to 0$ yields the differential equation

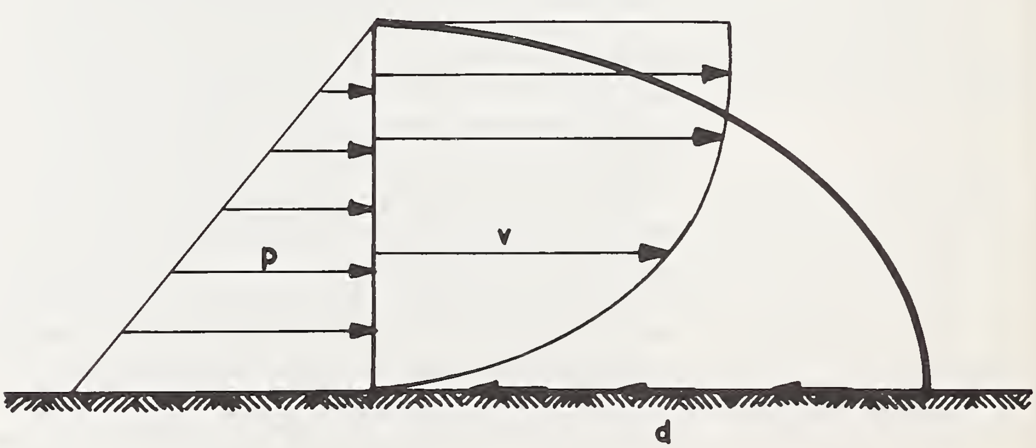

Figure 6.4. — Assumed flow pattern in stream front.

---

[8]. . . with the exception of those formulas like the Sayre-Albertson (6), which fail below a certain positive value of y. . .

$$\frac{dy}{dx} = S_0 - \frac{V_A^2}{C_h^2\, y} \tag{6.46}$$

The behavior y(x) is readily obtained from equation 6.46 by numerical integration. To start the process, it is noted that for $x \rightarrow x_A$, the right side increases without bound as $y \rightarrow 0$, while S_0 remains fixed. Thus, very close to the stream front, S_0 is negligible, and the differential equation becomes separable with a solution that depends upon the assumed variation of C_h with y. If the Manning formula (eq. 6.31) is used, the result is

$$y = \left(\frac{V_A^2\, n^2}{C_u^2}(x_A - x)\right)^{3/7} \tag{6.47}$$

In a horizontal border this expression is valid arbitrarily far back from the front as long as V is reasonably close to V_A. In a sloping border, equation 6.47 applies only insofar as $\frac{V_A^2\, n^2}{C_u^2\, y} \gg S_0$; in principle, it merely supplies the first step in a numerical, stepwise integration of equation 6.46, say by the modified Euler method.

The shape factor r_β (ϕ_{y_L} for the tip cell) can be estimated by integrating y(x) over the length of the cell, then dividing by cell length to get the average depth $\tilde{y}_{LR}$. The ratio of average depth to depth y_N at the left boundary of the tip cell is the shape factor, that is,

$$r_\beta = \frac{\tilde{y}_{LR}}{y_N} \tag{6.48}$$

since y_{N+1} is zero. Evidently, the shape factor will vary with the length of the tip cell. For a very short cell, in view of the 3/7 power of the variation, the shape factor is simply,

$$r_\beta = \frac{7}{10} \tag{6.49}$$

With increasing length, this factor increases. A unique, generalized solution for the depth profile near the front of a stream advancing with constant velocity on a sloping, impervious bed can be developed. The variation of y^* ($= y/y_n$) is found as a function of $x_A^* - x^*$ ($= [x_A - x]S_0/y_n$), in which y_n is the normal depth for the given velocity of advance and given border slope and roughness. (See sec. 6.8 for further discussion of dimensionless parameters.) Consequently the shape factor will also be a unique function of dimensionless tip-cell length δx_N^*. This relationship was computed and tabulated, and an empirical expression was devised to approximate the relation, namely.

$$r_\beta = 1.0 - 0.275\, e^{-0.3\, \delta x_N^*} \tag{6.50}$$

When needed, as in the passage from the first time step of solution to subsequent time steps (sec. 6.10), depth values can be obtained at points in the interior of the end cell by postulating a power-law variation of depth with distance from the brink; the power β used is that necessary to yield the given shape factor,

$$\beta = \frac{1}{r_\beta} - 1 \tag{6.51}$$

with, then,

$$\frac{y}{y_N} = \left(\frac{x_A - x}{x_A - x_N}\right)^\beta \tag{6.52}$$

Here, x_N is the location of the left end of the tip cell.

A similar procedure is invoked to estimate the shape factor in the tip cell under run-off conditions. Only, now, the downstream boundary of the cell is fixed, and the discharge (over an impenetrable surface), rather than the velocity, is constant, at the run-off rate q_{ro}. The appropriate differential equation, replacing equation 6.46, is

$$\frac{dy}{dx} = S_0 - \frac{q_{ro}^2}{C_h^2\, y^3} \tag{6.53}$$

The resulting power-law solution at values of $L - x$ so small that S_0 is negligible is

$$y = \left(\frac{q_{ro}^2\, n^2}{C_u^2}\,(L - x)\right)^{3/13} \tag{6.54}$$

in which L is the field length (x-coordinate of field end); the Manning formula for resistance was again employed, to obtain this result. Equation 6.54, thus, replaces equation 6.47. The shape factor, r_α for the run-off case,

$$r_\alpha = \frac{\tilde{y}_{LR}}{y_N} \tag{6.55}$$

is readily found for a very short cell length, namely

$$r_\alpha = \frac{13}{16} \tag{6.56}$$

Numerical integration of equation 6.54, integration of the results to yield $\tilde{y}_{LR}$ and hence r_α as a function of $L^* - x^{*}$[9], and fitting an empirical expression to the last yields the approximate relation for longer cells, namely

$$r_\alpha = 1 - 0.12\, e^{-0.6\, \delta x_N^*} \tag{6.57}$$

in place of equation 6.50. Again, the exponent in an approximately fitting power-law relation for depth,

$$\alpha = \frac{1}{r_\alpha} - 1 \tag{6.58}$$

Profiles in the vicinity of the blocked end of a border can also exhibit highly irregular behavior, as illustrated by the depth profile of figure 6.5. It is possible to make an estimate of the location of the reentrant corner by computing the volume that would have run off were the dike absent and then assuming that this volume forms a stagnant pool at the downstream end. This procedure provides an approximate profile shape, and so can lead to weighting factors. The complexity of the approach suggests, however, simply to increase the number of cells until the error from this source is reduced to tolerable levels. Indeed, the program BRDRFLW does this.

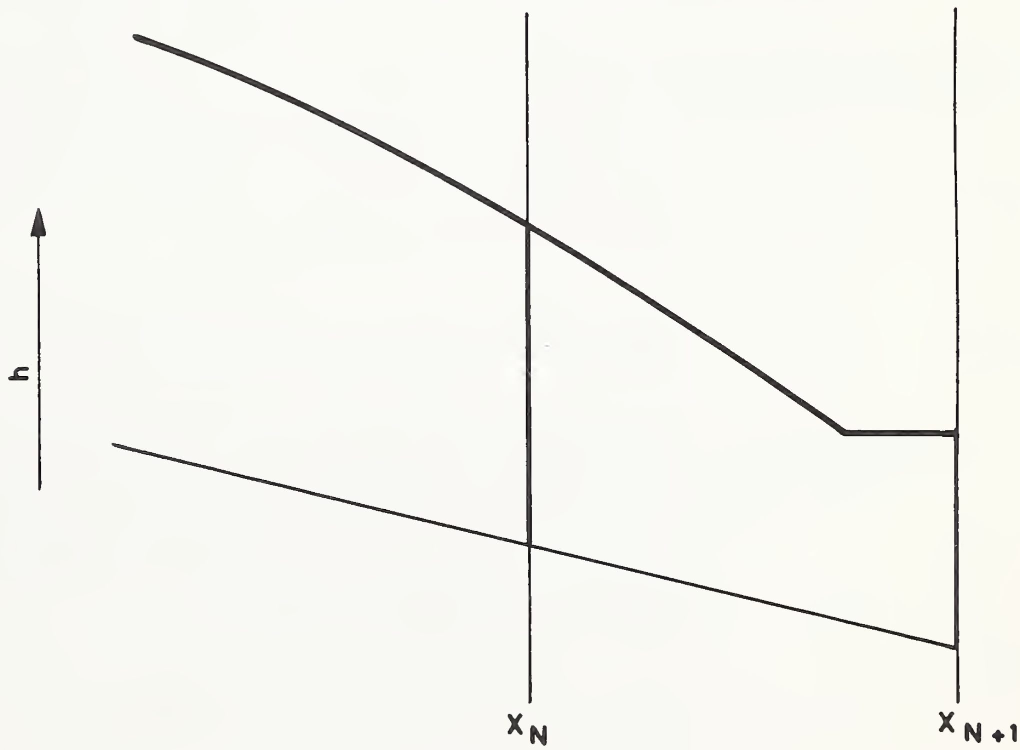

Figure 6.5.—Interaction of live stream with pond.

[9] $L^* = LS_0/y_n$.

During advance, a shape factor different from one-half is also needed for the z-profile in the lead cell, say at time t_i. The shape is determined by assuming that over a short time period prior to t_i, the stream had advanced at constant velocity V_A. At the instant t_i then, any point x behind the stream-front location x_A would have been wetted for a period of time

$$\tau = \frac{x_A - x}{V_A} \tag{6.59}$$

If the Kostiakov infiltration formula, $z = k\tau^a$, is assumed,

$$z(x,t_i) = k\left(\frac{x_A(t_i) - x}{V_A(t_i)}\right)^a \tag{6.60}$$

It follows that the z-profile in the lead cell is given by

$$\frac{z}{z_N} = \left(\frac{x_A - x}{\delta x_N}\right)^a \tag{6.61}$$

and the shape factor r_a for the lead cell is

$$\phi_{z_L} = r_a = \frac{1}{1 + a} \tag{6.62}$$

In the lead cell during advance, $z_{N+1} = 0$. Formula 6.62 is valid for long cells, as long as the advance velocity has not changed very much over the period of time necessary to advance a distance equal to the length of the cell. Of course, an infiltration equation differing from the monomial power law above can lead to a different shape factor.

Because the curvature of the infiltrated-depth profile near its downstream end persists for some distance upstream from an advancing front, and also for some time in the vicinity of field end after advance has been completed, a formula for the shape factors ϕ_{z_L} and ϕ_{z_R} was devised for general use. This formula, just for appropriate shape factors, is based on the assumption that the shape of the profile in any cell can be derived from a monomial power law in distance back from a fictitious (or real) advancing front. The location of this front is determined by given depths of infiltration z_L and z_R on the left and right sides of the cell, respectively, the cell length, $\delta x = x_R - x_L$, and the assumption that the power is a. With

$$\sigma = \left(\frac{z_R}{z_L}\right)^{1/a} \tag{6.63}$$

it follows that the distance ξ_L between x_L and the (real or fictitious) profile front where the infiltration depth drops to zero is given by

$$\xi_L = \frac{\delta x}{1 - \sigma} \tag{6.64}$$

Then with $\delta \forall_z$ the infiltrated volume for the cell, given by both the equations

$$\delta \forall_z = \frac{z_L \, \xi_L}{1 + a} - \frac{z_R \, \xi_R}{1 + a} = (\phi_{z_L} z_L + \phi_{z_R} z_R) \, \delta x \tag{6.65}$$

(in which $\xi_R = \xi_L - \delta x$) and the definition

$$\phi_{z_R} = 1 - \phi_{z_L} \tag{6.66}$$

it follows that

$$\phi_{z_L} = \frac{1 + \dfrac{a(1 - \sigma)}{1 - \sigma^{-a}}}{(1 + a)(1 - \sigma)} \tag{6.67}$$

These general formulas show that ϕ_{z_L} and ϕ_{z_R} both approach 1/2 as $z_R \rightarrow z_L$, and that ϕ_{z_L} approaches $1/(1 + a)$ (eq. 6.62), as $z_R \rightarrow 0$.

6.6 Solution of the Set of Nonlinear Algebraic Equations by the Newton-Raphson Technique: Successive and Single Linear Approximation

As indicated in section 6.3, application of mass conservation and force equilibrium to the N cells making up the total stream length yields 2N equations of the type 6.12 and 6.42; namely,

$$R_{c_K} = I_k - O_k - \delta \forall_{y_k} - \delta \forall_{z_k} + \delta \forall_{y_{known_k}} + \delta \forall_{z_{known_k}} = 0 \tag{6.68}$$

and

$$R_{m_k} = P_k + W_k - D_k = 0 \tag{6.69}$$

with $k = 1, 2, 3, \ldots, N$ identifying the cell. These contain the $2N + 2$ variables, y_k, q_k, $k = 1, 2, \ldots, N + 1$. The values y_{known}, q_{known} are presumed known and represent the solution at the previous time step. From the previous discussion on boundary conditions, q_1 is known,

$$\left.\begin{array}{lr} [\, q_1 = q_{in} & t \leq t_{co} \,] \\ & \\ \text{for} & \\ & \\ [\, q_1 = 0 & t > t_{co} \,] \end{array}\right\} \tag{6.70}$$

In the simplest case, q_1 is the constant inflow q_{in} until cut off. During advance,

$$q_{N+1} = y_{N+1} = 0 \tag{6.71}$$

but x_{A_i}, and hence δx_N is not known. The remaining cell lengths δx_k, $k = 1, 2, \ldots, N - 1$, are known from extrapolation of the advance over the previous time step. With uniform division of stream length into N parts (except for the tip cell), and uniform δt,

$$\delta x_k = \frac{x_{z_{i-1}} + (x_{A_{i-1}} - x_{A_{i-2}}) - x_{LB}}{N} \qquad k = 1, 2, \ldots, N - 1 \tag{6.72}$$

the upstream computational boundary $x_{LB} = 0$, provided recession has not begun.

During run off,

$$y_{N+1} = 0 \tag{6.73}$$

and q_{N+1} is unknown, while with ponding behind a dike,

$$q_{N+1} = 0 \tag{6.74}$$

and y_{N+1} is unknown.

The nonlinear nature of the force equation makes it necessary to solve the set of equations and boundary conditions iteratively, unless a locally linearized solution is considered adequate. In principle, as long as the change in value of a variable over a time step is small, relative to the value of the variable itself, the locally linearized solution is accurate and avoids the repeated calculations of an iterative solution. Thus, using a small enough value of time step will usually be adequate to insure the accuracy of the linearized solution. On the other hand, in those regions, such as near the trailing edge in recession where y and q are both very small, there is some question as to how small the changes thereof have to be to insure accuracy of the linear solution. Further, while the nonlinear solution requires iterative procedures, the time steps can be larger than in the linearized scheme. Until the user has gained familiarity with the behavior of the mathematical model, it is recommended that the iterative, nonlinear solution be used. For only then is the user assured that the equations of mass conservation and force equilibrium have been satisfied. In any event, the linear solution comprises, simply, the first step of the iterative solution.

It is desired, then, to find those values of y_k, q_k as satisfy the inequalities

$$\left.\begin{aligned} |R_{c_k}| &\le R_{c_{max}} \\ |R_{m_k}| &\le R_{m_{max}} \end{aligned}\right\} \quad k = 1, 2, \ldots, N \tag{6.75}$$

in which $R_{c_{max}}$ and $R_{m_{max}}$ are small quantities on the order of 0.000001 times the size of the individual members of the right-hand sides of equations 6.68 and 6.69. Substitution of first guesses, say y_{known_k}, q_{known_k}, for the unknown values yields residuals R_{c_k}, R_{m_k} generally greater than the maximum. So, the guesses must be adjusted by an amount as will reduce the residual. With j the iteration index, the quantities

$$\left.\begin{aligned} \xi_k &= \delta y_k = y_k^{j+1} - y_k^j \\ \eta &= \delta q_k = q_k^{j+1} - q_k^j \end{aligned}\right\} \tag{6.76}$$

are sought, in which the δ symbol refers to the change from one iteration to the next on a given time line. They are found by solution of the simultaneous set of linear equations

$$\left.\begin{aligned} \delta R_{c_k} &= \frac{\partial R_{c_k}}{\partial y_k}\xi_k + \frac{\partial R_{c_k}}{\partial y_{k+1}}\xi_{k+1} + \frac{\partial R_{c_k}}{\partial q_k}\eta_k + \frac{\partial R_{c_k}}{\partial q_{k+1}}\eta_{k+1} = -R_{c_k} \\ \delta R_{m_k} &= \frac{\partial R_{m_k}}{\partial y_k}\xi_k + \frac{\partial R_{m_k}}{\partial y_{k+1}}\xi_{k+1} + \frac{\partial R_{m_k}}{\partial q_k}\eta_k + \frac{\partial R_{m_k}}{\partial q_{k+1}}\eta_{k+1} = -R_{m_k} \end{aligned}\right\} \tag{6.77}$$

The partial derivatives are determined for the j^{-th} approximation to y_k and q_k by differentiating equations 6.68 and 6.69 and substituting the j^{-th} values of y_k and q_k. The set of equations 6.77 is linear and is solved by the methods of the next section. For $k = N$, during advance, since y_{N+1} and q_{N+1} are both known, η_{N+1} is defined as the correction to the length of the tip cell

$$\eta_{N+1} = x_A^{j+1} - x_A^j \qquad \text{(during advance)} \tag{6.78}$$

and the coefficients of η_{N+1} in equations 6.77 are, correspondingly, $\partial R_c/\partial x_A$ and $\partial R_m/\partial x_A$. These values occupy the slots in the coefficient matrix that would normally contain $\partial R_{c_N}/\partial q_{N+1}$ and $\partial R_{m_N}/\partial q_{N+1}$, as the latter are of no interest.

With y_L, q_L representing y_k, q_k, respectively, and y_R, q_R, y_{k+1}, q_{k+1}, respectively, the Newton-Raphson coefficients are, for each k,

$$\frac{\partial R_c}{\partial y_L} = -\theta\,\delta x_{JL} - \phi_{y_L}\,\delta x_{LR} \tag{6.79}$$

$$\frac{\partial R_c}{\partial q_L} = \theta\,\delta t \tag{6.80}$$

$$\frac{\partial R_c}{\partial y_R} = \theta\,\delta x_{MR} - \phi_{y_R}\,\delta x_{LR} \tag{6.81}$$

except for $k = N$ in the event that advance halted during the current time step. In that case,

$$\frac{\partial R_c}{\partial y_R} = -\phi_{y_R}\,\delta x_{LR} \tag{6.82}$$

because the movement of the right boundary does not "scoop in" any volume. Finally,

$$\frac{\partial R_c}{\partial q_R} = -\theta\,\delta t \tag{6.83}$$

During advance,

$$\frac{\partial R_c}{\partial x_R} = -\frac{\delta \forall_{y_{LR}} + \delta \forall_{z_{LR}}}{\delta x_{LR}} \tag{6.84}$$

all these partial derivatives stem from equation 6.68.

From equation 6.69 the force equation,

$$\frac{\partial R_m}{\partial y_L} = y_L + \phi_{y_L}(b_L - b_R) + 2\,\phi_{D_{y_L}}\,D\left(\frac{1}{\tilde{C}_h}\frac{\partial \tilde{C}_h}{\partial \tilde{y}} + \frac{1}{\tilde{y}}\right) \tag{6.85}$$

Here, the values D and $\tilde{y}$ are computed as per equations 6.32 and 6.34 or 6.39. The form of the derivative $\partial \tilde{C}_h / \partial \tilde{y}$ depends on the empirical expression used to evaluate $\tilde{C}_h$ (see sec. 3.4). With the Manning formula in force,

$$\frac{\partial \tilde{C}_h}{\partial \tilde{y}} = \frac{1}{6}\,\frac{\tilde{C}_h}{\tilde{y}} \tag{6.86}$$

in which $\tilde{C}_h$ is the Chezy C_h evaluated at the average value of y. Further,

$$\frac{\partial R_m}{\partial q_L} = -2\,\phi_{D_{q_L}}\,\frac{D}{\tilde{q}} \tag{6.87}$$

Some problems were experienced with convergence of the iterative scheme (or development of saw-tooth profiles near the receding trailing edge with the linear scheme) when this expression was used for the coefficient of δq_L (and, with $\phi_{D_{q_L}}$ replaced by $\phi_{D_{q_R}}$, for the coefficient of δq_R). These problems stemmed from the fact that near the trailing edge in recession, q values are very small. Equations 6.77, on the other hand, are based on Taylor-series expansions of y and q about y^i and q^i, truncated after the first-order term; good convergence depends on δq and δy being small relative to q and y. The quadratic term of the series expansion for q was approximately taken into account by the following procedure. It is noted that, approximately,

$$D_{j+1} = P_{j+1} + W_{j+1} \tag{6.88}$$

and that

$$= D_{j+1} = \frac{\delta x}{\tilde{C}_{h_j}^{\,2}\, \tilde{y}_j^2}(\tilde{q}_j + \delta \tilde{q})^2 + \frac{\partial D}{\partial \tilde{y}}\delta \tilde{y} \tag{6.89}$$

$$= D_j \left(1 + \frac{\delta \tilde{q}}{\tilde{q}_j}\right)^2 + \frac{\partial D}{\partial \tilde{y}}\delta \tilde{y} \tag{6.90}$$

while

$$P_{j+1} + W_{j+1} = P_j + W_j + \frac{\partial P}{\partial y_L}\delta y_L + \frac{\partial P}{\partial y_R}\delta y_R + \frac{\partial W}{\partial \tilde{y}}\delta \tilde{y} \tag{6.91}$$

Thus,

$$\left(1 + \frac{\delta \tilde{q}}{\tilde{q}_j}\right)^2 = \frac{P_j + W_j + \dfrac{\partial R_m}{\partial y_L}\delta y_L + \dfrac{\partial R_m}{\partial y_R}\delta y_R}{D_j} \tag{6.92}$$

On the assumption that, in the trailing region, R_m changes from one iteration to the next primarily as the result of changes in $\tilde{q}$, rather than $\tilde{y}$ (as was often found), one can write

$$\frac{\delta \tilde{q}}{\tilde{q}_j} = \sqrt{\left|\frac{P_j + W_j}{D_j}\right| - 1} \tag{6.93}$$

the absolute value signs being put in as a precaution against accidental negative values for P + W—recall that all these values are numerically very small in the trailing region of flow.

Thus, on the grounds that the quantity $\partial R_m/\partial q_L$ represents the coefficient of δq_L in the matrix of coefficients, it is modified by the factor f to the result,

$$\frac{\partial R_m}{\partial q_L} = -2\,\phi_{D_{q_L}} \frac{D}{\tilde{\bar{q}}} f \tag{6.94}$$

in which

$$f = 1 + \frac{1}{2}\left(\sqrt{\left|\frac{P+W}{D}\right|} - 1\right) \tag{6.95}$$

Worthy of note, f differs but little from unity. Similarly,

$$\frac{\partial R_m}{\partial q_R} = -2\,\phi_{D_{q_R}} \frac{D}{\tilde{\bar{q}}} f \tag{6.96}$$

There remains to set

$$\frac{\partial R_m}{\partial y_R} = -y_R + \phi_{y_R}(b_L - b_R) + 2\,\phi_{D_{y_R}} D\left(\frac{1}{\tilde{C}_h}\frac{\partial \tilde{C}_h}{\partial \tilde{y}} + \frac{1}{\tilde{y}}\right) \tag{6.97}$$

In the advance phase, in the tip cell,

$$\frac{\partial R_m}{\partial x_R} = \frac{W - D}{\delta x_{LR}} \tag{6.98}$$

6.7 Solution of the Linear System by the Double-Sweep Technique

At each iteration the linear system represented by equations 6.77 must be solved. The matrix of coefficients is sparse, in that non-zero values are clustered around the diagonal. The following efficient method of solution that utilizes this sparseness is based upon a scheme of Preissman, presented by Liggett and Cunge (4).

The given system can be represented schematically by the pair of equations

$$\left.\begin{aligned} a\,\xi_k + b\,\eta_k + c\,\xi_{k+1} + d\,\eta_{k+1} + g = 0 \\ p\,\xi_k + q\,\eta_k + r\,\xi_{k+1} + s\,\eta_{k+1} + t = 0 \end{aligned}\right\} \tag{6.99}$$

one such pair for each cell $k = 1, 2, \ldots, N$. Here the ξ_k and η_k represent the corrections δy_k, δq_k to be made at station k in the given iteration; the a, b, c, d represent the appropriate partial derivatives of R_c, while g is R_c itself. The p, q, r, s represent the partial derivatives of R_m, and t is R_m.

Auxiliary coefficients E_k and F_k are defined such that

$$\eta_k = E_k\,\xi_k + F_k \tag{6.100}$$

whatever the values η_k, ξ_k, prove to be. Of course equation 6.100 does not define E_k and F_k uniquely, since an infinite variety of value-pairs will satisfy it for any given pair of solution values η_k, ξ_k. However, any pair of values E_k, F_k which satisfy equation 6.100 will do. For example, for k = 1, a correct pair is

$$\left.\begin{aligned} E_1 &= 0 \\ F_1 &= \eta_1 \end{aligned}\right\} \tag{6.101}$$

in which η_1 is known from the upstream boundary condition.

A scheme is sought whereby E_{k+1} and F_{k+1} can be determined in terms of E_k and F_k. For then, all E and F could be determined sequentially for k = 2, 3, . . ., N + 1 in the so-called forward sweep. With ξ_{N+1} known from the downstream boundary condition, equation 6.100 would yield η_{N+1}. Furthermore, substitution of η_k from equation 6.100 into either of equations 6.99 would yield an expression for ξ_k in terms of ξ_{k+1}, η_{k+1}. This then would be used to obtain ξ_N from ξ_{N+1}, η_{N+1}. Equation 6.100 would then yield η_N, and so on, with k = N − 1, N − 2, . . ., 1, in execution of the backward sweep.

The desired relations for E_{k+1} and F_{k+1} in terms of E_k and F_k are readily, if tediously, found by substituting η_k from equation 6.100 into each of equations 6.99, then solving each equation for ξ_k and equating the results. Collection of terms yields an equation of the form

$$\eta_{k+1} = E_{k+1}\,\xi_{k+1} + F_{k+1} \tag{6.102}$$

in which

$$\left.\begin{aligned} E_{k+1} &= \frac{r\,G_1 - c\,G_3}{d\,G_3 - s\,G_1} \\ F_{k+1} &= \frac{G_4\,G_1 - G_2\,G_3}{d\,G_3 - s\,G_1} \end{aligned}\right\} \tag{6.103}$$

with

$$G_1 = a + b\,E_k \tag{6.104}$$

$$G_2 = g + b\,F_k \tag{6.105}$$

$$G_3 = p + q\,E_k \tag{6.106}$$

$$G_4 = t + q\,F_k \tag{6.107}$$

In the backward sweep

$$\left.\begin{aligned} \xi_k &= U\,\xi_{k+1} + V\,\eta_{k+1} + W \\ \eta_k &= E_k\,\xi_k + F_k \end{aligned}\right\} \quad (6.108)$$

with

$$U = -\frac{c}{G_1} \quad (6.109)$$

$$V = -\frac{d}{G_1} \quad (6.110)$$

$$W = -\frac{G_2}{G_1} \quad (6.111)$$

6.8 Nondimensional Forms of the Governing Equations

The program works in a dimensionless mode. This allows convenient entry of nondimensional data if a series of generalized runs are being made. When dimensioned input data are used, it is still an advantage to work in dimensionless mode, for the dimensionless variables are also *normalized* in some sense as well; that is, depths and discharges in the stream generally run in the range 0 to 1; dimensionless bottom slope in sloping borders is always unity, and so forth.

Dimensionless variables are ratios of the dimensioned variables to some pertinent characteristic value having the same dimensions. Dimensionless variables (starred) are defined as follows

$$\left.\begin{aligned} y^* &= \frac{y}{Y_0},\ q^* = \frac{q}{Q_0},\ x^* = \frac{x}{X_0},\ L^* = \frac{L}{X_0}, \\ t^* &= \frac{t}{T_0},\ \tau^* = \frac{\tau}{T_0},\ z^* = \frac{z}{Y_0},\ b^* = \frac{b}{Y_0} \end{aligned}\right\} \quad (6.112)$$

Here Y_0 is a characteristic depth, Q_0 is a characteristic discharge (per unit width), X_0 is a characteristic length, and T_0 is a characteristic time.

In sloping borders, the characteristic depth is taken as normal depth for the given inflow discharge and average bottom slope and roughness (DMLMOD = 1),

$$Y_0 = y_n\,(q_{in}, \bar{S}_0, n) \quad (6.113)$$

(with, say, the Manning formula in force). The average bottom slope $\bar{S}_0$ is given by the total change in bottom elevation divided by border length. The characteristic discharge is simply the initial inflow rate

$$Q_0 = q_{in} \tag{6.114}$$

The characteristic distance is given by

$$X_0 = \frac{Y_0}{\bar{S}_0} \tag{6.115}$$

and the characteristic time, by

$$T_0 = \frac{X_0 Y_0}{Q_0} \tag{6.116}$$

In horizontal borders, normal depth is infinitely great, so alternative definitions are necessary. With DMLMOD = 2,

$$Q_0 = q_{in} \tag{6.117}$$

as before, and

$$T_0 = t_{co} \tag{6.118}$$

and

$$X_0 Y_0 = Q_0 T_0 \tag{6.119}$$

as before, a convenient choice for the characteristic depth is

$$Y_0 = \frac{Q_0^{3/5} T_0^{1/5}}{C_{h_0}^{2/5}} \tag{6.120}$$

in which the Chezy C_h is evaluated at Y_0.

With either set of choices for the characteristic variables, the formulation of dimensionless drag turns out particularly simple.

Substitution of the products $y = y^* Y_0$, $x = x^* X_0$, $q = q^* Q_0$, etc, into the equation of mass conservation, 6.12, results in an equation of exactly the same form, but with all variables but the weighting factors starred, that is, dimensionless. Only the computation of z is affected by the transition to dimensionless variables. For with

$$z = k \tau^a + b^{10} \tau + c \tag{6.121}$$

---

[10]Note that b in this context is not the same as the b used elsewhere to represent bottom elevation.

it follows that

$$z^* = K^* \tau^{*a} + B^* \tau^* + C^* \tag{6.122}$$

in which

$$K^* = \frac{k\, T_0^a}{Y_0} \tag{6.123}$$

$$B^* = \frac{b\, T_0}{Y_0} \tag{6.124}$$

$$C^* = \frac{c}{Y_0} \tag{6.125}$$

K^*, B^*, and C^* are evidently dimensionless infiltration coefficients characteristic of the given irrigation. Worthy of note, the numerical values of these parameters are different in the two schemes of converting variables to nondimensional form.

Similar substitution into the equilibrium equation, 6.42, yields expressions for P and W in the starred variables that are identical in form to those with dimensioned variables, equations 6.24 and 6.25. Only in the case of sloping borders, the dimensionless bottom-elevation difference is $b_L^* - b_R^* = x_R^* - x_L^*$; in horizontal borders, of course, $b_L^* - b_R^* = 0$. Equation 6.39 for, now, the *dimensionless* drag intensity retains its form, except that the Chezy C_h is now a dimensionless version, different from equation 6.31. For both choices of characteristic variables, the dimensionless Chezy/Manning C_h is simply

$$C_h^* = R^{*1/6} \tag{6.126}$$

as can be readily proved by introducing both sets of dimensionless variables into the equilibrium equation.

The dimensionless inflow rate, for constant inflow to cut off, is simply unity. In the second system, $t_{co}^* \equiv 1$ by definition; in the first system, it is a variable. Field end is marked by $x^* = L^*$; of note, the numerical value of L^* is different in the two systems, for a given real, dimensioned L. In general, the variables of interest have differing numerical values for the same irrigation, viewed in the two systems of nondimensionalization.

In the first system (DMLMOD = 1), the dimensionless solution—controlling variables (as described in (8)) are, with uniform bottom slope and Manning resistance, the field length L^*, the infiltration parameters a, K^*, B^* C^*, and cut-off time t_{co}^*. In the second system, these are slope S_0^* and L^*, and a, K^* B^*, C^*.

6.9 Differential Forms of the Governing Equations

For comparison with other studies in the literature, it is worthwhile to express the integrated equations (integrated over cell length and a time increment) of mass conservation and equilibrium in differential form, as partial differential equations in x and t.

The equation of mass (volume) conservation, equation 6.12, is first written for a very short cell—short enough for the ϕ to be one-half—and for a short time increment. Then it is divided by δx_{LR} and by δt. Then δx_{LR} and δt are both made to approach zero. The weighted sums then assume much simpler forms. For example $\theta q_L + (1 - \theta)\, q_J \rightarrow q_L$, etc. Furthermore, in the limit, as $N \rightarrow \infty$,

$$\frac{\delta x_{JL}}{\delta x_{LR}}(y_L + z_L) - \frac{\delta x_{MR}}{\delta x_{LR}}(y_R + z_R) = -\frac{1}{N}\frac{dx_A}{dt}\,dt\,\frac{\partial(y + z)}{\partial x} \qquad (6.127)$$

approaches zero faster than $(q_L + q_R)/\delta x_{LR}$, and the "scooping in" of volume (the second term in the right of each of equations 6.13 and 6.14), stemming from the obliqueness of the computational grid, becomes negligible. The result in the limit is the, so called, equation of continuity,

$$\frac{\partial q}{\partial x} + \frac{\partial y}{\partial t} + \frac{\partial z}{\partial t} = 0 \qquad (6.128)$$

since

$$\phi_{y_L}\, y_L + \phi_{y_R}\, y_R = \tilde{y} \rightarrow y, \text{ etc.} \qquad (6.129)$$

The equilibrium equation, 6.42, written for a thin slice, following division by the volume of the slice $\tilde{y}\,\delta x_{LR}$ and passage to the limit as $\delta x_{LR} \rightarrow 0$, yields the result

$$\frac{\partial y}{\partial x} = S_0 - S_f \qquad (6.130)$$

in which S_f is given by equation 6.28, (eq. 6.129 was used in obtaining eq. 6.130).

Part II: Program Organization

6.10 The First Time Step

Time and advance are set to zero for the time index $i = 1$. The computation of the first time step seeks the advance and profile at $i = 2$. The time $t(2) = \delta t_1$, in which δt_1 is the size of the first time step.

Dimensionless values of $R_{c_{max}}$ and $R_{m_{max}}$ are each set to 0.000001. The weighting factor in time, θ, is set to 0.6.

The advance in the first time step is computed, with the entire stream length treated as a single (tip) cell, and appropriate weighting factors used in the equations. It is assumed that discharge increases according to a three-seventh power law from 0 to the value q_{in} in the course of the first time step; consequently the volume of inflow in the first time step is $0.7\ q_{in}\ \delta t_1$. This first step of calculation is always handled in fully nonlinear fashion, regardless of whether subsequent-time-step calculations are locally linearized or not. Once the stream length and upstream depth have been determined for the first time step, the length is subdivided into N cells.[11] The depths y_k at the juncture points $k = 2, 3, 4, \ldots, N$, are found by means of equation 6.52 with β taken from equation 6.51 (the total length is substituted for $[x_a - x_N]$). Infiltration depths z_k are found from equation 6.61 (with the same substitution of total stream length for δx_N). The discharges q_k are then given by the formula

$$q_k = q_{LB} \cdot \frac{y_k + z_k}{y_{LB} + z_{LB}} \qquad (6.131)$$

The program is then sent to section 6.18, End of Time Step.

6.11 Preparation of Trial Values for Each Successive Time Line

In equation 6.131, the subscript LB refers, as before, to conditions at the left (upstream) stream boundary; RB refers to the downstream (right) stream boundary. It follows that $k = 1$ corresponds to LB, while $k = N + 1$ corresponds to RB. During advance, x_a refers to x_{RB}. The subscripts L and R refer to k and $k + 1$, respectively.

For successive time steps, the procedure is to increase the time index i by one, and increment the time by δt. The time increment varies in accordance with one or another scheme, defined by the choice of DTMOD (sec. 3.9). In addition, it is convenient to compute the ultimate total volume of inflow as $V_Q = q_{in}\ t_{co}$, in which q_{in} is a constant inflow rate, and t_{co} is the cut-off time. On the other hand, the volume of inflow during the first time step is set to

[11]See section 3.9 (DTMOD) for possible variations on this scheme.

$0.7 \cdot q_{in} \cdot \delta t_1$ (sec. 6.10). Further, the cut off is smeared over one time step, so that the increment of inflow volume pertaining to the step that contains t_{co} is $(1 - \theta)q_{in}\delta t$. To reconcile all these factors, one time step is made just the right size to ensure that a time line falls precisely on the precutoff value given by

$$t_{pco} = t_{co} - (1 - \theta)\delta t_{std} + 0.3\,\delta t_1 \tag{6.132}$$

Then, t_{co} will fall at just that fraction of the standard time step after t_{pco} that will allow the inflow volume computed by increments over all the time steps to equal $q_{in} \cdot t_{co}$.

In any event, if t_i exceeds the specified t_{max}, the computations are ended in one of the two normal modes of termination. The other, standard, normal termination follows post-irrigation analysis, when the computed irrigation has been completed.

With computations continuing, first guesses are made for x_{LB}, x_{RB}, and x_k, y_k, q_k for all k. The left and right boundaries are assumed the same as on the previous time line, except during advance; then, for a first guess, the right boundary is assumed to advance at the same speed as in the previous time step. The x_k are found by subdividing the total computational stream length $x_{RB} - x_{LB}$ into N parts. The y_k and q_k are assumed equal to their values y_{known_k}, q_{known_k} on the previous time line. Bottom elevation and depths of infiltration are computed for all k. The value of discharge at the upstream boundary is computed and the correction $\delta q_1 = \eta_1 = q_1 - q_{known_1}$ to the first guess for discharge at LB is obtained.

6.12 Overview of the Iteration Cycle for Correcting Trial Values

At this point the iteration cycle is entered. If the locally linearized mode of solution has been chosen, the cycle is traversed just once. If the nonlinear, iterative mode is in force, the cycle is traversed repeatedly, the iteration index j increased by 1 each time, until R_c and R_m in every cell are reduced below $R_{c_{max}}$ and $R_{m_{max}}$, respectively, or j exceeds j_{max}. In the last case, the time step is cut in half and the calculations repeated, and so on, for a maximum of eight reductions. If convergence is still not achieved, the error message, "NO CONVERGENCE IN CELLS" is printed, and an abnormal exit (controlled[12] abort) is made.

[12]. . .as opposed to uncontrolled aborts, defined here, as aborts initiated by computer-system software. Any diagnostic information printed is then controlled solely by *that* software.

6.13 Cell Computations and Solution of the Resulting Set of Linear Equations

If R_c or R_m in any cell (eqs. 6.68, 6.69) exceed the permitted maximums, note is taken of that fact.[13] The partial derivatives (eqs. 6.79-98) comprising the coefficients of the corrections ξ_k, η_k, in equations 6.77 are computed and the equations solved by the double-sweep method outlined in section 6.7. The corrections for $k = 1, 2, \ldots, N + 1$ are added to the current (j^{-th}) approximations of the variables.

6.14 Elimination of Computed Negative Cell Lengths: Restructuring System of Nodes

If the stream is in the advance phase, every new profile is checked immediately for negative cell lengths. These can arise because the node distribution is based on the first guess for the advance increment. With closely spaced nodes near the leading edge, a negative correction to the advance increment can place the new right boundary upstream from an interior node point.[14]

The locations of the interior node points are not generally changed in response to the iterative adjustment of the stream boundaries, because this would add the location of the right stream boundary as unknown in the equations for each cell, instead of for just the downstream-boundary cell. This, in turn, would change the appearance of the matrix of coefficients for the system of linear correction equations. Instead of restricting the non-zero coefficients to a narrow band about the diagonal, the system would also have an additional vertical stripe of coefficients applying to the unknown stream length. This would require a major change in the method of solution of the equation set.

Instead, the internal nodes are left fixed in the hope that only the length of the last node will change in consequence of corrections to the advance increment. Only in the event that a negative correction exceeds the length of the right boundary cell does it become necessary to restructure the system of nodes. Then, a new node set is constructed, in accord with the given value of RDX,[15] but based on the corrected stream length. When this occurs, a recomputation for the time step is made, that is, the iterations are restarted from the beginning, with the original trial values of depth, discharge, and advance increment. Only the iteration counter continues to increment, so that the total number of iterations is always noted and does not exceed the maximum, j_{max}. Thus, even with the locally linearized-solution mode (LINMOD = 1), the number of iterations can, on occasion, exceed one.

[13]RFLAG is set to one, in contrast to the zero value set at the start of the iterations.

[14]. . .either because the ratio RDX is small, the number of cells NSTD is large, or the time step DT is large (see Input, line 10, sec. 3.10).

[15]Input, line 10, sec. 3.10.

6.15 Elimination of Computed Negative Stream Depth: Recession

Once the stream length is seen to consist of positive cell lengths only, all of the new *depths* are scanned for negative values, for the program operates under the general rule that no surface-stream computations will be performed with negative depths. Apart from the physical impossibility of a negative depth, certain terms in the governing equations, notably the drag term, have no mathematical meaning either, with a negative or zero depth, and any attempt to calculate drag with a non-positive depth will result in an unscheduled, system-controlled[16] abort. Computed depths, then, less than zero simply are not allowed in the surface stream.[17]

Apparent negative values can arise from either of two causes, one completely normal, the other evidence of a less-than-ideal computation. As regards the first cause, once inflow is cut off, depths at the rear of the surface stream continually decrease because of infiltration and, usually also, because of bulk flow in the downstream direction. In a stream with incipient front-end recession, the depths near the right stream boundary also decrease. Since each computed approximation to a variable value is based on equations linearized about the current value of the variable, and these are applied over a full time step of some given size, if the true result calls for a zero depth at some time within the duration of the time step, the computed depth at the end of the time step will be negative. This is a normal computation during recession, and the time of passage of the recession edge past a given x-station is estimated by linear interpolation between the computed depths at that station at the beginning and end of the time step. In a completely normal calculation, if several stations experience computed depths passing to negative values in a given time step, the station with the largest[18] computed negative depth lies at the boundary of the stream, and the neighboring stations exhibit computed negative depths progressively smaller[18] towards the interior of the stream (or, of course, positive depths progressively larger).

If the program is working well, in the sense that all functions of interest are changing smoothly and gradually with respect to time and distance, no negative depths will be computed in the interior of the profile unless all depths to the exterior of that point are also negative, as described above. An imperfect calculation, on the other hand, can lead to the development of saw-tooth profiles, in which some depth peaks are positive and some troughs negative. In particular, the drag term in the force-equilibrium equation is very sensitive to small errors in discharge or depth when the depth is very low. These small errors can lead to large errors in drag, with subsequent computation of saw-

---

[16]...as opposed to program-controlled.

[17]Zero depths are allowed only at the stream boundaries, for drag is not computed there.

[18]...in the absolute sense...

tooth profiles. Furthermore, use of imprecise weighting factors when cell lengths are large can also lead to saw-tooth profiles. If negative depths arise when all the surface depths are quite low near the end of the irrigation, reduction of the computational stream profile to those regions that are comprised of positive depths only, is a well justified means of getting useful final results from a troublesome calculation. If the saw teeth are of high amplitude, occurring in a region of large depth, however, then significant volumes of water will be lost in the calculation, and recession, either from the rear or from the front, will be computed as occurring too rapidly. This condition is signaled by a large, positive relative volume error (see post-irrigation analysis, sec. 5.5), well over 0.01; this circumstance alerts the user to the problem. The procedure for eliminating those portions of the profile that contain negative depths is outlined next.

The entire profile between x_{LB} and x_{RB} is scanned for negative depths and the location of each occurrence is noted. If none is found, the program proceeds to 6.16. If any are found, the largest length of stream either between a boundary and the nearest location of negative depth or between two locations of negative depths is selected as a basis for the new computational stream length. These new boundaries are considered tentative, pending examination of the depths there.

If either boundary has been stepped in toward the interior, the entire time step will be recomputed on the basis of the new stream length. This length now applies to both the accepted profiles at the beginning of the time step and the unknown profile at the end of the time step.[19] In other words, only a portion of the "old" stream—albeit the most significant portion—is used to advance the calculations to the new time line. On the other hand, if the largest stream length following the step-in process is less than 1 percent of field length, the irrigation is presumed over. The trailing recession edge is assumed to cross the new upstream boundary at the current time. Front-end recession is assumed to cross the new downstream boundary also at the current time. If such stepping in of a computational boundary constitutes the first indication of rear-end or front-end recession, recession from the corresponding old stream boundary is assumed to occur arbitrarily a half time step earlier. Once recession stations and times are noted, program control passes to post-irrigation analysis (sec. 5.5)

With a stream of working length, the depth at the tentative upstream boundary is checked first. If positive, the location is accepted as the new boundary and the tentative downstream boundary is viewed next. But if the depth there

[19]The iteration counter continues to be incremented, rather than set back to one.

is negative, recession has occurred from the old upstream boundary. If the depth at the old boundary location[20] has turned negative, the time of recession there is determined by linear interpolation between the depths computed there at the two times. If the depth is still positive, signifying a saw-tooth profile, recession from the old boundary is still assumed to have occurred, arbitrarily one-half of a time step earlier than the current time.

Then, a location with a small positive depth in the new profile is sought for the new computational boundary. The profile downstream from the tentative boundary location is scanned for a depth equal to or greater than a preset small value, y_{rec}.[21] If all depths are less than y_{rec}, the irrigation is assumed over. Any remaining surface water is added to the infiltrated depths by computing recession times commensurate with the additional time necessary to infiltrate those small depths. The program then passes to post-irrigation analysis.

But if a depth greater than y_{rec} is found at an interior node, the new computational boundary is placed at the location nearest the tentative boundary at which a depth equal to y_{rec} exists, as determined by linear interpolation between nodes. In preparation for a recomputation of the same time step with the new boundary, the upstream portion of the computational stream as it existed at the beginning of the time step is also truncated to this same new x-boundary. Only the portions interior to this point will enter into the volume-balance equations. The depth and discharge on this previous time line are found at this x by linear interpolation between nodes; the depth of infiltration there is found by applying the infiltration function to the appropriate infiltration time. Cell volumes for the new upstream-boundary cell are found by using the appropriate weighted averages of nodal surface and subsurface depth values.

In the stepping-in process, the total number of cells in the stream may change. If the boundary is moved more than one cell length from its previous position on the old time line, at least one cell will be lost from consideration. The node number at the left boundary is taken to be the number of the nearest node, on the old time line, upstream from the point where $y = y_{rec}$ on the new time line. This insures that the number of cells on the new and old time lines are the same. (After the downstream boundary has been dealt with, and prior to recomputation of the time step, the nodes are renumbered, so that the first node is always indexed one.)

---

[20]The old and new boundaries can be the same.

[21](dimensionless) $y_{rec} = 0.01$.

The same considerations are now applied to the tentative downstream boundary. If the depth there is nonnegative, the instructions described in the rest of this paragraph are bypassed. In the event of a negative depth, the boundary is stepped in, following calculation of a recession time for the old downstream boundary location, to the nearest location where a surface depth equals y_{rec}. If none is found, the irrigation is over; the remaining surface depths are added to the infiltration profile, and the program passes to post-irrigation analysis (sec. 5.5). If a new boundary *is* located, however, the old computational stream length is again truncated. If the resultant stream length is less than 1 percent of the field length, the recession edges are judged to pass the new boundaries at the current time, and the irrigation is deemed over; post-irrigation analysis commences. Otherwise, the dimensions and volumes of the downstream-boundary cells, on the previous and on the current time lines, are recalculated as for the upstream-most cell, prior to the recomputation of the entire time step.

In this way, even if a considerable shift in boundary location occurs in the course of a single time step, the computational grid never becomes very oblique. A cell boundary that is moved a great distance in the course of a time step can lead to considerable error in the cell mass-balance computations, if the infiltration profile is relatively deep and nonuniform.

Since whole cells may have been lopped off the stream in the step-in process, a renumbering of the nodes now takes place. The new total number of cells is noted. The new upstream-boundary node is numbered one, and the remaining nodes are numbered sequentially progressing downstream. The arrays describing conditions at each node, new and old x, bottom elevation, surface depth, discharge, and infiltration time and depth, are shifted in accordance with the new numbering.

At this point, that portion of the infiltrated volume $\forall_{z_{out}}$ that lies at the beginning of the time step outside the current boundaries of the stream is calculated and stored for subsequent use by the volume-balance check that is performed for diagnostic purposes at every time step.

Next, the new conditions at the right boundary are investigated.

6.16 Investigation of Potential Changes in Downstream Boundary Conditions

Apart from the possibility of front-end recession signaled by the computation of negative depths, which has been treated in the previous section, a number of other possibilities arise at the downstream boundary of the surface stream, and the program must branch accordingly. The first branching is determined by conditions at the beginning of the time step. Each of *these* paths then branches further, depending upon what has developed during the time step.

6.16.1 Advance at Beginning of Time Step

A stream that was advancing at the beginning of the time step will be computed for the end of the time step as (1) continuing advance, (2) exhibiting negative advance, that is, spontaneously receding from the front end, (sec. 6.16.1.1) or (3) crossing the field boundary (sec. 6.16.1.2).

When a positive advance increment is computed, the stream is ready for the next iteration, or the next time step,[22] or a change in boundary condition because field end has been crossed.

6.16.1.1 Front-End Recession at End of Time Step

A computed negative advance increment requires a recomputation of the time step. If the nonlinear approach has been chosen, the spontaneous front-end recession is not treated as such, that is, recomputation does not commence until the errors in mass and force balances have been reduced below the required tolerances in the iterations, thus confirming the computation of negative advance. With the linear approach, the first indication is sufficient. In any event, the recomputation is performed on the basis of front-end recession from a boundary located at the point of maximum advance (that is, the location of the right boundary at the beginning of the time step).[23]

6.16.1.2 Stream Encounters Field End: Runoff or Ponding at End of Time Step

When an advance computation shows the stream front crossing field end, in fact, advance was completed at some point during the current time step, and either runoff or ponding is occurring for the rest of the step. This calls for a recomputation of the time step with the new boundary conditions applied to the current time line. In the nonlinear approach, the iterations are allowed to continue normally to confirm stream arrival "past" field end. The time of arrival of the wave at field end is found by assuming a constant rate of advance over the time step equal to that computed for the time step in the "absence" of a downstream boundary.

The imposition of a new right-hand boundary, at $x = L$, calls for a repositioning of the nodes.[24] These are placed in accord with the number of cells remaining and with the given ratio r_{DX} of successive cell lengths.

---

[22] . . . whichever is appropriate, depending upon (1) whether a recomputation has been ordered because of boundary step-in, (2) whether the solution technique has been chosen locally linearized or fully nonlinear, and (3) whether the errors in mass and force balances are small enough (sec. 6.17).

[23] If this negative advance increment arises prior to inflow cut off, the computation is judged a failure, a message is printed to that effect and a controlled abort is executed.

[24] Without repositioning, it is possible, for example, for the new boundary location to lie upstream of the downstream-most cell(s).

For runoff, the first guesses for the new nodal values of depth and discharge are determined by interpolation among the last-computed values. Only the downstream-boundary value of depth is set to zero. The stream is now ready for recomputation.

For the ponding case, the first guess is arrived at by assuming that the surface and subsurface volumes for that portion of the stream computed as lying beyond field end (so-to-speak, "spilled" volume) are retained upstream from the end barrier in a standing pool. First the spilled volume is computed; then the nodes are repositioned in the new stream length, and tentative nodal values of depth and discharge are found by interpolation among the last-computed values. The dimensions of the pool are found by assuming its surface level, except in a transition cell in which the water-surface elevation varies linearly from the interpolated value on the upstream side to pool level on its downstream side; pool volume, of course, is known. All first-guess discharges in the pool are assumed zero. The stream is now ready for recomputation.

6.16.2 Runoff at Beginning of Time Step

If the right boundary was subject to runoff at the beginning of the time step, and the computed discharge there at the end of the time step is positive, this iteration is assumed completed, and the program passes to the instructions in section 6.17.

If, however, the discharge turns negative there, a recomputation is indicated, with new boundary conditions reflecting front-end recession. First, though, with a nonlinear computation, the iterations are allowed to run their course, to confirm the negative runoff. A further test, particularly pertinent to linear calculations, is applied to help ensure that the negative runoff computed truly signals the start of front-end recession, rather than an indication of saw-tooth behavior of a small-valued computed runoff function. In incipient front-end recession, the stream profile is concave upwards, while the profile upstream from a discharging overfall is concave downward. The last four nodal values of depth are examined to determine the sense of concavity of the profile. If the profile appears to be concave upward, it is taken as bona fide indication of front-end recession. With a concave-downward profile, the negative runoff is judged spurious, and the runoff phase is allowed to continue in the expectation that positive saw-tooth peaks will be computed shortly, or that soon the depth profile will turn concave upward and allow computed front-end recession to commence.

6.16.3 Ponding or Front-End Recession at Beginning of Time Step

For a stream undergoing ponding, or in front-end recession at the start of the time step, the iteration is complete at this point.

6.17 Branching at the End of the Iteration Cycle

At this point the program notes whether the recompute flag has been raised. If so, the iteration cycle is repeated at once. Otherwise, it is repeated only if the nonlinear mode of solution is in effect, and if R_c or R_m have exceeded the allowable maximum in any cell.

6.18 Calculations at the End of the Time Step

Once the computed stream geometry and discharge distribution for the current time line have been accepted, certain information pertinent to the profile is stored. The depths at both ends of the profile are compared with the maximums attained there, up to the current time line, and form new maximums if the old ones were exceeded. Further the maximum depth in the profile and its location are noted and compared with the global maximum for the irrigation, replacing the last if it is greater.

A measure e_{ss} of profile irregularity, the lack of smoothness is computed

$$e_{ss} = (y_{k+2} + y_k - 2y_{k+1}) - (y_{k+1} + y_{k-1} - 2y_k) \qquad (6.133)$$

for all k between 2 and N − 1; the maximum in the profile, TOOTH, is determined and compared with a global maximum.

Current surface and subsurface volumes, $\forall_y$ and $\forall_z$ respectively, are computed. and their sum is compared to the difference between the total volumes of inflow $\forall_Q$ and runoff $\forall_{ro}$ in a volume balance. The volume error

$$\forall_{err} = \forall_Q - \forall_y - \forall_z - \forall_{ro} \qquad (6.134)$$

is divided by the total inflow volume to obtain the relative volume error

$$PC_{v_{err}} = \frac{\forall_{err}}{\forall_Q} \qquad (6.135)$$

Total inflow and runoff volumes (for the entire extant period of irrigation) are incremented.

Profiles and/or an abbreviated current description of the stream are printed, if called for by the extant value of IDIAG (sec. 3.11). Profiles are plotted at this time upon demand (sec. 3.12).

The values $x_{known}(k)$, $b_{known}(k)$, $y_{known}(k)$, $q_{known}(k)$, $\delta\forall_{y_{known}}(k)$, $\delta\forall_{z_{known}}(k)$ are replaced by $x(k)$, $b(k)$, $y(k)$, $q(k)$, $\delta\forall_y(k)$, $\delta\forall_z(k)$, respectively for all $k = 1, 2, \ldots, N + 1$.

The program returns to section 6.11, Preparation of Trial Values for Each Successive Time Line.

7. The Kinematic-Wave Model

This chapter details the theory and program logic outlined in sections 5.3 and 5.4.

7.1 Introduction: Key Assumption—Relatively Large Bottom Slope

The kinematic-wave model is a numerical solution of a family of ordinary differential equations. In this introductory section, the governing partial differential equation leading to this family is derived. Reduction to the ordinary differential equations and their solution is relegated to subsequent sections.

In chapter 6, the unsteady flow in the surface stream was analyzed by breaking it up into computational cells, or slices. The depths and discharges at the cell boundaries and the total stream length were determined in a series of time steps by the solution of algebraic equations expressing, at each time step, mass conservation and equilibrium of forces for the water in each cell. The algebraic equations were, in fact, numerical approximations of time and space integrals entering into the exact expressions of mass conservation and force equilibrium. So, in general, one could say that the surface flow was analyzed through integral relationships applied to finite-sized slices of the surface stream for finite-sized time steps.

Alternately, the problem could be viewed mathematically as expressed in terms of partial differential equations. These are readily derived from equations 6.12 and 6.23 (as shown in sec. 6.9) and comprise the so-called equations of continuity

$$\frac{\partial q}{\partial x} + \frac{\partial y}{\partial t} + \frac{\partial z}{\partial t} = 0 \qquad (7.1)$$

and motion

$$\frac{\partial y}{\partial x} = S_0 - S_f \qquad (7.2)$$

Here, x and t are distance and time coordinates, respectively, q, y, and z are local, instantaneous discharge, surface depth, and infiltrated depth, respectively, S_0 is the local bottom slope, and S_f is the friction slope at the given x and t (defined by eq. 6.28.)

The forces on the water in each cell were assumed to arise from three sources; namely, the component of the weight in the direction of flow, the drag of vegetation and bottom directed opposite to the flow, and the difference in pressures exerted at the cell boundaries by the water in the neighboring slices upstream and downstream. Now for those flows in which the weight component proves much larger than the pressure difference, a major mathematical simplification becomes tenable. For then, equation 7.2 is approximated by the equality.

$$S_0 = S_f \tag{7.3}$$

which is, in fact, an algebraic or transcendental relation between depth and discharge at every point in the flow (eq. 6.28)

$$q^2 = C_h^2 y^3 S_0 \tag{7.4}$$

in which the right side is a function of x and y alone.[25] Further in equation 7.1, z is a function of infiltration time alone and hence, for any given x and t, is dependent on the past history of advance only. Indeed, then

$$\frac{\partial z}{\partial t} = i(\tau) \tag{7.5}$$

in which i is the infiltration rate, a function of τ, the infiltration time. Thus, equation 7.1 can be viewed as a partial differential equation in a single unknown, say y, in terms of two independent variables x and t,

$$c \frac{\partial y}{\partial x} + \frac{\partial y}{\partial t} + i = 0 \tag{7.6}$$

in which

$$c = \frac{dq(y)}{dy} \tag{7.7}$$

or with equation 7.4 in force,

$$c = \sqrt{S_0} \left(y^{3/2} \frac{dC_h}{dy} + \frac{3}{2} C_h y^{1/2} \right) \tag{7.8}$$

Finally, with the Chezy C_h expressed in terms of the Manning n (eq. 6.31)

$$c = \frac{5}{3} \frac{C_u}{n} \sqrt{S_0}\, y^{2/3} \tag{7.9}$$

As for the zero-inertia model, the program for kinematic-wave solutions works with dimensionless variables. The techniques for reducing variables and equations to dimensionless form are the same as described in section 6.8. The equations in this chapter have the same form regardless of whether the symbols stand for dimensioned variables or their dimensionless counterparts and can be viewed either way.

---

[25]. . .y alone, in the event of a constant bottom slope and roughness.

Equations like equation 7.6 describe a kind of wave motion called *kinematic*, in the nomenclature of Lighthill and Whitham (3), pioneers in the area. The name stems from the fact that all the variables in the governing equation (7.6) are kinematic in nature; that is, their dimensions involve length and time only. In a sense, the nomenclature is unfortunate, because equation 7.6, besides expressing the equation of continuity, which is certainly a kinematic relation, has also implied equation 7.3, a dynamic relation, stating equality of weight and drag force components.

This equality, describing uniform flow at normal depth at every point in the stream is met, approximately, whenever the depth gradient is small compared with the bottom slope. This will be true in the bulk of the surface stream when the bottom slope is relatively large. The method fails on the spot, as soon as a zero or adverse bottom slope is encountered.

At the very front of an advancing stream, and also at the brink of a free overfall, the depth gradient becomes very large, and there equation 7.3 is certainly not satisfied. Furthermore, behind an end block, where the ponded water is essentially stagnant, even on a steep slope, the depth gradient and bottom slope are essentially equal in magnitude. On the other hand, the condition of equation 7.3 is very well met in the trailing region of the surface stream in recession, a region that is generally difficult to compute on steep slopes with the zero-inertia model, because of the low depths there.

In general, limits to the reasonable application of kinematic-wave theory to border irrigation can be found by comparing the results thereof with those stemming from the zero-inertia model. Within those limits the zones of large negative depth gradient are effectively modeled by depth discontinuities. Also, behind a blocked border end, the water can be assumed a stagnant pool, having no effect on the stream plunging in. The stream calculations, performed with the kinematic-wave assumption, equation 7.3, in force are then simply terminated, in effect, at the point in the border marking the upstream boundary of the pond; the volume of the pond is determined by subtracting the infiltrated volume seeping out of the pond from the stream volume entering.

These techniques are detailed in the rest of this chapter, following an exposition in the next sections of the basic approach in solving equation 7.6.

7.2 Reduction to a Pair of Ordinary Differential Equations

By an appropriate change of independent variables, equation 7.6 can be transformed to a pair of ordinary differential equations, which can then be solved numerically. The first step consists in introducing an orthogonal s-n system oriented, at each point in the x-t plane, at some angle α (as yet undefined) to the x-t coordinates. In general, α will vary from point to point in the plane, as in figure 7.1, so that the s and n coordinates form two mutually orthogonal families of curves.

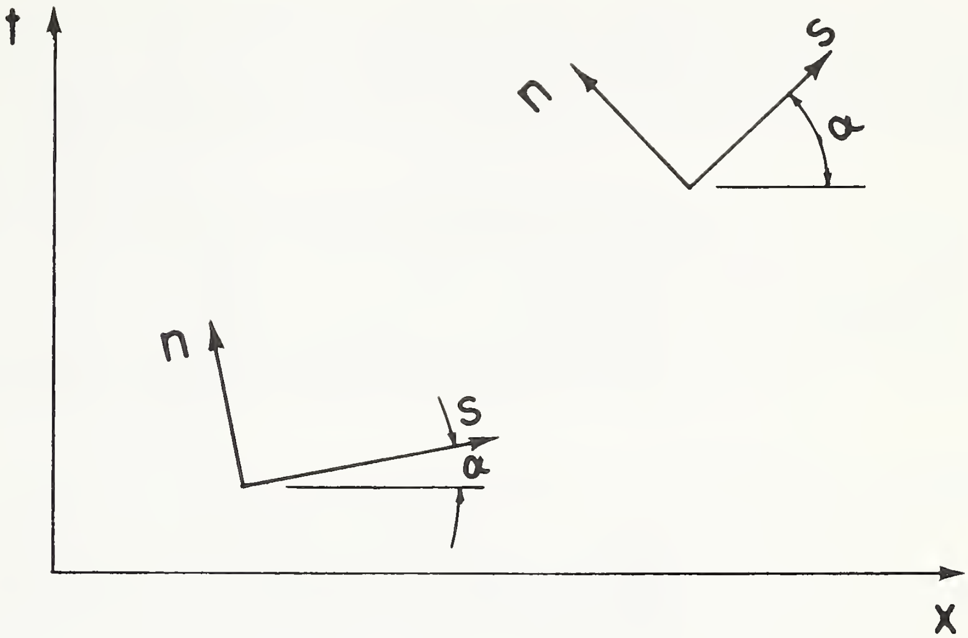

Figure 7.1.—The s-n coordinate system.

By the chain rule of differentiation, equation 7.6 is transformed to

$$c\frac{\partial y}{\partial s}\frac{\partial s}{\partial x} + c\frac{\partial y}{\partial n}\frac{\partial n}{\partial x} + \frac{\partial y}{\partial s}\frac{\partial s}{\partial t} + \frac{\partial y}{\partial n}\frac{\partial n}{\partial t} + i = 0 \tag{7.10}$$

With

$$\frac{\partial s}{\partial x} = \cos\alpha \quad \frac{\partial n}{\partial x} = -\sin\alpha \quad \frac{\partial s}{\partial t} = \sin\alpha \quad \frac{\partial n}{\partial t} = \cos\alpha \tag{7.11}$$

equation 10 can be written

$$(c\cos\alpha + \sin\alpha)\frac{\partial y}{\partial s} - (c\sin\alpha - \cos\alpha)\frac{\partial y}{\partial n} + 1 = 0 \tag{7.12}$$

If now α is chosen at each point in the x-t plane, in accord with the value of c that in fact exists there, such that

$$\cot\alpha = c \tag{7.13}$$

the coefficient of $\partial y/\partial n$ in equation 7.12 vanishes, and this equation (since $c = \cos\alpha/\sin\alpha$, and $\cos^2\alpha + \sin^2\alpha = 1$) can be written as the ordinary differential equation,

$$\frac{1}{\sin\alpha}\frac{dy}{ds} + i = 0 \tag{7.14}$$

But

$$\frac{1}{\sin \alpha} \frac{dy}{ds} = \frac{dy}{dt} \tag{7.15}$$

as can be seen from figure 7.2, and so equation 7.14 takes the simple form

$$\frac{dy}{dt} = -i \tag{7.16}$$

valid along a so-called characteristic curve, whose equation is given by

$$\frac{dx}{dt} = c \tag{7.17}$$

Equation 7.17 follows from equation 7.13, when the relations depicted in figure 7.2 are taken into account. Equations 7.16 and 7.17 represent the ordinary differential equations equivalent to the single partial differential equation 7.6.

The x-t plane can be thought of as blanketed with a family of these characteristic curves (the s-coordinate curves), for which equation 7.17 expresses the slope at any point in terms of the depth there. Along any such curve, the depth decreases with time as the result of infiltration, in accord with equation 7.16. The general appearance of these curves will be depicted in section 7.4, once an important complication, intersection of characteristic curves, has been dealt with.

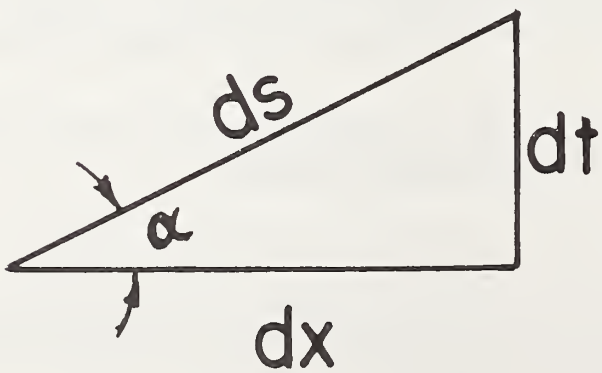

Figure 7.2.—Relation between differentials.

7.3 Intersection of Characteristics: The Kinematic Shock

The formation of kinematic-shock discontinuities will be studied first for a special case—the gradual increase of a preexisting uniform flow in a channel with zero infiltration and constant roughness and bottom slope. The results will then be viewed in the light of conditions that, in fact, exist in a border-irrigation flow.

Figure 7.3 depicts the characteristic curves, or simply *characteristics*, pertaining to an initially uniform flow in a reach of impervious channel, steep enough for the wave motion therein to be described by kinematic-wave theory. At time zero, let the discharge gradually increase. This simplified case retains the essential features necessary to extend the results to the case of flow with infiltration.

In the given special case, the characteristics are all straight lines, each bearing a single, constant value of depth and discharge; in the region of uniform flow the characteristics are parallel. Their slope, on $t = 0$, is given by equations 7.17 and 7.18. At $x = 0$, the increasing discharge is accompanied by an inverse slope increasing with time. Consequently, the characteristics intersect. The significance of the intersection will be dealt with in due course. Of immediate concern are the conditions governing the time and place of intersection of a neighboring pair of characteristics, as depicted in figure 7.4.

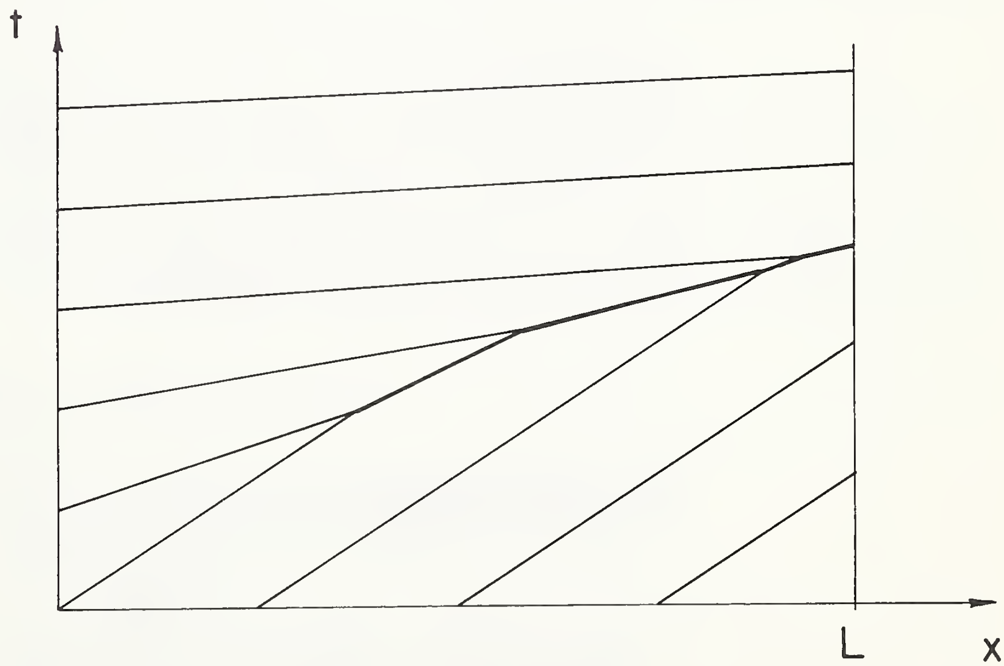

Figure 7.3.—Formation and propagation of kinematic shocks.

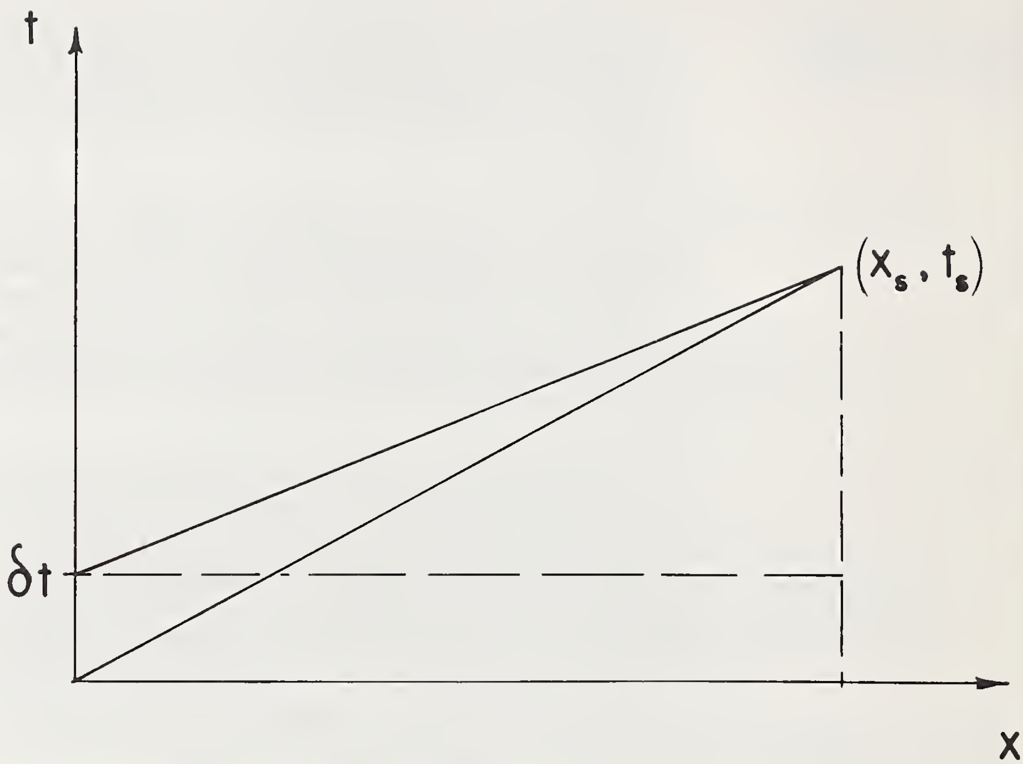

Figure 7.4.—Intersection of a neighboring pair of characteristics.

Of course, the smaller is δt, the more nearly are the characteristics, emanating from $x = 0$ at $t = 0$ and $t = \delta t$, parallel. At the same time, the smaller is their initial separation, so that intersection is more easily achieved. It turns out that as δt approaches zero, limiting values of the coordinates (x_s, t_s) of intersection are approached. Indeed, with c and dc/dt the inverse slope and its rate of increase, respectively, at $x = 0$ at time zero, then $c + (dc/dt)\delta t$ is the inverse slope of the characteristic emanating from $x = 0$ at $t = \delta t$. The triangles constructed in figure 7.4 show that

$$c = \frac{x_s}{t_s} \text{ and } c + \frac{dc}{dt}\delta t = \frac{x_s}{t_s - \delta t} \tag{7.18}$$

With x_s eliminated from equations 7.18, and δt made smaller and smaller, it is evident that in the limit,

$$t_s = \frac{c}{dc/dt} \tag{7.19}$$

$$x_s = \frac{c^2}{dc/dt} \tag{7.20}$$

From these results, it is evident that an abrupt increase in discharge (and hence c) at the left boundary will result in immediate formation of a shock. Further, it is clear that as the initial depth (and c) decreases, the intersection occurs ever earlier. In the limit, even a gradual increase in discharge, from zero, will lead to immediate shock formation.

Since the only effect of infiltration and variable slope and roughness is to give the characteristics some curvature, these qualitative results are unchanged[26] for an irrigation stream in a pervious border. Thus, the motion of the surge onto the field commences, from the start, as a kinematic shock. The significance of this is discussed next.

Again, the argument is presented for the simplified case—uniform, impervious channel. The qualitative conclusions are not altered for the flow in border irrigation. It has already been pointed out that each characteristic carries its own constant value of depth. Thus, as two characteristics approach each other, the longitudinal distance between the two different depth values decreases. As the intersection occurs, the heretofore steepening profile becomes actually vertical, that is, a discontinuity. This abrupt step change in depth constitutes the profile of the kinematic shock.[27]

A shock-discontinuity propagates at a velocity different from the velocity of either of the kinematic waves associated with the depths on its high and low sides, and turns out to lie in between these values. Elementary mass-conservation applied to a thin slice of space through which the shock is moving, as in figure 7.5, shows that shock-propagation velocity w_a is the same as velocity V_a of the water just behind the wave front.

Indeed, let x_1 be a plane fixed in space through which water is flowing and which is located a very small distance δx behind the shock front. Let x_a be a moving plane, fixed in the shock front of height y_a. At the given instant, the volume of water between x_1 and x_a is growing at the rate w_a y_a plus small quantities associated with the infiltrated volume and the gradually changing depth behind the shock. The volumetric rate of flow into the region between x_1 and x_a is Vy_a, plus a small quantity associated with the depth gradient and

---

[26]As very small x_s are considered, any curvature short of infinite will not be apparent and infinite curvature cannot arise even at the wave front where the infiltration is infinite, because the surface depth never drops to zero, for otherwise the velocity must also.

[27]. . . that is, as viewed in this study, in which $S_0 = S_f$ is strictly observed. It is possible (see, for example, Henderson (2)) to obtain a more realistic shock-front profile by relaxing this condition in the vicinity of the front, allowing instead both a depth gradient and local and convective accelerations, assuming only a profile *slowly* changing in shape.

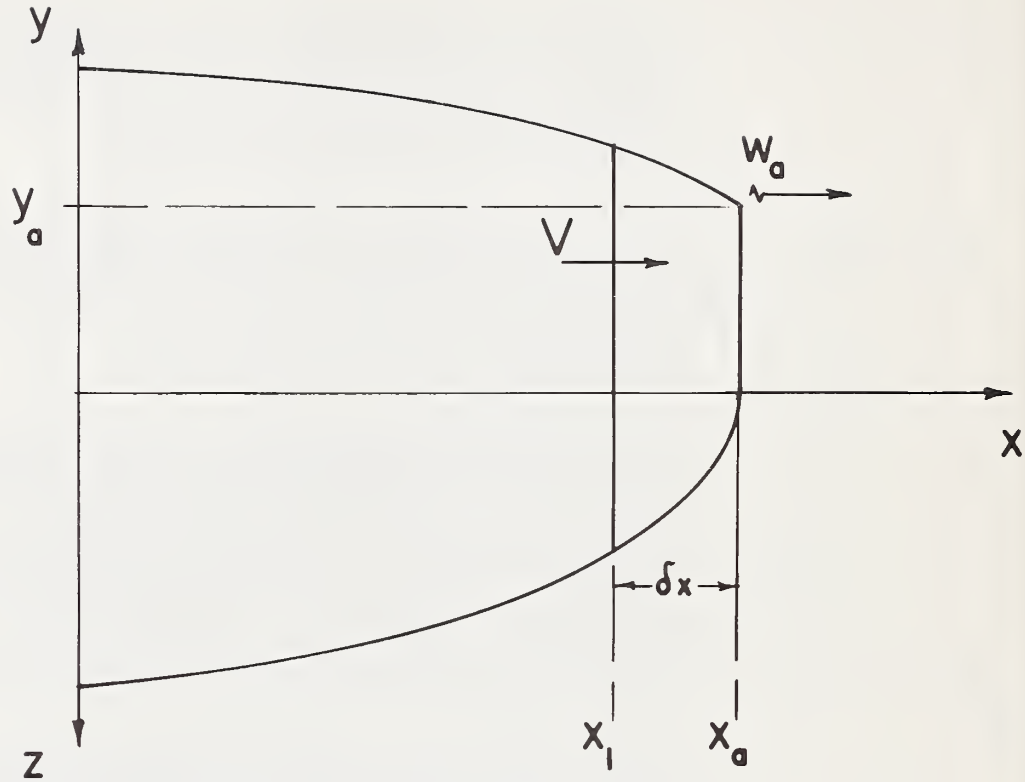

Figure 7.5.—Shock propagation speed.

δx between x_1 and x_a. But the volumetric inflow rate at x_1 must equal the rate of growth of volume between x_1 and x_a. Further, as δx is considered smaller and smaller, the small correction terms become negligible. Thus,

$$\frac{dx_a}{dt} = w_a = V_a = \frac{q_a}{y_a} \tag{7.21}$$

in which V_a, q_a, and y_a are the values of V, q, and y, respectively, when $\delta x \rightarrow 0$.

7.4 Pattern of Kinematic Waves in Border Irrigation

The front of the irrigation stream, then, moves out from the origin of the x-t plane as a depth discontinuity. The shock trajectory is intersected by successive kinematic waves emanating from the left boundary. At each intersection, the depth on the high side of the shock is that carried by the kinematic wave; the shock-propagation speed leaving the intersection reflects the new depth and discharge on its high side. A complete pattern of trajectories is shown in figure 7.6. Visible are the intersections of the advancing shock trajectory with a succession of kinematic-wave trajectories, each emanating from the upstream field boundary at an ever greater value of time. The arrival of waves at the right boundary subsequent to the arrival of the stream front there yields runoff from field end. Upon cutoff, a fan of kinematic-wave trajectories radiates outward from the cutoff point (x = 0,

$t = t_{co}$). Some reach field end to contribute to runoff. The rest terminate (with zero depth) in the interior of the field; their end points constitute the recession curve.

The border utilized in the construction of figure 7.6 was uniform in slope and roughness, and the inflow rate was held constant until cutoff. The kinematic-wave trajectories curve upwards slightly because of the effect of infiltration along their lengths (eqs. 7.16, 7.17, 7.8); the advance trajectory also curves upward, reflecting the decreasing depth on the upstream side of the shock.

When the shock reaches field end, advance is over. Successive kinematic-wave trajectories each bring a value of discharge to field end; this constitutes the runoff (or rate of ponding if a dike is assumed at field end). In the event that high-side shock depth reduces to zero before reaching field end, advance halts spontaneously and, usually, front-end recession follows.

Recession from the upstream end commences immediately after cutoff, as discharge and depth fall to zero simultaneously in the normal-depth kinematic-wave approximation. However, during the instant that the depth is falling, kinematic waves are still being generated, each at a successively lower value of inverse slope. Each of these waves is subject to the conditions of equation 7.16. Some of them, those with the larger starting depths, may yet get to field

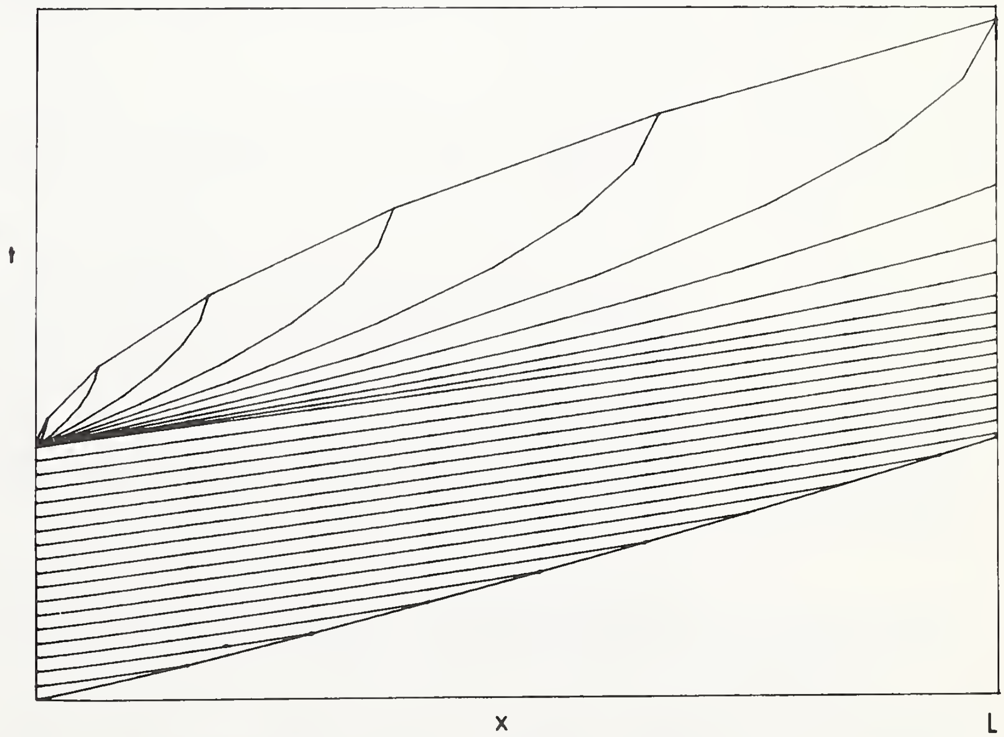

Figure 7.6.—Complete network of characteristic curves.

end and provide some runoff. Those with smaller starting depths end spontaneously, somewhere in the border, as the depth upon them reduces to zero because of infiltration. These end points mark the trajectory of the recession curve.

7.5 Program Organization

7.5.1 Definition of Mesh Density

The denseness of the network of characteristic curves originating prior to cutoff is governed by the time increments δt separating the characteristics emanating from the upstream boundary. This is chosen on the basis of the input variable N_{STD}, entered in line 10 (sec. 3.10),

$$\delta t = \frac{L}{N_{STD}} \left(\frac{1}{w_a} - \frac{1}{c} \right) \tag{7.22}$$

in which w_a and c are computed for the initial inflow rate. This makes the number of points defining the advance curve somewhat greater than N_{STD}.[28]

7.5.2 Construction of First Increment of Advance

The first step in constructing the network of characteristics is accomplished by a call to the subroutine KWCDA, which is described in detail in section 7.6. In brief, it computes the intersection of a segment CA of a kinematic-wave trajectory with a segment DA of the shock trajectory (advance curve). In this case, C and D are both on $x = 0$, (see fig. 7.7) and are separated by the time increment δt.

The subroutine returns the coordinates (x_a, t_w) of point A, and the depth y_a, discharge q_a, celerity c, and advance speed w_a there.

7.5.3 Construction of the Family of Characteristics Before Cutoff

Subsequently, the program constructs each successive kinematic-wave trajectory in a series of distance steps. The node points have the same x-values as the node points on the advance curve below. When a given kinematic-wave trajectory has been constructed out to the current limits of the advance curve, the subroutine KWCDA is called to construct both the final segment of the kinematic-wave trajectory and the final segment of the advance curve. Their intersection provides a new node location for the mesh.

It is presumed that as the kinematic wave trajectories are constructed, one by one, separated at their upstream end by the time increment δt (eq. 7.22), eventually one will be encountered for which the last segment straddles field end.

---

[28]With zero infiltration and constant bottom slope and roughness, it would be just $N_{STD} + 1$.

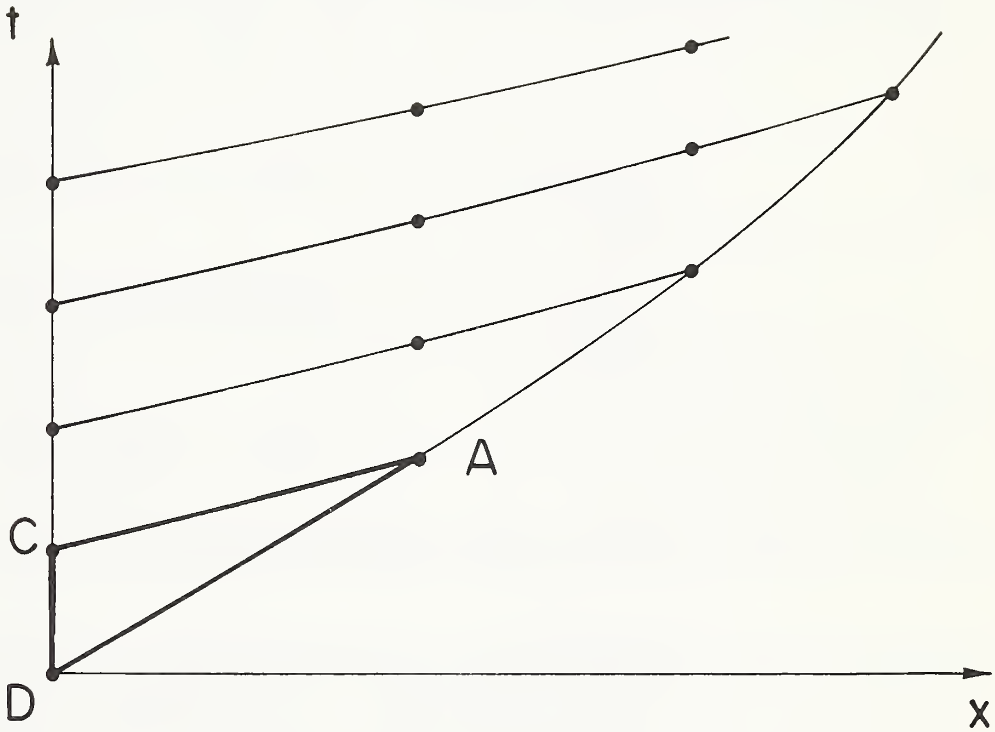

Figure 7.7. — First step in construction of network of characteristics.

The time of arrival of the stream at field end is determined by interpolation along the advance curve. The value of runoff (or rate of increase of ponded volume), that is, the discharges at $x = L$ on both the kinematic-wave trajectory and the advance trajectory are found by equation 7.4 after the depths have been found there by interpolation.

Henceforth, at least until cutoff, field end constitutes the x-location of the downstream-most node in the network of characteristic curves. The net is built up through repeated use of KWBC on each characteristic; the downstream-most value of discharge on each constitutes the rate of runoff or increase in ponded volume. Each characteristic is identified by its index i (which should not exceed 100 to stay within array dimensions).

7.5.4 Post Cutoff Family of Characteristics

After inflow cutoff, a number N_{rec} of kinematic-wave trajectories is chosen sufficiently large to define the fan emanating from $x = 0$, $t = t_{co}$. In general, those members of the fan bearing the largest discharge values, initially, will reach the right boundary. The rest will turn upward and end spontaneously, within the border length, as the discharge thereon reduces to zero. The number of characteristics in the fan is given by the formula

$$N_{rec} = 2 + \frac{L}{\delta t \cdot c_1} \tag{7.23}$$

in which c_1 is the celerity associated with the discharge before cutoff. This number has proved to provide a network after cutoff comparable in density to the portion before cutoff.

To ensure a reasonably uniform distribution of members within the fan, the following formula provides the starting value of discharge q(1) for each member,

$$q(1) = q_1 \left(\frac{N_{rec} - j_{rec}}{N_{rec}} \right)^{2.5} \tag{7.24}$$

in which q_1 is, for the moment, the precutoff value of inflow, and j_{rec} is an index for characteristics within the fan.

The trajectory of each member of the fan is computed by repeated use of KWBC. Each characteristic, as it reaches the last node, at field end, provides a value of discharge, for runoff or ponded-volume increase. Sooner or later, however, a characteristic will be encountered that fails to reach field end (a negative depth will be computed).

At this time a subroutine, KWEND, is introduced. KWEND is designed to compute a kinematic-wave trajectory all the way to its end ($y = 0$), given the location and discharge at its starting point. This subroutine, described in detail in section 7.8, chooses its own node locations, independent of the node distribution on the advance curve. This proves necessary because of the great curvature and small inverse slopes encountered on the characteristics as their trailing ends ($y = 0$) are approached (see fig. 7.6).

First, KWEND is used repeatedly, in an iterative scheme to find that value of discharge q(1) at the starting point ($x = 0$, $t = t_{co}$) of a characteristic such that its end point, $y = 0$, falls right on field end, $x = L$. A discharge greater than this critical value yields a characteristic with its end value, x_{end}, greater than L, while one less than this value, results in a characteristic ending at an x less than L.[29] In the vicinity of the correct value of q(1), the relation between q(1) and x_{end} is essentially linear; this provides relatively quick convergence of the iterative scheme. The time coordinate of the end point of the critical characteristic marks the end of the runoff function $q_{ro}(t)$, and also the last point on the recession function $x_{rec}(t)$.

At this point in the program, N_{rec} is redefined

$$N_{rec} = N_{STD} \tag{7.25}$$

and j_{rec} is reset to zero. At the same time q_1 in equation 7.24 is set to the critical value q(1) just found.

Subsequently, equation 7.24 is used to yield starting discharge values for each of N_{rec} characteristics (as j_{rec} is incremented by one for each successive characteristic), the end points of which will define the recession curve at x values interior to 0 and L. The subroutine KWEND constructs each such characteristic and, in particular, the x and t coordinates of its end point. When all the characteristics have been computed and all end points have been joined to form the recession function, the program branches, depending on the given downstream boundary condition.

With DBC = 1 entered as input data (sec. 3.5), to signify free flow off border end, the computation of runoff and recession are accepted, and the program proceeds to post-irrigation analysis (sec. 5.5). With DBC = 2 (ponding), the program computes the elevation of a pool at field end whose volume equals that computed as runoff. The upstream-most extent of that pool marks the downstream limit of validity of the recession curve as computed earlier. The rest of the recession curve is calculated as resulting from infiltration of a still pond. When this computation is completed, the program proceeds to post-irrigation analysis (sec. 5.5).

[29]A value of IDIAG $\geq$ 4 will result in a printout describing each trial characteristic; IPLOTC $\geq$ 2 will result in a plot of each trial trajectory.

7.5.5 The Hybrid Model: Recession, Only, Computed by Kinematic-Wave Theory

With the option SOLMOD = 5 in force, the flow is calculated by zero-inertia theory until the stream has reached field end and also until recession has started from the upstream end. Then, the surface-depth profile computed for that time, called t_{kwstt}, is modified for transfer to kinematic-wave theory, and the rest of the irrigation is computed on *that* basis.

The depth values in the profile are adjusted by averaging neighboring values to assure a monotonically increasing depth with distance. In the front, where the depth gradient is basically negative, the depth is held constant. Surface-water volume is preserved by shortening the stream as necessary.

A kinematic-wave trajectory is then assumed to emanate from each node on the time line $t = t_{kwstt}$, with the starting conditions derived from the depth pertaining to that node. The subroutine KWEND is called to construct each characteristic. If any characteristic proves to cross field end instead of terminating within the border, the time of crossing and the discharge at that time are found by interpolation to contribute to the runoff function.

As described in section 7.5.4, the recession curve is found by joining the ends of the kinematic-wave trajectories which terminate within the border. The passage of the recession curve through field end is found by interpolation between the two termination points closest to field end, one on each side (fig. 7.8).

7.6 Subroutine KWCDA

This subroutine is called every time that the intersection of a segment of a characteristic and a segment of the advance trajectory must be computed. Thus, it is called to compute the last segment of every characteristic during the advance phase. It performs a numerical integration of equations 7.16, 7.17, and 7.21 over segments of the characteristic and advance trajectories pictured in figure 7.9.

The integration of equation 7.16,

$$y_A - y_c = - \int_C^A i \, dt \qquad (7.26)$$

is not trivial, because $i \to \infty$, as $t \to t_A$. A change of variables, however, solves the problem. Indeed,

$$\begin{aligned}\int_{t_C}^{t_A} i dt &= \int_{\tau_C}^{\tau_A} i \frac{dt}{d\tau} d\tau = \left(\frac{\overline{dt}}{d\tau} \right) \int_{\tau_c}^{\tau_A} i d\tau \\ &= - \left(\frac{\overline{dt}}{d\tau} \right) z_C \frac{t_A - t_C}{\tau_C} z_C\end{aligned} \qquad (7.27)$$

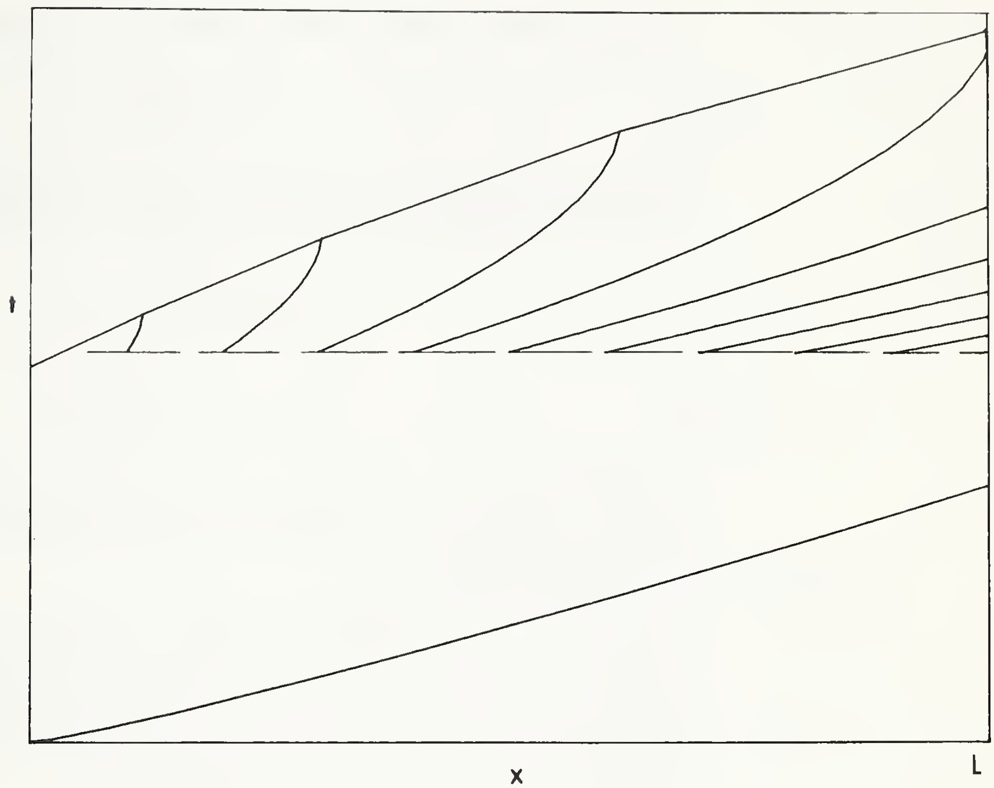

Figure 7.8.—Characteristic curves in hybrid model.

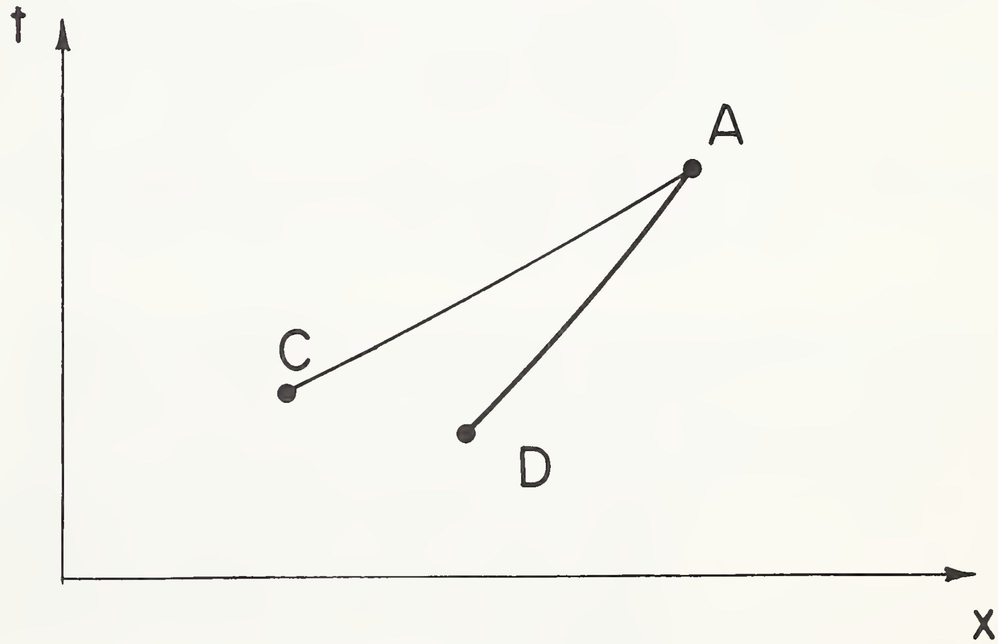

Figure 7.9.—Intersection of characteristic and advance curves.

Thus, a numerical approximation to equation 7.26 is given by

$$y_C - y_A = \frac{z_C}{\tau_C}(t_A - t_C) \tag{7.28}$$

Equation 7.28, which has y_A and t_A as unknowns, is solved simultaneously with the following approximations to equations 7.17 and 7.21, respectively,

$$\frac{x_A - x_C}{t_A - t_C} = \frac{c_C + c_A}{2} \tag{7.29}$$

$$\frac{x_A - x_D}{t_A - t_D} = \frac{w_D + w_A}{2} \tag{7.30}$$

which introduce the additional unknown x_A. There are no further unknowns, because c_A and w_A are uniquely tied to y_A through equations 7.8, 7.4 and the last of equations 7.21.

If the linear mode of solution is in effect (that is, LINMOD = 1—sec. 3.9), the segments in figure 7.9 are assumed straight lines, so that $c_C = c_A$, $w_D = w_A$, and a direct solution is possible. With the nonlinear option (LINMOD = 2). the equations are solved iteratively. If the iterations fail to converge in 20 steps, the entire set of iterations is repeated with the results of each step printed to aid in a diagnosis of the problem.

7.7 Subroutine KWBC

The aim of this subroutine is to construct a segment of kinematic-wave trajectory. Given the conditions at its start, at point B in figure 7.10, namely, x_B, t_B, y_B, τ_B, z_B, q_B, c_B, the x-coordinate of its end point x_C, and the time coordinate t_D of the advance curve at the point $x_D = x_C$, KWBC determines the remaining conditions at the end point, t_C , y_C, τ_C, z_C, q_C, c_C.

This is achieved by a numerical integration of the equations 7.16 and 7.17, that is, by simultaneous solution of algebraic approximations to their integrals, namely,

$$\frac{y_C - y_B}{t_C - t_B} = -\frac{z_C - z_B}{\tau_C - \tau_B} \tag{7.31}$$

$$\frac{x_C - x_B}{t_C - t_B} = \frac{c_B + c_C}{2} \tag{7.32}$$

Equation 7.31 is derived from equation 7.16 in a manner essentially the same as that leading to equation 7.28. Equation 7.32 is the same as equation 7.29 in meaning. With $\tau_C = t_C - t_D$, and z_C and c_C unique functions of τ_C and y_C, respectively, equations 7.31 and 7.32 are solved simultaneously for the unknowns t_C, y_C.

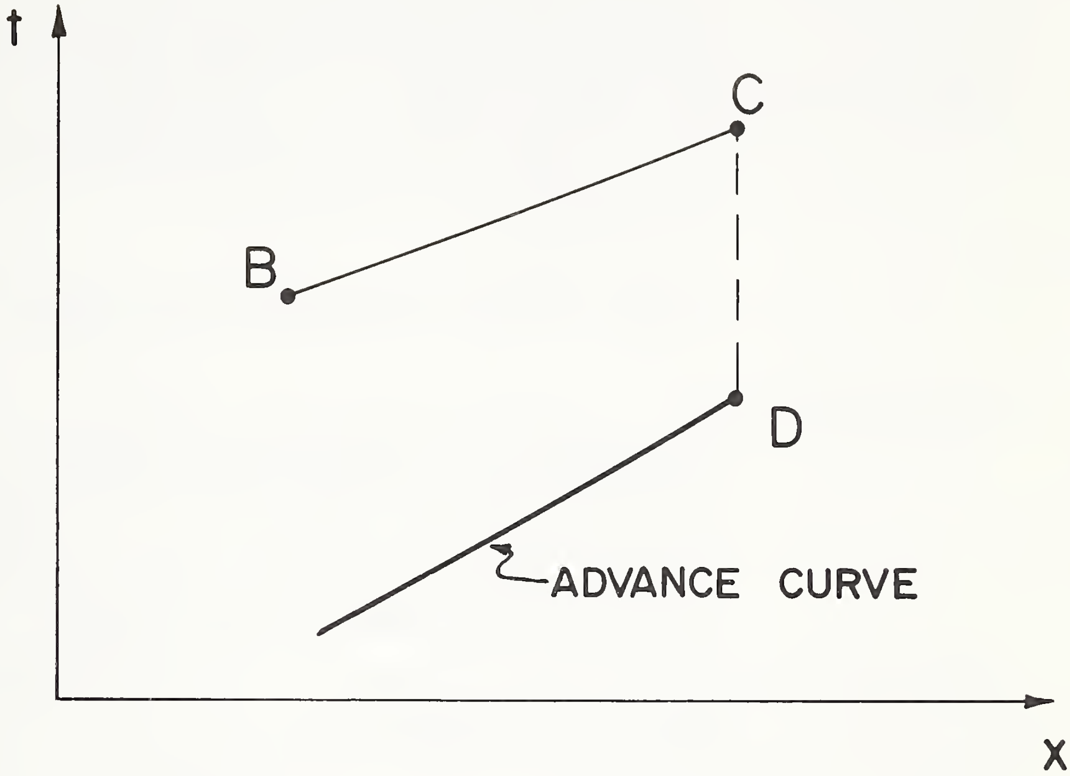

Figure 7.10.—Construction of a segment of the kinematic-wave trajectory.

In the linear mode (LINMOD = 1—sec. 3.9), it is assumed that BC is a straight line, and hence that $c_B = c_C$. This permits direct solution of equation 7.32 for t_C. followed by another direct solution, of equation 7.31, for y_C. In the nonlinear mode (LINMOD = 2), BC is considered a segment of the second-degree curve described by equation 7.32 with $c_B \neq c_C$, and an iterative Newton-Raphson solution is required. The linear solution then constitutes the first guess. If the iterations fail to converge within 20 cycles, all iterations are repeated with the results of each cycle printed as a diagnostic.

7.8 Subroutine KWEND

This subroutine requires given x and t coordinates and a given discharge at that place and time.[30] The subroutine constructs a kinematic-wave trajectory (characteristic) emanating from the given point and bearing the given value of discharge. The trajectory is constructed to its end, where the discharge and depth have fallen to zero as the result of infiltration. Knowledge of the advance curve and infiltration function is a requirement for the use of KWEND.

[30]. . .and, hence, depth, celerity, infiltration depth, and so forth.

The characteristic is constructed in *time* steps, by numerical integration of equations 7.16 and 7.17 over each step. The size of the step is given before the successful construction of each segment. At first, the step is based on the assumption that the total length of characteristic will be composed of $N = N_{STD}$[31] segments. The segments are numbered in order, with the index $k = 2$ referring to the first segment.[32] The label B is given to the start of the segment and C to the end of the segment.

At the start of the calculation for each segment, an estimate is made of the time t_{end} at which the entire trajectory will end, namely,

$$t_{end} = t_D + \tau(z_{end}) \tag{7.33}$$

In equation 7.33, t_D is the time at which the advance curve arrived at the point in the field x_B, at which the current segment starts, and $\tau(z_{end})$ is the time it would take, with the given infiltration function, to infiltrate a depth $z_{end} = z_B + y_B$. Clearly, the more nearly vertical is the remainder of the characteristic leaving point B, and the more nearly horizontal the advance curve, the more nearly correct will this estimate be.

The projected size of the time step encompassed by the segment under construction is given by the formula

$$\delta t = \frac{t_{end} - t_B}{N - k + 2} \tag{7.34}$$

and then,

$$t_C = t_B + \delta t \tag{7.35}$$

An attempt is made to construct the segment by simultaneous solution of numerical approximations to the integrals of equations 7.16 and 7.17, namely,

$$\frac{y_C - y_B}{t_C - t_B} = - \frac{z_C - z_B}{\tau_C - \tau_B} \tag{7.36}$$

which is the same as equation 7.31, and

$$\frac{x_C - x_B}{t_C - t_B} = \frac{c_B + c_C}{2} \tag{7.37}$$

---

[31]. . .entered as data input (see sec. 3.10).

[32]k is also the index of the node points on the characteristic.

a restatement of equation 7.32. Equation 7.36 suffers from a potential problem. Quite possibly, at some point in its length, the kinematic-wave trajectory will parallel the advance curve below. Then the denominator of the expression in the right side will vanish. The program is prepared for this eventuality — the denominator is monitored and when its absolute value falls below 0.000001, equation 7.36 is replaced by

$$\frac{y_C - y_B}{t_C - t_B} = - i_C \tag{7.38}$$

with i computed at the current trial location of C.

In the linear mode of solution (LINMOD = 1—see sec. 3.9), equation 7.37 is solved first, for x_C, in the assumption that $c_C = c_B$. With t_D the time the advance curve crosses x_C, $z_C = z(\tau_C)$ is found for

$$\tau_C = t_C - t_D \tag{7.39}$$

This allows solution of equation 7.36 (or 7.38) for y_C.

With LINMOD = 2 (the nonlinear solution mode), the linearized solution forms the first guess in an iterative solution of equations 7.36 (or 7.38) and 7.37 for x_C and y_C. If 20 iterations prove insufficient for convergence, all 20 are repeated and the results printed for diagnosis of the problem. In the event that y_C turns negative, δt is cut in half and the sequence of instructions commencing with equation 7.35 is repeated.

When all N segments have been completed, a final end point, upon which y = 0, is computed in accordance with the equations

$$x_{end} = x_C + \frac{q_C}{i_{end}} \tag{7.40}$$

$$t_{end} = t_C + \frac{y_C}{i_{end}} \tag{7.41}$$

in which C represents the end of the last segment computed. Equation 40 is an approximation to the integral of equation 7.17, for with equations 7.7 and 7.16 in force,

$$x_{end} - x_C = - \int_{t_C}^{t_{end}} \frac{dq}{dy} \frac{dy/dt}{i} dt = - \int_{t_C}^{t_{end}} \frac{1}{i} dq = \frac{q_C}{\bar{i}} \tag{7.42}$$

Equation 7.41 is, of course, an approximation to the integral of equation 7.16. In both equations 7.40 and 7.41, i_{end} is an approximation to $\bar{i}$.

References

(1) Bassett, D.L., D. D. Fangmeier, and T. Strelkoff. 1980. Hydraulics of surface irrigation. *In* Jensen, M. (ed.), Design and operation of farm irrigation systems, ch. 12. American Society of Agricultural Engineers. [Monograph.]

(2) Henderson, F. M. 1966. Open channel flow. The Macmillan Company, New York.

(3) Lighthill, M. J., and G. B. Whitham. 1955. On kinematic waves: I—Flood movement in long rivers. Proceedings of the Royal Society (London), ser. A, vol. 229, No. 1178.

(4) Liggett, J. A., and J. A. Cunge. 1975. Numerical methods of solution of unsteady flow equations. *In* K. Mahmood and V. Yevjevich (eds.), Unsteady flow in open channels, ch. 4. Water Resources Publications, vol. I. Fort Collins, Colo.

(5) Katopodes, N. D., and T. Strelkoff. 1977. Dimensionless solutions of border-irrigation advance. Journal of the Irrigation and Drainage Division, American Society of Civil Engineers, vol. 103, No. IR4, Proceedings Paper 13400, p. 401-417.

(6) Sayre, W. W., and M. L. Albertson. 1961. Roughness spacing in rigid open channels. American Society of Civil Engineers Proceedings 87 (HY3): 121-150.

(7) Smith, R. E. 1972. Border irrigation advance and ephemeral flood waves. Journal of the Irrigation and Drainage Division, American Society Civil Engineers Proceedings 98, No. IR2, Paper 8979, p. 289-307.

(8) Strelkoff, T., and A. J. Clemmens. 1981. Dimensionless stream advance in sloping borders. Journal of the Irrigation and Drainage Division, American Society of Civil Engineers Proceedings 107, No. IR4 Paper 16747, p. 361-382.

(9) ______ and N. D. Katopodes. 1977. End depth under zero-inertia conditions. Journal of the Hydraulics Division, American Society of Civil Engineers Proceedings 103, No. HY7, Paper 13053, p. 699-711.

(10) ______ and N. D. Katopodes. 1977. Border irrigation hydraulics with zero inertia. Journal of the Irrigation and Drainage Division, American Society of Civil Engineers Proceedings 103, No. IR3, Paper 13189, p. 325-342.

(11) U.S. Department of Agriculture, Soil Conservation Service. 1974. Border irrigation. *In* SCS National Engineering Handbook, ch. 4, sec. 15.

Appendix: Example Input/Output

Printout from a sample run is presented.

Input keyboard entries are marked by an arrow. Immediately after the entry is completed, the program echoes back the information received. This fulfills two purposes: (1) It verifies that the intended data were received and (2) if the program is used in batch mode with punched-card input, the echoed data following the printed prompts provide a record of the data input.

```
**********************************BORDER-IRRIGATION-FLOW PROGRAM**********************************

                                                                                   08 JUN 83      18.17.30
 ELAPSED CP TIME (SECONDS)  =    35.065
 CU-S USED                  =   115.276
 CU-S REMAINING             =   584.724


 INTERACTIVE USERS -- POSITION PAPER FOR PROMPTS   THEN ENTER (LINE 1) 1 FOR A FRESH START ---
                                                         2 TO CHANGE DESIGN PARAMETERS -- ZREQ,QIN,TCO ---
                                                         3 TO CHANGE SOLUTION MODES -- SOLMOD,LINMOD,DTMOD,ISUPZA,ZADMOD ---
                                                         4 TO CHANGE SOLUTION PARAMETERS -- NSTD,RDX,DTSTD,TMAX,JMAX ---
                                                         5 TO CHANGE LEVEL OF DIAGNOSTICS AND/OR PLOTTING FLAGS ---
                                                         0 TO STOP ---


 1
  1
  (LINE 2)............... IDENTIFY THIS RUN ...............
 EXAMPLE #1
 EXAMPLE #1
  ENTER (LINE 3) --  INFMOD DMLMOD ---
 2,1
  2 1
  ENTER (LINE 4) SOIL AND CROP HYDRAULIC PROPERTIES --  RUFMOD RUF AN  INFMOD K A B C ---
 2, 0.04, 0,   1, 1, 0.5, 0, 0.
  2 .04 0. 1 1. .5 0. 0.
  ENTER (LINE 5) FIELD GEOMETRY --  L DBC SOMOD ---
 1200, 1, 1
  1200. 1 1
  ENTER (LINE 6) AVERAGE BOTTOM SLOPE --  SOAVG ---
 0.0005
  .0005
  ENTER (LINE 7) MANAGEMENT PARAMETERS -- ZREQ Q TCO ---
 1.5, 0.2, 40
  1.5 .2 40.
  ENTER (LINE 9) SOLUTION PARAMETERS --  SOLMOD LINMOD DTMOD ISUPZA ZADMOD ---
 2, 2, 0,0,0
  2 2 0 0 0
  ENTER (LINE 10) NUMERICAL SOLUTION PARAMETERS --  N(STD) RDX DT(STD) TMAX JMAX ---
 20, 1, 1, 0, 0
  20 1. 1. 0. 0
  ENTER (LINE 11) DIAGNOSTIC PARAMETERS --  IDIAG IDCH ID2 IPRZA FLGPVE ---
 0,0,0,0,0
  0 0 0 0 0.
  ENTER (LINE 12) PLOTTING PARAMETERS --  IPLOTW  IPLOTY IPLOTH IPLOTC IPWAIT  ---
 0,0,0,0,0
  0 0 0 0 0
 1
```

```
********************************************** B O R D E R  I R R I G A T I O N  F L O W **********************************************

                                                                                                                08 JUN 83     18.21.01

EXAMPLE #1


                          H Y D R A U L I C  P R O P E R T I E S  O F  C R O P  A N D  S O I L
                                 D I M E N S I O N E D                  D I M E N S I O N L E S S

ROUGHNESS ---
 MANNING N  (COEFFICIENT) =   .0400 FT**(1/6)        =   .0400 M**(1/6)       EXPONENT = 0.
                                                  DIMENSIONLESS DRAG COEFFICIENT      D* =  .1000E+01

INTAKE CHARACTERISTICS ---                  IN INFILTRATION FORMULA  Z = K*T**A + B*T + C    --

                        K = 1.0000     IN/HR**A      = 2.5400     CM/HR**A
                          =  .1291E+00 IN/MIN**A     =  .3279E+01 MM/MIN**A
                          =  .1389E-02 FT/SEC**A     =  .4233E-03 M/SEC**A
                                                                                K* =  .1389E+00
                        A =  .5000                   =  .5000                   A  =  .5000
                        B = 0.     IN/HR             = 0.     CM/HR             B* = 0.
                        C = 0.     IN                = 0.     CM                C* = 0.


                                        B O R D E R  G E O M E T R Y
                                 D I M E N S I O N E D                  D I M E N S I O N L E S S
```

```
FIELD LENGTH          L =1200.0 FT                = 365.8 M                L* =  .1410E+01
AVG. FIELD SLOPE   SOAVG = .0005000               =  .5000E-03             SO* =  .1000E+01
PLANE SURFACE

OPEN-END BORDER


                        I R R I G A T I O N - M A N A G E M E N T   P A R A M E T E R S
                               D I M E N S I O N E D                D I M E N S I O N L E S S


REQUIRED APPLICATION     = 1.50 IN                = 3.81 CM               ZREQ* = .2937E+00
UNIT INFLOW RATE         = .2000 CFS/FOOT         =18.581 LITERS/SEC-M      QIN* =  .1000E+01
CUT-OFF TIME             =  40.00 MIN             =  .667 HR               TCO* = .1325E+01


             C H A R A C T E R I S T I C   P A R A M E T E R S   I N   D I M E N S I O N L E S S   F O R M S

CHARACTERISTIC DEPTH BASED ON NORMAL DEPTH   YO=YN,  XO=YO/SO,  TO=XO*YO/QO

                               D I M E N S I O N E D                D I M E N S I O N L E S S
NORMAL DEPTH           YN = .4256 FT              = .1297 M                     = .1000E+01
FROUDE NUMBER AT NORMAL DEPTH  ............................................. FN = .1270E+00
CHARACTERISTIC DEPTH  YO = .4256E+00 FT           = .1297E+00 M

CHARACTRISTIC LENGTH  XO = .8511E+03 FT           = .2594E+03 M
CHAR'STIC DISCHARGE   QO = .2000E+00 CFS/FOOT     = .1858E+02 LITERS/SEC-M
CHARACTERISTIC TIME   TO = .3018E+02 MIN          = .1811E+04 SEC


                                                                       TOP = .2173E+03 MIN     = .1304E+05 SEC
                                                                       XOP = .6128E+04 FT      = .1868E+04 M
                                                                  P = .7200E+01


                             N U M E R I C A L   S O L U T I O N   P A R A M E T E R S

ZERO-INERTIA  (EQUILIBRIUM)  SOLUTION
DEPTH AND DISCHARGE FUNCTIONS ARE TREATED AS FULLY NONLINEAR
MAXIMUM ALLOWABLE NUMBER OF ITERATIONS   JMAX = 20
WHEN WATER SURFACE OF COMPUTATIONAL STREAM IS ESSENTIALLY LEVEL, INFILTRATION IS ASSUMED TO BE THAT OF LEVEL POOL(S)

NUMBER OF CELLS IN STREAM = 20
STANDARD TIME STEP     DT =  1.00 MIN              = .017 HR               DT* = .3313E-01
DT=DT(STD)/N(STD) FOR FIRST N(STD) TIME STEPS.  THEN DT=DT(STD)
                    TMAX = 780.00 MIN              =  13.0 HR             TMAX* = .2584E+02


                                  ZERO-INERTIA (EQUILIBRIUM) MODEL
```

POST-IRRIGATION SYNOPSIS

.... U L T I M A T E   I N F I L T R A T I O N   P R O F I L E ....

K	X	TA	TR	Z	TA MIN	TR MIN	X METERS	Z CM	X FEET	Z IN
1	0.	0.	.2887E+01	.2360E+00	0.	87.1	0.	3.1	0.	1.21
5	.1410E+00	.8171E-01	.3471E+01	.2557E+00	2.5	104.8	36.6	3.3	120.0	1.31
9	.2820E+00	.1897E+00	.4119E+01	.2753E+00	5.7	124.3	73.2	3.6	240.0	1.41
13	.4230E+00	.3094E+00	.4584E+01	.2872E+00	9.3	138.4	109.7	3.7	360.0	1.47
17	.5640E+00	.4369E+00	.4990E+01	.2964E+00	13.2	150.6	146.3	3.8	480.0	1.51
21	.7049E+00	.5702E+00	.5354E+01	.3038E+00	17.2	161.6	182.9	3.9	600.0	1.55
25	.8459E+00	.7080E+00	.5674E+01	.3095E+00	21.4	171.3	219.5	4.0	720.0	1.58
29	.9869E+00	.8495E+00	.6008E+01	.3155E+00	25.6	181.4	256.0	4.1	840.0	1.61
33	.1128E+01	.9942E+00	.6315E+01	.3204E+00	30.0	190.6	292.6	4.2	960.0	1.64
37	.1269E+01	.1141E+01	.6603E+01	.3246E+00	34.5	199.3	329.2	4.2	1080.0	1.66
41	.1410E+01	.1291E+01	.6761E+01	.3248E+00	39.0	204.1	365.8	4.2	1200.0	1.66
	.1410E+01			0.			.3658E+03	0.	.1200E+04	0.

.... M E A S U R E S   O F   M E R I T   O F   C O M P U T A T I O N ....

COMPUTATIONAL VOLUME BALANCE   VQ= .1325E+01   VZ= .4196E+00   VRO= .9017E+00   .... RELATIVE VOLUME ERROR = .2932E-02
MAXIMUM SIZE OF SAW TEETH IN PROFILES --   ITM= 4 KTM= 2 TOOTHM= .138E+00 IRTM=228 KRTM= 3 RTOOTM= .302E+01

.... S Y N O P S I S   O F   R E S U L T S   O F   I R R I G A T I O N ....

		HOURS	MINUTES	DIMENSIONLESS
T CO	(TIME OF CUT OFF)	.67	40.00	.1325E+01
T L	(DURATION OF ADVANCE)	.65	38.97	.1291E+01
T R	(TIME RECESSION STARTS AT UPSTREAM END)	1.45	87.15	.2887E+01
T FR	(TIME RECESSION STARTS AT DOWNSTREAM END)	3.52	210.95	.6989E+01
T E	(TIME ALL SURFACE WATER DISAPPEARS)	3.52	210.95	.6989E+01

		ENGLISH FT**3/FT	METRIC M**3/M	DIMENSIONLESS
V Q	(APPLIED VOLUME)	480.000	44.594	.1325E+01
V Z	(INFILTRATED VOLUME)	151.969	14.119	.4196E+00
V RO	(RUNOFF VOLUME)	326.623	30.345	.9017E+00

		ENGLISH	METRIC	DIMENSIONLESS	% OF APPLIED DEPTH
Y MAX U	(MAXIMUM DEPTH OF SURFACE STREAM ATTAINED AT UPPER END)	.42 FOOT	12.68 CM	.9776E+00	
Y MAX D	(MAXIMUM DEPTH OF SURFACE STREAM ATTAINED AT LOWER END)	0. FOOT	0. CM	0.	
Y MAX	(MAXIMUM DEPTH OF SURFACE STREAM ATTAINED AT ANY POINT)	.42 FOOT	12.68 CM	.9776E+00	
X YMAX	(LOCATION OF POINT OF MAXIMUM DEPTH)	0. FOOT	0. M	0.	
Z MIN	(MINIMUM DEPTH OF INFILTRATION)	1.21 INCH	3.06 CM	.2360E+00	25.1 %
Z MAX	(MAXIMUM DEPTH OF INFILTRATION)	1.70 INCH	4.33 CM	.3337E+00	35.5 %
Z LQ	(AVERAGE LOW-QUARTER DEPTH OF INFILTRATION)	1.34 INCH	3.39 CM	.2614E+00	27.8 %
Z REQ	(REQUIRED DEPTH OF INFILTRATION)	1.50 INCH	3.81 CM	.2937E+00	31.3 %
Z Q	(AVERAGE APPLIED DEPTH VQ/L)	4.80 INCH	12.19 CM	.9399E+00	100.0 %
Z AVG	(AVERAGE INFILTRATED DEPTH VZ/L)	1.52 INCH	3.86 CM	.2976E+00	31.7 %

Z

RO

```
        (AVERAGE DEPTH OF RUNOFF     VRO/L) ..................................  3.27 INCH   8.30 CM    .6396E+00      68
                                                                                                                      .0 %

Z DP ZREQ  (AVERAGE DEPTH OF DEEP-PERCOLATION VOLUME BASED ON GIVEN REQUIRED DEPTH)   .06 INCH    .16 CM    .1261E-01     1.3 %
Z DP ZMIN  (AVERAGE DEPTH OF DEEP-PERCOLATION VOLUME BASED ON ZREQ = ZMIN)            .31 INCH    .80 CM    .6159E-01     6.6 %
Z DP ZLQ   (AVERAGE DEPTH OF DEEP-PERCOLATION VOLUME BASED ON ZREQ = ZLQ)             .19 INCH    .49 CM    .3762E-01     4.0 %
Z U ZREQ   (AVERAGE OF INFILTRATED DEPTHS LESS THAN OR EQUAL TO REQUIRED DEPTH)      1.46 INCH   3.70 CM    .2850E+00    30.3 %
Z U ZMIN   (AVERAGE OF INFILTRATED DEPTHS LESS THAN OR EQUAL TO ZMIN)                1.21 INCH   3.06 CM    .2360E+00    25.1 %
Z U ZLQ    (AVERAGE OF INFILTRATED DEPTHS LESS THAN OR EQUAL TO ZLQ)                 1.33 INCH   3.37 CM    .2600E+00    27.7 %

UC C       (CHRISTIANSEN UNIFORMITY COEFFICIENT) ..........................................   .931
UC H       (HSPA UNIFORMITY COEFFICIENT) ..................................................   .933
DU         (DISTRIBUTION UNIFORMITY              ZMIN/ZAVG) ...............................   .793
DU LQ      (LOW-QUARTER DISTRIBUTION UNIFORMITY    ZLQ/ZAVG) ..............................   .879
RP         (RUNOFF FRACTION IN PERCENT            VRO/VQ  ) ...............................  68.05%
                                                                         BASED ON   BASED ON    BASED ON
                                                                        GIVEN ZREQ  ZREQ=ZMIN   ZREQ=ZLQ
IE         (IRRIGATION EFFICIENCY                  ZU/ZQ  ) ..............   30.32%     25.11%      27.66%
UZ         (USEFUL FRACTION OF INFILTRATED VOLUME  ZU/ZAVG) ..............    .958       .793        .874
SE         (STORAGE EFFICIENCY                     ZU/ZREQ) ..............   97.02%    100.00%      99.43%
AAP        (PERCENT OF TOTAL AREA ADEQUATELY IRRIGATED) ..................   63.22%    100.00%      88.08%
DR         (DEFICIENCY RATIO, AVERAGE DEFICIT IN UNDERIRRIGATED AREA, PERCENT OF ZREQ)  8.11%        4.77%

CU-S USED FOR THIS RUN  =    39.044



********************************BORDER-IRRIGATION-FLOW PROGRAM********************************

                                                                                        08 JUN 83      18.24.02
ELAPSED CP TIME (SECONDS)  =    52.697
CU-S USED                  =   158.196
CU-S REMAINING             =   541.804


INTERACTIVE USERS -- POSITION PAPER FOR PROMPTS   THEN ENTER (LINE 1) 1 FOR A FRESH START ---
                                                  2 TO CHANGE DESIGN PARAMETERS -- ZREQ,QIN,TCO ---
                                                  3 TO CHANGE SOLUTION MODES -- SOLMOD,LINMOD,DTMOD,ISUPZA,ZADMOD ---
                                                  4 TO CHANGE SOLUTION PARAMETERS -- NSTD,RDX,DTSTD,TMAX,JMAX ---
                                                  5 TO CHANGE LEVEL OF DIAGNOSTICS AND/OR PLOTTING FLAGS ---
                                                  0 TO STOP ---
```


☆ U.S. GOVERNMENT PRINTING OFFICE: 1985 - 617-884 - 814/40204